

**THE INTERANNUAL AND INTERDECADAL VARIABILITY
OF THE BORNEO VORTEX
DURING BOREAL WINTER MONSOON**

A Dissertation

Presented to

The Faculty of the Graduate School

At the University of Missouri

In Partial Fulfillment

Of the Requirements for the Degree

Doctor of Philosophy

By

MOHD HISHAM MOHD ANIP

Dr. Anthony R. Lupo, Dissertation Supervisor

MAY 2012

The undersigned, appointed by the dean of the Graduate School,
have examined the dissertation entitled

**THE INTERANNUAL AND INTERDECADAL VARIABILITY
OF THE BORNEO VORTEX
DURING BOREAL WINTER MONSOON**

Presented by Mohd Hisham Mohd Anip

A candidate for the degree of
Doctor of Philosophy of Soil, Environment and Atmospheric Sciences
And hereby certify that, in their opinion, it is worthy of acceptance.

Professor Anthony R. Lupo

Professor Stephan Montgomery Smith

Associate Professor Patrick S. Market

Associate Professor Neil Fox

ACKNOWLEDGEMENTS

First and foremost, I would like to thank Dr. Anthony R. Lupo for guiding me through the completion of my dissertation. He really made me comfortable and I enjoyed every moment I spent with him during the progress of this work. I will never forget all the valuable experiences and knowledge I have gained from him.

I would also like to give my utmost gratitude to Dr. Patrick S. Market, Dr. Neil Fox and Dr. Montgomery Smith for being part of my dissertation committee members. Without your helpful suggestions and comments, I do not think I will be able to complete this work.

Endless thanks also go to the top management of Malaysian Meteorological Department for putting their confidence in me and giving me an opportunity to further my studies and the Government of Malaysia for the scholarship during my four-year study at this university.

Finally, my deep appreciation goes to my beloved wife, Zuana Tahir, for being unconditionally supportive and patient, my three children for being understanding and my parents for the encouragements. All of them have given me strength in the completion of my PhD. journey.

TABLE OF CONTENTS

Acknowledgements	ii
List of Figures	v
List of Tables	xi
Abstract	xv
Chapter	
1. Introduction	1
1.1 Backgrounds	3
1.2 Study Objectives	10
2. Methodology	12
2.1 Study domain	12
2.2 Data	13
2.3 Procedure	15
2.4 Climate variability	19
2.4.1 Pacific Decadal Oscillation (PDO)	19
2.4.2 El Nino Southern Oscillation (ENSO)	21
2.4.3 Quasi-Biennial Oscillation (QBO)	22
2.4.4 Tropospheric Biennial Oscillation (TBO)	24
3. Climatological results and discussions	27
3.1 Borneo vortex frequency	27

3.2 Borneo vortex center	46
3.3 Borneo vortex system and lifespan.....	72
3.4 Borneo vortex intensity	88
3.5 The onset and retreat dates of the Borneo vortex	110
3.6 Discussions	129
4. Case Studies	133
4.1 Background mean fields	134
4.2 Weak and moderate Borneo vortices (3 December 1991)	143
4.3 Strong Borneo vortex (9 January 2009)	153
5. Summary and conclusions	164
Appendix A	170
References	181
Vita Auctoris	189

LIST OF FIGURES

Figure	Page
1.1 Primary synoptic-scale circulation features over Southeast Asia during winter monsoon. “C” indicates the cyclonic circulation, which is known as Borneo vortex (adapted from Johnson and Zimmerman, 1986).....	2
2.2.1 Domain of the study area to determine the Borneo vortices bounded by 2.5°S and 7.5°N latitudes and 102.5°E and 117.5°E longitudes.....	13
3.1.1 Seasonal Borneo vortex frequency for 41 winter monsoon between 1970/71 and 2010/11 seasons. The red-dashed line is the 4 th order polynomial trendline and the black line is the linear trendline of the vortex frequencies.....	31
3.1.2 Monthly total of Borneo vortex frequency throughout 41 winter monsoon seasons.....	32
3.1.3 An event where two Borneo vortices were observed at 0000 UTC on 7 December 2008. The vortex centers are marked as yellow ‘X’. The white lines with arrows are the streamlines of the wind flow and the color-shaded areas indicate the wind speed of 2 ms ⁻¹ or greater.....	34
3.1.4 The seasonal frequency of Borneo vortex for 41 winter monsoon seasons plotted as Fourier power spectra with the ordinate displaying the magnitude of the Fourier coefficient and the abscissa displaying the period of cycles per 41 years. The blue-and green-dashed lines indicate the 95% and 80% confidence level against the white-noise background, respectively.....	38
3.2.1 One of the Borneo vortices that was observed to rotate in the counterclockwise direction in the Southern Hemisphere, which formed at 0000 YTC on 7 January 1995. The center is marked as yellow “X”. The color-shaded area indicates the wind speed of 2 ms ⁻¹ or greater.....	47
3.2.2 Red “X”s are the position of the seasonal averages of Borneo vortex centers for 41 winter monsoon between 1970/71 and 2010/2011 seasons and the yellow star is the long-term average position of all the vortex centers throughout the study period.....	52

3.2.3	The seasonal longitudinal (top) and latitudinal (bottom) positions of the Borneo vortex centers for 41 winter monsoon between 1970/71 and 2010/11 seasons. The red-dashed line is the 3rd order polynomial trendline and the black line is the linear trendline of the vortex positions.....	54
3.2.4	Monthly averages of latitudinal (top) and longitudinal (bottom) position of the Borneo vortex centers throughout 41 winter monsoon seasons.....	56
3.2.5	Monthly position of the Borneo vortex centers (blue “X”s) based on the latitude-longitude average for 41 winter monsoon seasons. The yellow star is the long-term average and the red box is the study domain.....	57
3.2.6	The position of the seasonal Borneo vortex centers for 41 winter monsoon between 1970/71 and 2010/2011 seasons. The brown “X” indicates the vortex center during the PDO1 period while the blue “+” during PDO2. The yellow star is the long-term average position of the vortex center throughout the study period.....	58
3.2.7	The seasonal latitudinal (top) and longitudinal (bottom) positions of the Borneo vortex centers for 41 winter monsoon seasons plotted as power spectra with the ordinate displaying the magnitude of the Fourier coefficient and the abscissa displaying the period of cycles per 41 years. The blue- and green-dashed lines indicate the 95% and 80% confidence level against the white-noise background, respectively.....	61
3.2.8	The position of the seasonal Borneo vortex centers for 41 winter monsoon between 1970/71 and 2010/2011 seasons. The brown “X” indicates the vortex center during the EN years, the blue “+” is LN and the grey “*” is NEU year. The yellow star is the long-term average position of the vortex center throughout the study period.....	63
3.2.9	The position of the seasonal Borneo vortex centers for 41 winter monsoon between 1970/71 and 2010/2011 seasons. The brown “X” indicates the vortex center during the east QBO mode and the blue “+” is west QBO. The yellow star is the long-term average position of the vortex center throughout the study period.....	66
3.2.10	The position of the seasonal Borneo vortex centers for 41 winter monsoon between 1970/71 and 2010/2011 seasons. The grey “X” indicates the vortex center during the weak TBO mode and the blue “+” is strong TBO. The yellow star is the long-term average position of the vortex center throughout the study period.....	69

3.3.1	Seasonal mean of Borneo vortex system lifespan between 1970/71 and 2010/11 winter monsoon seasons. The black line indicates the linear trendline and red-dashed line is the 3rd order polynomial trendline.....	79
3.3.2	The seasonal lifespan of Borneo vortex systems for 41 winter monsoon seasons plotted as Fourier power spectra with the ordinate displaying the magnitude of the Fourier coefficient and the abscissa displaying the period of cycles per 41 years. The blue- and green-dashed lines indicate the 95% and 80% confidence level against the white-noise background, respectively.....	81
3.4.1	Monthly distribution of Borneo vortex frequency of different intensities.....	93
3.4.2	The seasonal Borneo vortex frequency for weak (blue line), moderate (brown line) and strong (green line) intensities throughout 41 winter monsoon between 1970/71 and 2010/11 seasons. The red-dashed lines are the 3 rd order polynomial trendlines.....	96
3.4.3	The seasonal Borneo vortex frequency for weak (top), moderate (middle) and strong (bottom) intensities plotted as Fourier power spectra with the ordinate displaying the magnitude of the Fourier coefficient and the abscissa displaying the period of cycles per 41 years. The blue- and green-dashed lines indicate the 95% and 80% confidence level against the white-noise background, respectively.....	100
3.5.1	The position of the first and last Borneo vortex centers that had been detected in each winter monsoon between 1970/71 and 2010/11 seasons. The blue “X” indicates the first vortex and brown “+” is the last vortex of the season. Yellow ‘star’ is the long-term mean Borneo vortex position as analyzed in section 3.2.....	113
3.5.2	The date of the first (Top) and last (Bottom) Borneo vortex observed in each winter monsoon between 1970/71 and 2010/11 seasons over the study region. The black line indicates the linear trendline and red-dashed line is the 3 rd order polynomial trendline.....	115
3.5.3	The onset and retreat dates of the first (Top) and last (Bottom) Borneo vortex, respectively, observed in each winter monsoon between 1970/71 and 2010/11 seasons plotted as Fourier power spectra with the ordinate displaying the magnitude of the Fourier coefficient and the abscissa displaying the period of cycles per 41 years. Blue-dashed lines indicate significant interval at 99% confidence level against the white-noise	

	background The blue- and green-dashed lines indicate the 95% and 80% confidence level against the white-noise background, respectively.....	119
4.1.1	The 0000 UTC seasonal mean streamlines of 925 hPa wind field for winter monsoon between 1979/80 and 2010/11 seasons. Brown-dashed line is the trough and blue star is the center of Borneo vortex long-term mean position determined from section 3.2.....	135
4.1.2	The analysis of 0000 UTC seasonal mean divergence (s^{-1}) at 925 hPa chart throughout winter monsoon between 1979/80 and 2010/11 seasons. The blue star is the center of Borneo vortex long-term mean position determined from section 3.2.....	135
4.1.3	The analysis of 0000 UTC seasonal mean vorticity (s^{-1}) at 925 hPa chart throughout winter monsoon between 1979/80 and 2010/11 seasons. The blue star is the center of Borneo vortex long-term mean position determined from section 3.2.....	139
4.1.4	The analysis of 0000 UTC seasonal mean vertical velocity ($Pa s^{-1}$) at 925 hPa chart throughout winter monsoon between 1979/80 and 2010/11 seasons. The blue star is the center of Borneo vortex long-term mean position determined from section 3.2.....	139
4.1.5	The analysis of 0000 UTC seasonal mean potential vorticity ($K m^2 Kg^{-1} s^{-1}$) at 925 hPa chart throughout winter monsoon between 1979/80 and 2010/11 seasons. The blue star is the center of Borneo vortex long-term mean position determined from section 3.2.....	141
4.2.1	The analysis chart of 925 hPa wind direction (white lines) and speed (color-shaded area in ms^{-1}) at 0000 UTC on 3 Dec 1991. The yellow 'X' is the center of Borneo vortex.....	143
4.2.2	The analysis charts of 0000 UTC wind at 925 (top), 850 (middle) and 700 (bottom) hPa pressure levels on 3 December 1991. Brown-dashed line is the trough and "C" is the center of cyclonic circulation.....	145
4.2.3	The analysis of 0000 UTC horizontal divergence (s^{-1}) at 925 hPa chart on 3 December 1991. The black and purple stars are the center of moderate and weak vortices, respectively.....	147
4.2.4	The analysis of 0000 UTC horizontal relative vorticity (s^{-1}) at 925 hPa chart on 3 December 1991. The black and purple stars are the center of moderate and weak vortices, respectively.....	148

4.2.5	The vertical cross section between A and B in Fig. 4.2.4 of 0000 UTC horizontal relative vorticity (s^{-1}) at 1000 to 100 hPa pressure levels on 3 December 1991. The black and purple stars are the center of moderate and weak vortices, respectively.....	148
4.2.6	The analysis of 0000 UTC vertical velocity/omega ($Pa s^{-1}$) at 925 hPa chart on 3 December 1991. The black and purple stars are the center of moderate and weak vortices, respectively.....	150
4.2.7	The analysis of 0000 UTC potential vorticity ($K m^2 Kg^{-1} s^{-1}$) at 925 hPa chart on 3 December 1991. The black and purple stars are the center of moderate and weak vortices, respectively.....	150
4.2.8	The vertical cross section between A and B in Fig. 4.2.6 of 0000 UTC potential vorticity ($K m^2 Kg^{-1} s^{-1}$) at 1000 to 100 pressure levels on 3 December 1991. The black and purple stars are the center of moderate and weak vortices, respectively.....	151
4.3.1	The analysis chart of 925 hPa wind direction (white lines) and speed (color-shaded area in ms^{-1}) at 0000 UTC on 9 January 2009. The yellow 'X' is the center of Borneo vortex.....	153
4.3.2	The analysis charts of 0000 UTC wind at 925 (top), 500 (center) and 400 (bottom) hPa pressure levels on 9 January 2009. Brown-dashed line is the trough and "C" is the cyclonic circulation center.....	155
4.3.3	The analysis of 0000 UTC horizontal divergence (s^{-1}) at 925 hPa chart on 9 January 2009. The black star is the center of strong vortex.....	157
4.3.4	The analysis of 0000 UTC horizontal relative vorticity (s^{-1}) at 925 hPa chart on 9 January 2009. The black star is the center of strong vortex.....	157
4.3.5	The cross section between A and B in Fig. 4.3.4 of 0000 UTC relative vorticity (s^{-1}) at 1,000 to 50 hPa pressure levels on 9 January 2009. The black star is the center of strong vortex.....	159
4.3.6	The analysis of 0000 UTC vertical velocity/omega ($Pa s^{-1}$) at 925 hPa chart on 9 January 2009. The black star is the center of strong vortex.....	159
4.3.7	The analysis of 0000 UTC potential vorticity ($K m^2 Kg^{-1} s^{-1}$) at 925 hPa chart on 9 January 2009. The black star is the center of strong vortex.....	161

4.3.8 The cross section between A and B in Fig. 4.3.7 of 0000 UTC potential vorticity ($\text{K m}^2 \text{Kg}^{-1} \text{s}^{-1}$) at 1,000 to 50 hPa pressure levels on 9 January 2009. The black star is the center of strong vortex..... 161

LIST OF TABLES

Table	Page
2.4.1 Periods of the PDO phases from Lupo et al. (2007).....	20
2.4.2 Years of ENSO phases according to JMA definition taken from http://coaps.fsu.edu/jma.shtml	22
2.4.3 Seasons of QBO phases.....	24
2.4.4 Seasons of TBO phases.....	26
3.1.1 Monthly and seasonal frequencies of Borneo vortices during Malaysian winter monsoon periods between November and February for 1970/71 to 2010/11 seasons.....	29
3.1.2 The seasonal and monthly averages of Borneo vortex frequency.....	30
3.1.3 Total number of days that Borneo vortices were observed during winter monsoon between November and February for 1970/71 and 2010/11 seasons.....	34
3.1.4 The seasonal averages of the Borneo vortex frequency stratified by PDO phases.....	37
3.1.5 The seasonal averages of the Borneo vortex frequency stratified by ENSO years. "*" denotes the value is statistically significant at 90% confidence level.....	39
3.1.6 The seasonal averages of the Borneo vortex frequency stratified by ENSO in PDO phases.....	41
3.1.7 The seasonal averages of Borneo vortex frequency stratified by QBO phases.....	43
3.1.8 The seasonal averages of Borneo vortex frequency stratified by TBO phases.....	44
3.1.9 The seasonal averages of the Borneo vortex frequency stratified by ENSO in TBO phases. "*" denotes the value is statistically significant at 90% confidence level.....	45

3.2.1	Monthly and seasonal locations of Borneo vortex centers during 41 winter monsoon seasons.....	49
3.2.2	Monthly and seasonal averages of Borneo vortex centers based on latitude (Lat)-longitude (Long) positions (degree) during 41 winter monsoon seasons.....	51
3.2.3	The average positions of the Borneo vortex centers stratified by PDO phases. "*" denotes the value is statistically significant at 90% confidence level.....	60
3.2.4	The average positions (degree) of the Borneo vortex centers stratified by ENSO years. "*" denotes the value is statistically significant at 99% confidence level.....	64
3.2.5	The average positions (degree) of the Borneo vortex centers stratified by ENSO in PDO phases. "+" and "*" denotes the value is statistically significant at 95% and 90% confidence level, respectively.....	65
3.2.6	The average positions (degree) of the Borneo vortex centers stratified by QBO phases.....	68
3.2.7	The average positions (degree) of the Borneo vortex centers stratified by TBO phases.....	70
3.2.8	The average positions (degree) of the Borneo vortex centers stratified by ENSO in TBO phases. "*" denotes the value is statistically significant at 99% confidence level.....	70
3.3.1	The monthly and seasonal number of Borneo vortex systems.....	74
3.3.2	The seasonal and monthly average number of Borneo vortex systems.....	75
3.3.3	The monthly and seasonal average lifespan of the Borneo vortex systems.....	76
3.3.4	The seasonal and monthly average lifespans (days) of the Borneo vortex systems.....	77
3.3.5	The seasonal mean of Borneo vortex lifespan (days) stratified by ENSO years.....	82

3.3.6	The seasonal mean of Borneo vortex lifespan (days) stratified by QBO phases.....	83
3.3.7	The seasonal mean of Borneo vortex lifespan (days) stratified by TBO phases.....	84
3.3.8	The seasonal mean of Borneo vortex lifespan (days) stratified by ENSO in TBO phases.....	85
3.3.9	The seasonal mean of Borneo vortex lifespan (days) based on the sample groups of tropical cyclone activity from Zuki and Lupo (2008).....	87
3.4.1	Monthly and seasonal frequencies of Borneo vortices based on their intensity. Weak (W), moderate (M) and strong (S) intensities correspond to the wind speed around the vortex within 2.5° X 2.5° grid square with at least 2-5 ms ⁻¹ , 5-10 ms ⁻¹ and greater than 10 ms ⁻¹ , respectively.....	91
3.4.2	The long-term seasonal and monthly mean of Borneo vortex frequency with different intensities.....	95
3.4.3	The Borneo vortex seasonal average frequency of different intensities stratified by PDO phases. "*" denotes the value is statistically significant at 95% confidence level.....	98
3.4.4	The Borneo vortex seasonal average frequency of different intensities stratified by ENSO years. "*" denotes the value is statistically significant at 90% confidence level.....	101
3.4.5	The Borneo vortex seasonal average frequency of different intensities stratified by PDO periods and ENSO years. "+" and "*" denotes the value is statistically significant at 99% and 90% confidence level, respectively.....	102
3.4.6	The Borneo vortex seasonal average frequency of different intensities stratified by QBO phases.....	104
3.4.7	The Borneo vortex seasonal average frequency of different intensities stratified by TBO phases. "*" denotes the value is statistically significant at 95% confidence level.....	105
3.4.8	The Borneo vortex seasonal average frequency of different intensities stratified by TBO and ENSO phases. "*" denotes the value is statistically significant at 90% confidence level.....	107

3.4.9	The seasonal mean quantity of Borneo vortex with strong intensity based on the sample groups of tropical cyclone activity from Zuki and Lupo (2008).....	109
3.5.1	The seasonal dates and locations of the first and last Borneo vortex observed over 41 winter monsoon between 1970/71 and 2010/11 seasons.....	111
3.5.2	The seasonal mean dates of the first and last Borneo vortex detected over the study domain as stratified by PDO phases.....	118
3.5.3	The seasonal mean dates of the first and last Borneo vortex detected over the study domain as stratified by ENSO years. “+” and “*” denotes the value is statistically significant at 99% and 90% confidence level, respectively.....	121
3.5.4	The seasonal mean dates of the first and last Borneo vortex detected over the study domain as stratified by PDO and ENSO phases. “+” and “*” denotes the value is statistically significant at 95% and 90% confidence level, respectively.....	123
3.5.5	The seasonal mean dates of the first and last Borneo vortex detected over the study domain as stratified by QBO phases.....	125
3.5.6	The seasonal mean dates of the first and last Borneo vortex detected over the study domain as stratified by TBO phases. “*” denotes the value is statistically significant at 90% confidence level.....	126
3.5.7	The seasonal mean dates of the first and last Borneo vortex detected over the study domain as stratified by TBO and ENSO phases. “*” denotes the value is statistically significant at 99% confidence level.....	127

ABSTRACT

The boreal winter monsoon over the Malaysian region has long been associated with heavy rainfall activity and flood disaster. One of the main features that characterize this monsoon is the presence of Borneo vortices. The main purpose of this study is to identify these vortices and determine their long-term climatological behavior over 41 winter monsoon seasons that ran between November and February of the following year from 1970 to 2010. Once congregated, the vortices are divided into five different seasonal aspects, which include the frequency, position, lifespan, intensity, and onset and retreat dates of the first and last vortex of the season.

2,278 of Borneo vortices were identified throughout the study period. Out of this number, about 77% were considered as the weak type of vortex, 17% moderate and 5% strong. More than 60% of the vortices were discovered on a water body and the vortex long-term mean position was located at 2.4°N and 110.6°E, which is just off coast of the Borneo Island. In addition, the vortex systems have a mean lifespan of 3.6 days, which suggests that they are a synoptic type of weather event. The first vortex of the season tended to appear in early November while the last one generally left the region by end of February.

All of the polynomial long-term trends of the vortex aspects show a pattern that emulates the (Pacific Decadal Oscillation) PDO interdecadal variability

except in the case of the vortex system lifespan. Besides the PDO, the vortex aspects also demonstrate strong signals of emulating the (El Niño Southern Oscillation) ENSO, (Tropospheric Oscillation Oscillation) TBO and/or (Quasi Biennial Oscillation) QBO interannual variability when their time-series data are transformed into a function of oscillation through the Fourier power spectra analysis.

The data from each aspect of the Borneo vortices were then compared with all these interdecadal and interannual variabilities using the compositing analysis technique. The outcomes reveal that the majority of the vortex aspects show strong feedback with regard to different phases of the ENSO, TBO and PDO events, but not the QBO. Furthermore, the EN signal is found to be strong in PDO1 period while the LN signal is strong in PDO2. Also, it was discovered that the EN tends to weaken the TBO event, while the impact was reversed during the LN years. Even though most of the relationships identified here show strong confidence levels, however, some were not strong enough to be considered as statistically significant. In addition, this study also examined two selected events in order to find the differences among the Borneo vortices of different intensities based on their convective parameters.

CHAPTER 1

INTRODUCTION

Toward the end of every year, the region located southward of 10°N latitude around Southeast Asia, which includes Malaysia, is shrouded regularly by rain-laden clouds. During this period, the lower tropospheric wind predominantly becomes northeasterly as the monsoon trough from East Asia migrates southward toward the equator. This indicates that the northeast monsoon, which is also known as the winter monsoon, has completely set into the area. In general, the onset of Malaysian winter monsoon begins in early or middle November and persists until early March (MMD, 2012). During its peak period, some parts of the country receive excessive amounts of rainfall. This may be followed by possibly severe floods that lead to the damage of crops and property, and loss of lives.

Described as the most active convective region near the equator (Krishnamurti et al., 1973), this area does not only receive large amounts of rainfall, but it is also an area of intense latent heat release, which is the greatest source of global heat energy during boreal winter (Ramage, 1968). Due to its

significant impact, a lot of studies have been carried out with regard to this winter monsoon in this region including its dynamics, and synoptic features and structures (e.g. Ramage (1968), Cheang (1977, 1978), Murakami (1979), Houze et al. (1981), Johnson and Zimmerman (1986), Bate et al. (1989), Chang et al. (1979, 1980, 2005b)). Among all these studies, one of the fields that has gained scholars' interests, and has since flourished in tropical meteorological studies after World War II, is the presence of low tropospheric cyclonic disturbances near the equator, as depicted in Fig. 1.1. These synoptic-scale weather systems frequently form off coast of the Borneo Island. Owing to that, they are sometimes called as the Borneo vortices.

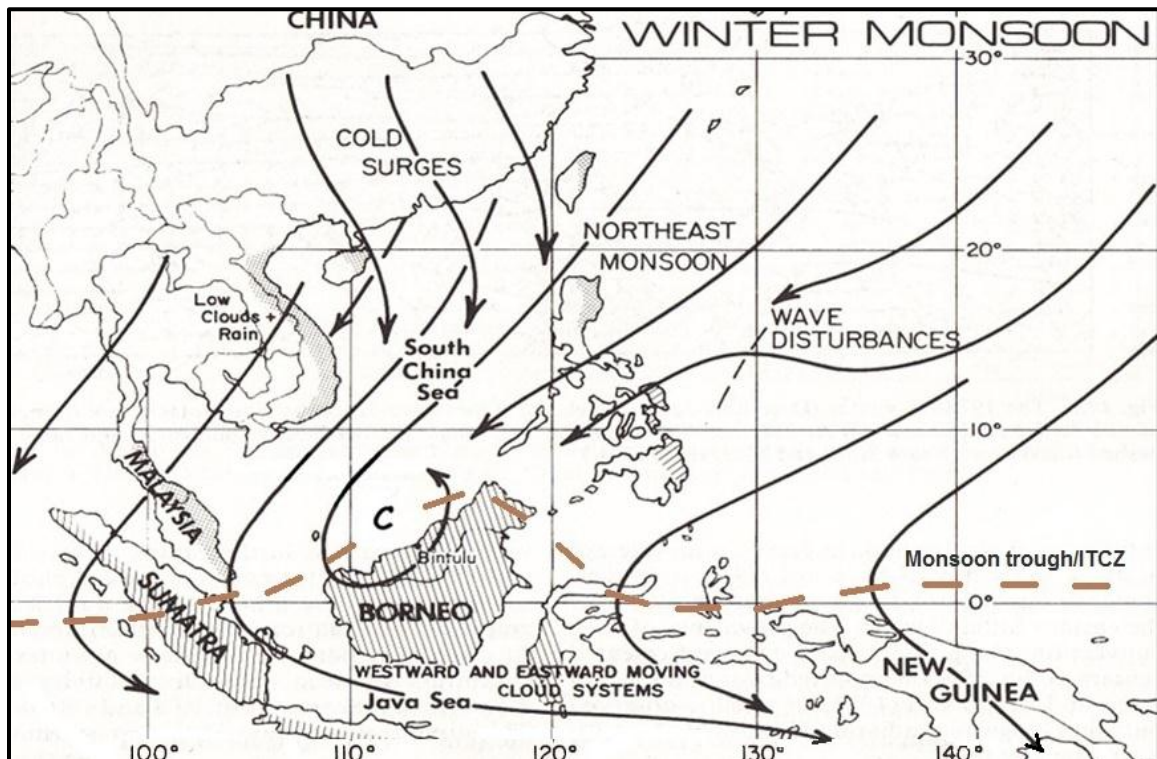


Fig. 1.1: Primary synoptic-scale circulation features over Southeast Asia during winter monsoon. "C" indicates the cyclonic circulation, which is known as Borneo vortex (adapted from Johnson and Zimmerman, 1986).

1.1 Background

The Borneo vortex is one of the two synoptic systems that characterize the winter monsoon weather in southern part of South China Sea (Chang et al., 2005b) including the Malaysian region. It forms and embeds in the monsoon trough (Cheang, 1977 and 1987), i.e. part of the Inter-Tropical Convergence Zone (ITCZ), and regularly occurs in association with low-level northeasterly monsoon flow from the higher latitudes. According to Johnson and Chang (2007), the vortex affects weather in the vicinity of Malaysian region by producing torrential rainfall, and influences the planetary-scale circulation through the release of enormous amounts of latent heat.

However, the presence of such vortex systems are not only restricted within this region, but can also be found in other parts of the equatorial belt. There has been considerable controversy over its origin ever since this type of vortex was first identified in the tropics. Riehl et al. (1948), Palmer (1952), Fett (1966) and Yanai et al. (1968) claimed that the vortex develops from equatorial easterly wave disturbances, while Sadler (1967) suggested that its formation is due to the wind shear between two opposing flows.

Detailed studies of the synoptic features and structures of some of these vortices occurring in December 1973 winter monsoon over the South China Sea in the Malaysian region by Cheang (1977) reveal that they can be generated from both processes. Evidence showed by him demonstrates that apart from being able to spawn in the west Pacific as a result of equatorial easterly wave

disturbances, the vortex could also form from lateral shear in the zonal easterly flow over the South China Sea.

Furthermore, according to Cheang (1977), this kind of shear may contribute to the development of barotropic instability, which then leads to the formation of such vortices in the region. Through this study, he also suggested that the vortex intensity is possibly maintained by a complex combination of conditional instability of the second kind (CISK) mechanism, and mixed barotropic and baroclinic instability. However, this idea was not supported by Murakami (1977). Instead, he claimed that the barotropic instability plays an insignificant part in the maintenance of such vortices over the South China Sea, which on the other hand, could be accounted for only by baroclinic processes.

Prior to 1970, it had been customary for Malaysian meteorologists to ascribe the cause of heavy rainfall over the Malaysian region during winter monsoon to the presence of these equatorial vortices. This condition was re-emphasized by Cheang (1977) in his synoptic studies of the vortices. In addition, he suggested that the intensification of these vortices depends very much on the outbreak of cold surges that come all the way from intense high pressure area in central Asia. The outbreak causes the northwesterly cold air to flow out from the anticyclone system and turning northeasterly with the presence of mid-tropospheric trough along the East Asia coast. It continues to move along the coast of China across the South China Sea before reaching the Malaysian region and interacts with the vortices.

These cold surges are believed to be the most important transient disturbance embedded within the mean monsoon circulation (Zhang et al., 1997b). Their presence has been known to impact the intensity of the Asian winter monsoon by many researchers prior to Cheang's (1977) works, such as by Wexler (1951), Ramage (1955, 1971), Riehl (1969) and Krishnamurti et al. (1973). However, Cheang's research is considered to be more detailed and explicit, and have helped Malaysian meteorologists to further understand these systems and provide better forecasting during the winter monsoon.

Upon realizing the importance of winter monsoon mechanisms, including the Borneo vortex, a group of international scientists was established to run series of observations in December 1978 known as Winter Monsoon Experiment (WMONEX) over the southern part of the South China Sea. This experiment was part of the Global Atmospheric Research Program (GARP) in order to obtain a comprehensive data set that would allow researchers to study various aspects of the winter monsoon, particularly within the Malaysian region (Greenfield and Krishnamurti, 1979).

The initiation of this experiment had gained wide attention among some scholars of tropical meteorology field even before its commencement date. However, their scope of research only centered on the interaction between the cold surge and the Borneo vortices over the South China Sea, such as Chang et al. (1979) and Chang and Lau (1980). Apart from that, Chang and Lau (1980) had also investigated the connection between the intensification of the vortices

and the enhancement of East Asia local Hadley circulation, as well as the strengthening of Walker cells along the equator. Their findings appear to match with earlier studies done by Bjerknes (1969) and Krishnamurti et al. (1973).

More studies related to these vortices were conducted once the data of WMONEX become available through meteorological World Data Centers after the completion of the experiment. Daily streamline analyses run by Chen et al. (1986) indicate that a persistent, quasi-stationary vortex in the low-level wind field is anchored to the Borneo coast. In another study, Houze et al. (1981) and Johnson and Priegnitz (1981) showed that the winter monsoon convection that produced heavy rainfall off the coast of Borneo was not only affected by the oscillation of the low-level land-sea breeze, but also increased its activity with the presence of the Borneo vortex and northeasterly cold surge. Without the vortex, the low level northeast monsoon winds would produce subsidence where convection is suppressed. Apart from the cold surge, Mower et al. (1984) found that the topography of Borneo, Peninsular Malaysia and Sumatra play an important role in the formation and intensification of the vortices, as Cheang (1977) pointed out beforehand.

After a lot of aggressive work was done in the 70's and 80's, the study of Borneo vortex eventually came to an end. No new research had been explored until the new millennium emerged due to the surprise formation of Typhoon Vamei adjacent to the Malaysian region on 27 December 2001. The study by Chang et al. (2003) revealed that the development of this typhoon was a result of

two interacting systems, a weak Borneo vortex that drifted into the southern tip of the South China Sea and remained there for four days, and a strong and persistent cold surge that created a large background cyclonic vorticity at the equator. Statistically, they hypothesized that the probability of a similar equatorial development is estimated to recur once in every 100 to 400 years.

As a consequence of this unique event, scholars began to give more attention to the vortex once again. Chang et al. (2005b) found that the vortex helps to divert low-level moisture from the regions of Sumatra and southern Peninsular Malaysia to western and southern parts of Borneo during the presence of cold surge. Although the interaction between the vortex and strong cold surge results in the largest and most intense region of deep convection over the west coast of Borneo, the strong northeast monsoon winds cause a shift of the vortex center such that much of the vortex lies over Borneo inland rather than over the water body of South China Sea. For this reason, the development and organization of the vortex into a tropical storm is impossible, except for few occasions. However, without the presence of the vortex, the region of deep convection shifts southward towards Java and northern Australia.

Many studies have shown that the presence of a cold surge in Malaysian region tends to increase the strength of the Borneo vortex. However, further analysis by Chang et al. (2005b) demonstrates that the presence of the Madden Julian Oscillation (MJO) in this area also has a noticeable effect on both the cold surge and vortex appearance. The frequency of surges is reduced during periods

when the MJO is present. Often the MJO-scale circulation pattern directly opposes the cold-surge wind pattern. Therefore, weak surges may be more inhibited during periods when the MJO-scale circulations are strong.

Due to primary impact of the MJO on cold-surge intensity and vortex frequency, more Borneo vortices form during non-MJO periods. In this study, they also found that during periods when the active convection portion of the MJO is passing over the Malaysian region, the occurrence of the vortex may be more related to the cyclonic shear to the north of anomalous equatorial westerlies rather than the northeasterly monsoon wind. This could be related to what Sadler (1967) had suggested in his earlier study on the origin of this equatorial vortex.

During the 2006/07 winter monsoon season, southern Peninsular Malaysia was inundated by the worst flood ever experienced within this area in a century. According to Tangang et al. (2008), one of the reasons behind this devastating episode was due to the absence of the Borneo vortex. Instead of generating a strong counter-clockwise turning of the northeasterly winds in the presence of the Borneo vortex to enhance the convection over western and southern parts of Borneo, its absence inhibited low-level moisture from being transported over the west coast of Borneo and reduced deep convection in this area.

As a result, the northeasterlies penetrated anomalously far south from their normal position in a straight trajectory and formed deep convection that

dumped the heavy rainfall and spawned major flooding over southern Peninsular Malaysia due to the blocking effect of the elevated terrain of Sumatra. They found that the absence of the vortex was associated with the enhanced of easterly winds over north Java owing to the formation of MJO deep convection in the Indian Ocean region and hence prohibited the counter-clockwise turning to take place.

Apart from the synoptic and dynamics features of this vortex that have been explored, Juneng and Tangang (2010) take a different approach by studying the long-term trends of the vortex between 1962 and 2007. In their analyses, they found that the frequency of vortex occurrences had increased throughout the study period. Also, the trend shows a significant northward shift of the latitudinal position of the vortex center towards the open sea, which then could modify the life cycle of the vortex because of less intense vortex-land interaction. Through this finding, they hypothesize that the shift of the vortex center is due to the intensification of the easterly component of the northeasterly cold surge in this region, which could result in weaker steering of the vortex further south towards the Borneo land mass. Due to this flow alteration, the vortex system remained longer over the water body, which thereafter leads to more vortex day counts.

After examining most of previous work conducted by many researchers related to this field, it appears that very little effort has been devoted to study the climatological aspects of these vortices. Looking at the work initiated by Juneng

and Tangang (2010), there is still ample room to explore in order to further understand the climatological behaviors of the Borneo vortex in addition to its dynamics and synoptic features.

1.2 Study objectives

It has been realized that the presence of Borneo vortex over the Malaysian region creates a great impact in terms of the rainfall distribution throughout the country during the winter monsoon season. Therefore, it is important to comprehend the vortex climatology characteristics so that Malaysian meteorologists, particularly, can make use of the outcome of these works and generate better forecasting for the safety of general public. Owing to that, the goal of this study is to identify and investigate the climatological behaviors of the Borneo vortex in further depth. In order to achieve this goal, several objectives need to be set, i.e.:

- a) To pinpoint the presence of Borneo vortices within a designated domain during Northern Hemisphere winter monsoon between 1970/71 and 2010/11 seasons based on the criteria set by previous works. Instead of using re-analysis data from National Center for Environmental Prediction (NCEP) as were done in all the former studies related to these vortices, this study is going to apply re-analysis data provided by European Centre for Medium-range Weather Forecasts (ECMWF) due to its higher resolution products.

- b) To sort the vortices into respective seasons and months in accordance to their frequency, location, intensity, lifespan, and onset and retreat dates upon identifying their existence. Once everything is in place, statistical and time-series analyses are performed using the standard statistical tools in order to describe their long-term climatological behaviors.

- c) To apply a Fourier transformation onto the seasonal distribution of all the Borneo vortices aspects in order to detect significant signals of interannual and/or interdecadal variability that may exist and match them with the periodicity of any existing global natural climate oscillations, such as El-Nino Southern Oscillation (ENSO), Tropospheric Biennial Oscillation (TBO), Quasi-Biennial Oscillation (QBO) and Pacific Decadal Oscillation (PDO), using the conventional compositing analyses technique.

- d) To perform case studies of random Borneo vortices of different intensities in order to understand the dynamic and synoptic behaviors and features that differentiate among them.

In regard to all the goal and objectives, we hypothesize that, within the study domain, the interannual and interdecadal variability of the seasonal Borneo vortex frequency, location, lifespan, intensity, and onset and retreat dates during the boreal or Northern Hemisphere winter monsoon emulates certain tropical climate oscillations.

CHAPTER 2

Methodology

2.1 Study domain

There is no specific definition with regards to the region where the Borneo vortex should be confined. Chang et al. (2005b) set a domain of 2.5°S–7.5°N latitude and 107.5°E–117.5°E longitude in order to search for this vortex, while Juneng and Tangang (2010) considered all vortices formed within 5°S-15°N latitude and 98°E-120°E longitude as Borneo vortex. As for this study, the domain is set between 2.5°S and 7.5°N latitude, and 102.5°E and 117.5°E longitude, as depicted in Fig. 2.1.1, which is slightly bigger than the one established by Chang et al. (2005b).

This domain was chosen because it represents the area with higher density of vortex occurrences as observed by earlier researchers. The area is also within the center of action between the vortex and the northeasterly cold surge that has been investigated to further enhance the vortex intensity. In addition, all the studies related to the impact of this vortex conducted by previous scholars are found to be limited within this area, such as Cheang (1977, 1978),

Houze et al. (1981), Johnson and Zimmerman (1987), Chang et al. (2003, 2005b), Tangang et al. (2008), and Juneng and Tangang (2010).



Fig. 2.1.1: Domain of the study area to determine the Borneo vortices bounded by 2.5°S and 7.5°N latitudes and 102.5°E and 117.5°E longitudes.

2.2 Data

For this work, the 0000 UTC reanalysis wind data obtained from ECMWF were used to identify the existence of Borneo vortices within the focus region during Northern Hemisphere winter monsoon events between 1970 and 2010 beginning on 1st of November until 28th or 29th of February of the following year for each season. Only data at the 925 hPa pressure level were chosen because the vortices have been known to form at low tropospheric levels (Gray (1975),

Cheang (1977), Johnson and Priegnitz (1981), and Chang et al. (2005b)). The data can be easily retrieved through the ECMWF website at <http://data-portal.ecmwf.int>. ECMWF is an intergovernmental organization supported by 34 European countries, centered in Reading, United Kingdom. It has been recognized by most meteorological communities as one of the best meteorological centers in the world that generates numerical weather products for operational and research purposes.

Ever since the ECMWF began its operation in early 1980's, it has produced three different types of operational global atmospheric reanalysis data namely ERA-15, ERA-40 and ERA-Interim. The ERA-15 provides the reanalysis data between 1979 and 1993, ERA-40 between 1957 and 2002, and ERA-Interim, i.e. the latest product among them, is an 'interim' reanalysis of the period 1989 till present in preparation for the next-generation extended reanalysis (Simmons et al., 2007). Since these works are focusing on Borneo vortex events that form between 1970/71 and 2010/11 winter monsoon seasons, only the reanalysis data produce by ERA-interim and ERA-40 were engaged here.

ERA-Interim is an improved version of ERA-40. The number of its pressure levels increased from ERA-40's 23 to 37 levels and additional cloud parameters are also included. It has a better horizontal grid resolution of 1.5° X 1.5°, which is one of the finest among the operational global atmospheric reanalysis system currently available, while ERA-40 grid resolution is only 2.5° X 2.5°. Other advances in the ERA-Interim data assimilation over the ERA-40

system are: 12 hour four-dimensional variational assimilation (4D-Var), better formulation of background error constraint, new humidity analysis, improved model physics, quality control of data drawing on experience from ERA-40, variational bias correction of satellite radiance data, improvements in radiosonde temperature and surface pressure bias handling, more extensive use of radiances, and improved fast radiative transfer model and assimilation of rain affected SSM/I (Special Sensor Microwave/Imager) radiances through 1D-Var (Simmons et al., 2007).

Even though the ERA-Interim provides the best data set for this study, which may represent the actual atmospheric condition at any chosen time, the data are only available from 1989 onwards. Since the study required data for 41 winter monsoon events started from 1970/71 season, part of the data set will be obtained from ERA-40. Thus, reanalysis data of ERA-40 cover the winter monsoon events from 1970/71 to 1988/89 seasons while ERA-Interim (Version 1.0) provide the data from 1989/90 onwards.

2.3 Procedure

The data obtained from ECMWF were in a network Common Data Form (netCDF) format, i.e. a special format that has been adopted for earth, ocean, and atmospheric sciences studies. This kind of data format can only be read and manipulated by limited number of software packages. The one used for this study is known as Integrated Data Viewer (IDV). It is free software provided by Unidata

program center of University Corporation for Atmospheric Research (UCAR) through its website at <http://www.unidata.ucar.edu/software/idv>. Once the data are in a readable format, the next step is to try to identify the Borneo vortices within the domain throughout the study period.

The method applied here to locate a Borneo vortex was based on earlier work done by Chang et al. (2003 and 2005b), which also has been used by Juneng and Tangang (2010). The vortex is established whenever there is a closed cyclonic circulation on the 0000 UTC 925 hPa wind field of the ECMWF reanalysis data within the study domain set in Fig. 2.1.1. In addition, the wind speed should be at least 2 ms^{-1} or more in any segment of the $2.5^\circ \times 2.5^\circ$ grid square within which the center circulation was located.

Once both requirements were fulfilled, the circulation was considered as a Borneo vortex. All the information of each of the vortices was then documented, which includes the date of its occurrences and the location of the vortex center, as pinpointed at the center of the closed cyclonic circulation of the streamlines analysis analyzed by the IDV, in the form of its latitude and longitude position. By doing so, one can discover not only the total number of vortices, but also its commencement and retreat dates from the study domain.

In addition to treating the vortices as individual entities, this study has also examined them in groups, named as systems. A system was determined to exist when a Borneo vortex was first identified and remained stationary or moved from its original position in the next observation time until it finally decayed. All these

actions should take place within the study domain. For the case of vortices that were first formed outside the domain and then move into it, the establishment of such systems begins as soon as the vortex enters the study domain. The arrangement was the same as for the case of the last vortex before the system vanishes. Once a vortex moves out from the domain, the system was considered dissipated. Through this method, the information that was gained not only provides the number of Borneo vortex systems throughout the study period, but one can also infer the lifespan of each system.

As mentioned earlier, the identification of the Borneo vortices was done by using the wind field. Through this field, the vortex intensity was classified according to the wind speeds that wrap the vortex center. The intensity of the Borneo vortices was considered as weak if all the wind speeds within $2.5^\circ \times 2.5^\circ$ grid square from the vortex center were 5 ms^{-1} or less. If any portion of the grid square had a wind speed greater than 5 ms^{-1} , but less than or equal to 10 ms^{-1} , the vortices were categorized as moderate, while vortices of strong intensity were generated by the wind speed greater than 10 ms^{-1} .

Once all the data had been congregated, they were then arranged according to seasons and months. The next step was to perform the traditional statistical analyses found in many standard textbooks, such as Neter et al. (1993). The time-series analyses were carried out in order to determine the long-term trends of the events. Subsequently, their interannual and interdecadal

variability was identified through the method of power-spectrum analysis via a fast Fourier transform (FFT) algorithm.

The Fourier analysis is a decomposition of the time series events into a sum of sinusoidal components, i.e. a mathematical method for transforming a function of time into a function of oscillation or cycle (Bloomfield, 2000). The method is commonplace in the study of Earth sciences and has greatly enhanced our understanding and forecast capabilities for cyclical phenomena that recur on interannual, interdecadal and millennial scales, such as El Nino Southern Oscillation (ENSO), Quasi-Biennial Oscillation (QBO), Pacific Decadal Oscillation (PDO) and Milankovitch cycles (Brooks, 2011). Unfortunately, this method filters out the signal induced by smaller timescale phenomena, such as Madden-Julian Oscillation (MJO), hence making it beyond the scope of this research.

In these analyses, the FFT was calculated with advanced math tool software, known as Mathcad. The outcomes were in complex numbers. Owing to that, the modulus function was applied before the final values were plotted on a graph. Since the energy transported by the wave is proportional to the square of the amplitude or magnitude, and therefore, the power spectral density is the square of the modulus of the Fourier transform.

Any significant peaks that were found on the graph will represent the number of oscillations or cycles of the explored Borneo vortex aspects throughout the study period, which could be associated with the atmospheric oscillations cause by ENSO, QBO and/or PDO. Afterwards, the seasonal data of

that particular aspect will be sorted accordingly to match the variability of those atmospheric events in order to detect any feedbacks. This could be done through standard statistical analyses known as compositing analyses technique. The outcomes were tested for significance, which could be found in many standard statistics textbooks, such as Neter et al. (1993).

2.4 Climate Variability

In the tropics there are several oscillations that are known to cause the variation to the climate patterns as a result of different intraseasonal, interseasonal, interannual and interdecadal timescales. However, the type of climate variability that has been discussed in these works was restricted only to PDO, ENSO, QBO and TBO events due to the limitation of FFT spectral method as stated earlier. Furthermore, those climate oscillations are believed to play a vital role in governing the interannual and interdecadal variability of the climatology of the Borneo vortex over the study region. Before we proceed to the next chapter, each of the climate oscillations needs to be defined and explained first prior to analyzing and discussing all the results.

2.4.1 Pacific Decadal Oscillation (PDO)

The term PDO was first coined by a Fisheries scientist, Hare (1996) while researching the connections between Alaska salmon production cycles and

Pacific climate that he believed to persist every 20-to-30 years. However, it was later redefined by Mantua et al. (1997) and Minobe (1997) as a 50 to 70 year sea surface temperature (SST) variation within the Pacific Ocean Basin. Gershunov and Barnett (1998) called this oscillation the North Pacific Oscillation and its positive (warm) phase is characterized by an anomalously deep Aleutian low, cold western and central North Pacific waters, warm eastern Pacific coastal water, and warm central and eastern tropical Pacific waters, while the reverse conditions characterized the negative (cool) phase. In addition, Lupo and Johnston (2000) referred the warm phase as PDO1 and cold as PDO2.

Based on those conditions, PDO2 was observed to take place from 1947 to 1976, and then switched to PDO1 between 1977 and 1998. In 1999, it was believed to switch phase again into PDO2 and remained as it is to the present as discussed by many scholars, such as Kerr (1999), Houghton et al. (2001), Lupo et al. (2007) and Birk et al. (2010). The summary of those periods is shown in Table 2.4.1 below, where 22 seasons of the study period are found to be in cold phase while the remaining falls under PDO1 period.

PDO Phase	Period
PDO2 (Cold)	1947 - 1976
PDO1 (Warm)	1977 - 1998
PDO2 (Cold)	1999 – present

Table 2.4.1: Periods of the PDO phases from Lupo et al. (2007).

2.4.2 El Nino Southern Oscillation (ENSO)

The ENSO is commonly known as El Nino. According to Trenberth (1997), the term El Nino originally applied to an annual weak warm ocean current that ran southward along the coast of Peru and Ecuador about Christmas time and only subsequently became associated with the unusually large warmings that occur every few years (i.e. considered to be 3 to 7 years by many scientists based on its recurrence time period) and change the local and regional ecology.

The coastal warming, however, is often accompanied by a much more extensive anomalous ocean warming to the International Date Line, and it is this Pacific basinwide phenomenon that forms the link with the anomalous global climate patterns. The atmospheric component tied to El Nino is termed the Southern Oscillation. Scientists often call the phenomenon where the atmosphere and ocean collaborate together as ENSO. El Nino (EN) then corresponds to the warm phase of ENSO. The opposite La Nina (LN) phase consists of a basinwide cooling of the tropical Pacific and thus the cold phase of ENSO.

From the above definition, lots of researchers have come out with different type of indices to determine and measure the ENSO years and intensity. For this study, the index issued by Japan Meteorology Agency (JMA) was preferred. A complete list and the detailed description of the JMA ENSO index can be found at the Center for Ocean and Atmospheric Prediction Studies (COAPS) website at <http://coaps.fsu.edu/jma.shtml>.

Briefly, the index classifies a year as EN, LN and neutral (NEU) based on the five month running-mean of spatially averaged sea surface temperature anomaly over the tropical Pacific Ocean bounded by the area of 4°N, 4°S, 150°W and 90°W. The index values used to define EN years are those equal or greater than +0.5°C for six consecutive months including October, November, and December, and then the ENSO year of October through September in the following year is categorized as EN year. If the index values are equal or less than –0.5°C, it is categorized as a LN year and a NEU year for the remaining values. Based on all these requirements, the list of the ENSO years covered for this study is given in Table 3.1.6, in which 21 seasons happened to be in NEU years, while 10 times apiece in LN and EN periods.

EI Nino	La Nina	Neutral
1972		
1976		1977-1981
1982	1970-71	1983-85
1986-87	1973-75	1989-90
1991	1988	1992-1996
1997	1998-99	2000-01
2002	2007	2003-05
2006	2010	2008
2009		

Table 2.4.2: Years of ENSO phases according to JMA definition taken from <http://coaps.fsu.edu/jma.shtml>.

2.4.3 Quasi-Biennial Oscillation (QBO)

As described by Reed et al. (1961), QBO is a remarkably regular oscillation of the zonal wind between easterlies and westerlies in the equatorial

stratosphere with a mean periodicity of about 28 to 30 months (2 to 2.5 years). During one half of this period, easterlies propagate from upper stratosphere to lower stratosphere and during the other half they are replaced by westerly winds. The alternating wind regimes develop at the top of the lower stratosphere and propagate downwards at about 1 km per month until they are dissipated at the tropical tropopause.

Therefore, this zonal wind as well as its temperature anomalies does not penetrate significantly below the tropopause (Baldwin et al., 2001). Because of that behavior, the impact of QBO oscillation toward the climate variability over the tropics has been nominal. The most promising connection was found in the interannual variation of Atlantic hurricane activity studied by Gray (1984) where it tends to be active and stronger when the overlying QBO is westerly and less active and weaker during the opposite phase.

Generally, the QBO phases can be quantified from the zonal component of the wind vector over the tropics using the upper atmospheric data at 30 hPa or 50 hPa levels. For this study, we established those phases by using the 30 hPa level data of mean monthly zonal wind observed at Gan Island/Maldives (1970 to 1975) and Singapore (1976 to 2011) radiosonde stations. The data could be retrieved from the website of Institute of Meteorology, University of Berlin at <http://www.geo.fu-berlin.de/en/met/ag/strat/produkte/qbo/index.html>.

The seasonal phases were determined based on the average of mean monthly zonal wind speed for November until February in order to match the

winter monsoon season studied here between 1970/71 and 2010/11. Through this procedure, the seasons turn out to be either in easterly or westerly phase, which make the analyses more straightforward and easy to understand. Finally, the list of the QBO phases was established as in Table 2.4.3 given below, which demonstrates that 21 out of 41 seasons are in the easterly phase while the remaining are westerly.

West QBO		East QBO	
2010/11	1987/88	2009/10	1989/90
2008/09	1985/86	2007/08	1988/89
2006/07	1984/85	2005/06	1986/87
2004/05	1982/83	2003/04	1983/84
2001/02	1980/81	2002/03	1981/82
1999/00	1978/79	2000/01	1979/80
1998/99	1977/78	1997/98	1976/77
1994/95	1975/76	1996/97	1974/75
1992/93	1973/74	1995/96	1972/73
1990/91	1971/72	1993/94	1970/71
		1991/92	

Table 2.4.3: Seasons of QBO phases.

2.4.4 Tropospheric Biennial Oscillation (TBO)

The TBO as defined by Meehl (1997) is the tendency for a relatively strong monsoon to be followed by a relatively weak one, and vice versa, with the transitions occurring in the season prior to the monsoon involving coupled land–atmosphere–ocean processes over a large area of the Indo-Pacific region. The condition of strong or weak convection over India and Indo-China during the

summer monsoon persists over the Maritime Continent, which include the study domain, and Australian monsoon region in the succeeding autumn and winter, following the seasonal migration of the convective center.

Its signals have been detected in a form of rainfall patterns in association with sea level pressure and SST conditions over India (Meehl (1987) and Yasunari (1990)), Indonesia (Yasunari and Suppiah, 1988), East Asia (Chang and Li, 2000) and Australia (Meehl and Arblaster, 2002). According to Meehl (1987), the periodicity of this oscillation is 2 to 3 years, which is about the same return period as the QBO event. However, it is surprising to know that there is no official list of TBO years based on its phases similar to the one established for the case of ENSO, PDO and QBO events.

Since a lot of studies use rainfall amount as the main indicator to determine the monsoon intensity, the same approach has been adopted here in order to quantify the TBO phases over the study region. The rainfall data from Kuching weather observation station, which is located roughly at the center of study domain at 1.5°N latitude and 110.3°E longitude as shown in Fig. 2.1.1, have been selected to run these analyses. With respect to its location, this station seems to be the most ideal site to represent the study domain as to quantify the TBO phases.

The rainfall data were obtained from Monthly Climatic Data for the World publication, which could be retrieved online from the National Climate Data Center website at <http://www7.ncdc.noaa.gov/IPS>. By summing up all the

monthly rainfall from November to February for each winter monsoon season, it gave the total amount for each respective season throughout the study period. The winter monsoon is considered relatively strong if the rainfall amount for that season is greater than the previous one and weak if the amount is less.

The method used here seems to be simplistic and straightforward, and does not adequately characterize the episodic nature of year-to-year variations of this event. However, the same approach has also been applied by previous scholars like Fasullo (2004). Throughout the study period, it was found that there were 21 seasons of relatively strong winter monsoon, which could be associated with strong TBO phase, while the remaining 20 seasons were relatively weak as listed in Table 2.4.4 below.

Strong TBO		Weak TBO	
2008/09	1988/89	2010/11	1989/90
2007/08	1987/88	2009/10	1986/87
2006/07	1985/86	2005/06	1984/85
2003/04	1983/84	2004/05	1982/83
2001/02	1981/82	2002/03	1980/81
1999/00	1979/80	2000/01	1978/79
1998/99	1976/77	1996/97	1977/78
1997/98	1975/76	1993/94	1974/75
1995/96	1973/74	1992/93	1972/73
1994/95	1970/71	1990/91	1971/72
1991/92			

Table 2.4.4: Seasons of TBO phases.

CHAPTER 3

Climatological results and discussions

Following the methods described in the previous chapter, all the necessary information related to the establishment of the Borneo vortex that fulfill the requirements set for these studies during the Malaysian winter monsoon between 1970/71 and 2010/11 seasons were documented and discussed accordingly.

3.1 Borneo vortex frequency

After analyzing all the 925 hPa daily wind fields throughout the study period, it turns out that not all the vortices were generated within the study domain. There are also cases where the vortices originated outside the domain before they managed to move into it. For such events, any vortex that was found to develop over the western Pacific and move all the way into the domain will not be considered as one of the Borneo vortices. This is because the vortex should be the one that is formed within or adjacent (i.e. within 2.5° from the domain's

border) to the study domain set in Fig. 2.1.1. Besides this restriction, there were several cases in the month of November, where the vortices formed as a result of southwesterly wind flow prior to the onset of winter monsoon season. As for this type of formation, it was also not considered as a Borneo vortex since the defined vortex is supposed to be the one that is generated owing to the prevailing winds with respect to winter monsoon events, i.e. either easterly or northeasterly.

By taking all these restrictions into consideration, 2,278 vortices have been recognized as Borneo vortices and were used for further analyses throughout this study. The vortices were then summarized and tabulated, as in Table 3.1.1, according to their respective month and season that they were formed. The outcomes show a wide range of variation during the seasons where the highest number of vortices are observed in 1971/72 and 1983/84 seasons with 74 occurrences while 1997/98 season records the lowest quantity with 32 vortices. On average, 55.6 vortices are generated in each winter monsoon season as calculated in Table 3.1.2, which would be considered as the long-term seasonal mean of this study.

The vortex seasonal frequency was then transformed into a time-series graph, as depicted in Fig. 3.1.1, which displays a vigorous fluctuation pattern from one season to another. It clearly indicates that the vortex frequency may have significant interannual and/or interdecadal variability in their seasonal distribution. The studies by Juneng and Tangang (2010) show that the vortex frequency has a significant linear upward trend with an increased rate of about

Season	Nov	Dec	Jan	Feb	Frequency
2010/11	9	20	12	7	48
2009/10	18	18	8	4	48
2008/09	17	29	19	8	73
2007/08	5	22	13	10	50
2006/07	8	23	25	9	65
2005/06	11	11	20	16	58
2004/05	10	17	10	6	43
2003/04	13	16	13	2	44
2002/03	13	9	14	5	41
2001/02	11	17	10	9	47
2000/02	10	14	19	9	52
1999/00	13	22	14	18	67
1998/99	10	15	17	11	53
1997/98	12	10	5	5	32
1996/97	6	20	10	14	50
1995/96	16	15	17	16	64
1994/95	8	20	8	2	38
1993/94	14	12	13	7	46
1992/93	26	14	6	5	51
1991/92	22	22	4	2	50
1990/91	4	15	8	7	34
1989/90	20	13	13	1	47
1988/89	13	13	12	15	53
1987/88	9	26	19	8	62
1986/87	11	12	10	6	39
1985/86	16	22	12	9	59
1984/85	10	26	16	13	65
1983/84	9	24	21	20	74
1982/83	8	21	11	5	45
1981/82	11	19	14	10	54
1980/81	12	26	13	14	65
1979/80	24	17	16	13	70
1978/79	19	23	10	10	62
1977/78	13	21	13	8	55
1976/77	24	20	15	13	72
1975/76	21	19	18	10	68
1974/75	13	18	23	18	72
1973/74	14	24	12	18	68
1972/73	14	15	18	7	54
1971/72	19	27	17	11	74
1970/71	14	15	22	15	66
Total:	550	762	570	396	2,278

Table 3.1.1: Monthly and seasonal frequencies of Borneo vortices during Malaysian winter monsoon periods between November and February for 1970/71 to 2010/11 seasons.

7% per decade between 1962 and 2007 winter monsoon seasons. However, the result found in this work was the opposite. This disparity could possibly be due to different kinds of data sources and criteria set in both works, which include the domain, number of seasons and duration of winter monsoon periods. It could also be a result of the choices of time periods used.

	All	Nov	Dec	Jan	Feb
No. of seasons	41	41	41	41	41
Total vortices	2,278	550	762	570	396
Vortex average	55.6	13.4	18.6	13.9	9.7

Table 3.1.2: The seasonal and monthly averages of Borneo vortex frequency.

The linear regression line in Fig. 3.1.1 demonstrates that the tendency of the vortex frequency follows a downward slope, which suggests that the seasonal number of vortices is decreasing from one season to another throughout this study period. However, the trend is statistically insignificant based on the R-Squared (R^2) value of 0.1995, which indicates a weak correlation between the trendline and the seasonal vortex frequency. The R^2 value nearly doubles to 0.3639 when their relationship is measured using a 4th order polynomial regression line, which suggests that the polynomial trendline is the better-fit line for determining the long-term trend of the seasonal Borneo vortex frequency for these analyses.

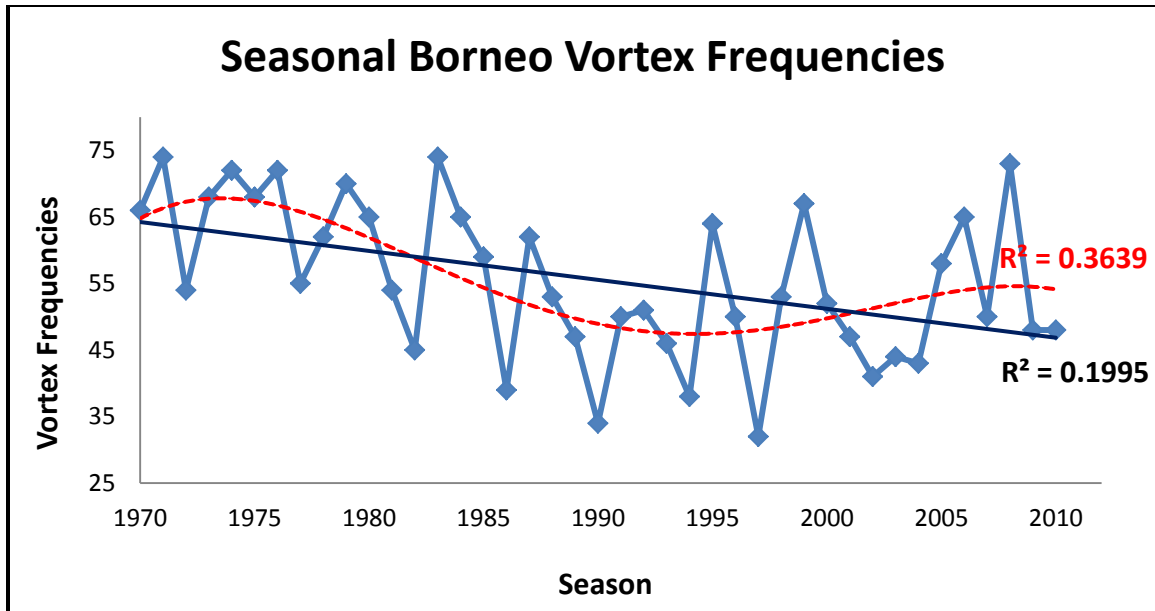


Fig. 3.1.1: Seasonal Borneo vortex frequency for 41 winter monsoon between 1970/71 and 2010/11 seasons. The red-dashed line is the 4th order polynomial trendline and the black line is the linear trendline of the vortex frequency.

The polynomial line has one convex curve at the middle and two partly-concaves slopes at the beginning and the end of the study period that tends to follow the pattern of PDO variability. Additional information about PDO can be found in section 2.4.1. The polynomial trendline shows that more Borneo vortices are generated during the cold PDO periods that happen prior to 1976 and from 1999 onward, while the number declines during the warm PDO phase that occurred between 1977 and 1998. Further analyses about this relationship will be explored later in this section together with the influence of other natural climate oscillations.

In terms of their total monthly distribution, the information gained from Table 3.1.1, Table 3.1.2 and Fig. 3.1.2 reveals that the highest number of

vortices is observed in December with a total of 762 occurrences, which represents 33.5% of the entire events. It is followed by January with 570, November with 550 and February with 396 vortices, which are equivalent to 25.0%, 24.1% and 17.4% of all vortices, respectively.

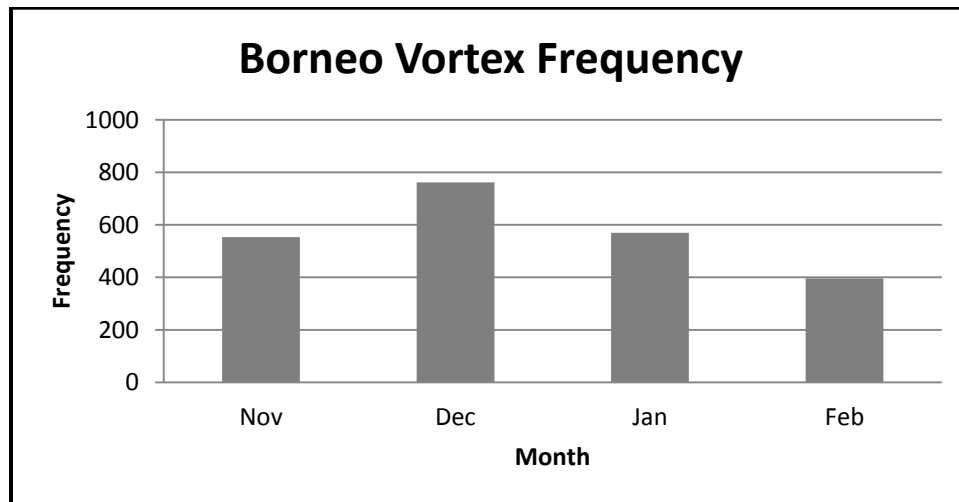


Fig. 3.1.2: Monthly total of Borneo vortex frequency throughout 41 winter monsoon seasons.

Based on the long-term mean of 55.6 Borneo vortices per season, the domain monthly average is calculated to be 13.9 vortices. However, the records in Table 3.1.2 reveal that the month of November documented 13.4 vortices per season, 18.6 in December, 13.9 in January and 9.7 in February. This shows that the number of Borneo vortices monitored in December is far greater than any other monthly average, while during November and January, their averages are about the same as the long-term mean quantity. As for February, its average is far below the long-term mean. Therefore, according to these analyses, the busiest month for the arrival of Borneo vortices over this region is in December, followed by January, November and February, respectively.

A study by Chang et al. (2005b) on the monthly mean convection over this region between December and February demonstrates that it is very active in December and became less energetic as the winter monsoon progresses. Since the formation of any vortex is always associated with convective processes, the results found here match well with their findings. December is also known to be the most active period in this winter monsoon based on its rainfall amount. This implies that the more vortices develop in this area, the more active the monsoon should become, which later could lead to greater rainfall distribution throughout this region. The relationship between the presence of these vortices and the amount of rainfall produced have been discussed by many scholars, such as Cheang (1977), Houze et al. (1981), Johnson and Priegnitz (1981), Chang et al. (2005a) and Tangang et al. (2008).

In general, out of 2,278 vortices that have been identified throughout the study period, each vortex tends to form on a different day except for 19 cases in which two vortices were found to appear within the same day. Those events were discovered to occur only during winter monsoon active months, i.e. 12 cases in November while the remaining occurred in December. One example of such cases is shown in Fig. 3.1.3, which took place on 7 December 2008. Owing to these types of cases, out of 4,930 days that cover the whole study period of 41 winter monsoon seasons between November and February, it turns out that the Borneo vortices were found on 2,259 different days, which accounting for almost 46% of the total timespan of the study period, as summarized in Table 3.1.3.

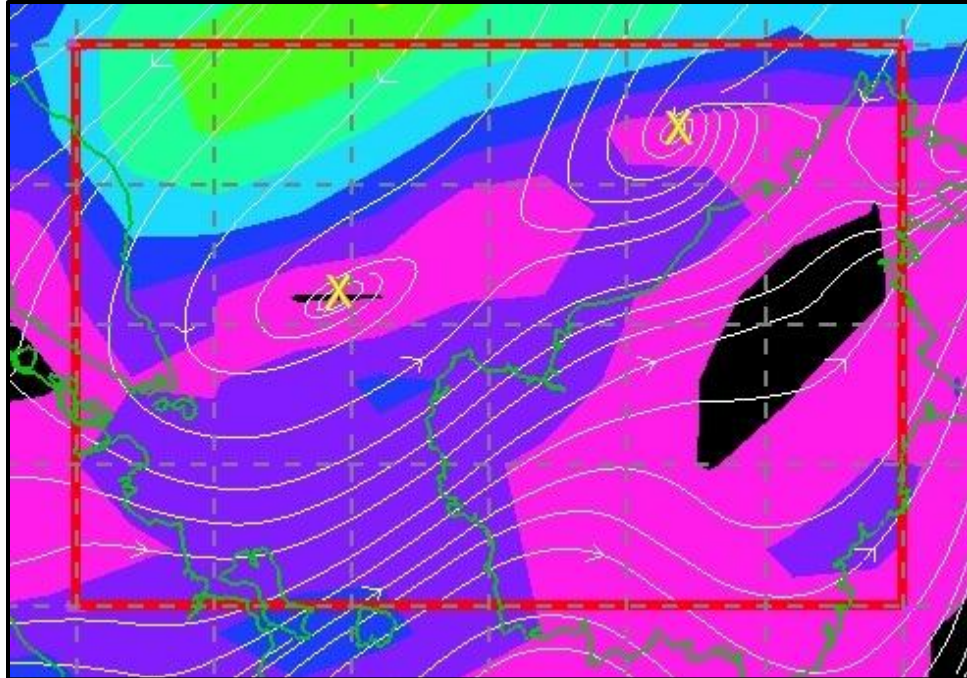


Fig. 3.1.3: An event where two Borneo vortices were observed at 0000 UTC on 7 December 2008. The vortex centers are marked as yellow 'X'. The white lines with arrows are the streamlines of the wind flow and the color-shaded areas indicate the wind speed of 2 ms^{-1} or greater.

	All	Nov	Dec	Jan	Feb
Total days (a)	4,930	1,240	1,271	1,271	1,158
Total days with vortex (b)	2,259	548	755	570	396
Average in percentage (b)/(a)	46%	44%	59%	45%	34%

Table 3.1.3: Total number of days that Borneo vortices were observed during winter monsoon between November and February for 1970/71 and 2010/11 seasons.

This percentage indicates that the probability for the vortices to form in this region is considerably high. Because of this tendency, the Borneo vortex has been considered as a persistent feature of Malaysian winter monsoon (Johnson and Houze, 1987). A study by Chang et al. (2004b) reveals that the number of

convective vortices in this region is the most compared to any other regions within the equatorial belt of the Asian-Australian monsoon area due to the effective interaction between northeasterly winds and the surrounding terrain. However, the number of days with a vortex that has been identified here is much higher than Chang et al. (2005b) discovered in their work, which encompassed only 33% of the season as compared to 46% here. This large disparity is possibly due to different sources of data and criteria set in both studies, which include the domain, number of seasons and period of winter monsoon event.

In terms of individual months as itemized in Table 3.1.3, the number of days in December has been observed as having more Borneo vortices than any other months of winter monsoon season over this region. Out of 1,271 total days, the vortex has occurred on 755 different days, which covered 59% of the December timespan. Subsequently, it was followed by the months of November and January came out with almost similar percentage, i.e. 44% and 45%, apiece, from 548 and 570 total days with vortices in each respective month. While the lowest number of days having Borneo vortices was monitored in February. Out of 1,158 total days, the vortices were found only on 394 days, about 34% of February timespan.

Based on these analyses, it is shown that the greatest chance for any observation within the study domain to encounter Borneo vortex during winter monsoon is in December. For this reason, most of the case studies and experiments related to this vortex were done in the month of December, such as

Winter MONEX experiment (Greenfield and Krishnamurti, 1979) and work of Cheang (1977 and 1978) and Chang et al. (1979 and 1980). Additionally, this month has also been considered as the most active winter monsoon period according to studies by Cheang (1987), Chang et al. (2005b), etc., possibly due to more days of having Borneo vortices. If this is the case, therefore, after the month of December, the sequence of the most active period for winter monsoon should be followed by January, November and finally February.

Referring to Fig. 3.1.1, it appears that the long-term polynomial trend of seasonal numbers of Borneo vortex exhibits a pattern that is similar to the PDO oscillation. Therefore, further analyses were done here by applying the compositing analyses technique, i.e. by separating the seasonal data in Table 3.1.1 according to respective PDO phases listed in Table 2.4.1. Subsequently, the numbers were totaled and averaged accordingly before being summarized in Table 3.1.4. The outcomes show that, on average, 53.1 vortices are formed seasonally during PDO1 phase while the number is relatively greater in the course of PDO2 with 58.4 vortices per season when compared to the long-term mean, which matches with the curve regression line displayed in Fig. 3.1.1.

This variation implies that PDO2 has a tendency to enhance the development of the Borneo vortex in this region, and hence increase its frequency, while the impact of PDO1 is likely to be the opposite. Taking the assumption that the data are normally distributed, the means were tested for significance using a simple two-tailed p-value from t-test since the sample sizes

are relatively small ($N < 30$), as suggested in Neter et al. (1993). The results show that the seasonal mean of both PDO phases are statistically insignificant compared to the vortex long-term mean as shown in Appendix A.

	All	PDO1	PDO2
No. of seasons	41	22	19
Total vortices	2,278	1,168	1,110
Vortices per season	55.6	53.1	58.4

Table 3.1.4: The seasonal averages of the Borneo vortex frequency stratified by PDO phases.

Besides the PDO, there are probably other natural climate oscillations that might also influence the variability of the Borneo vortex frequency throughout the study period over this region. They could be determined through the method known as power-spectral analysis by transforming the time series data in Table 3.1.1 into cyclical series using the FFT algorithm as described in Section 2.3. The final outcomes of this transformation were materialized in a periodogram presented in Fig 3.1.4 after filtering out the first and the last peaks of the power-spectrum in order to avoid confusion in interpreting the spectra gained here.

The significance of the power-spectral was then tested at the 95% confidence level against a white-noise background. The results show that the spectra has a very prominent peak at cycle number 10, which indicates that the seasonal Borneo vortex frequency has variability with a return period of 4 years. At present, the only natural event over the tropics that has a cycle of such period

is the ENSO. At 80% confidence level, more peaks related to ENSO were detected, i.e. at cycle number 6 and 13, which are associated with the recurrence period of about 7 and 3 years, respectively (General description about ENSO had been discussed in section 2.4.2).

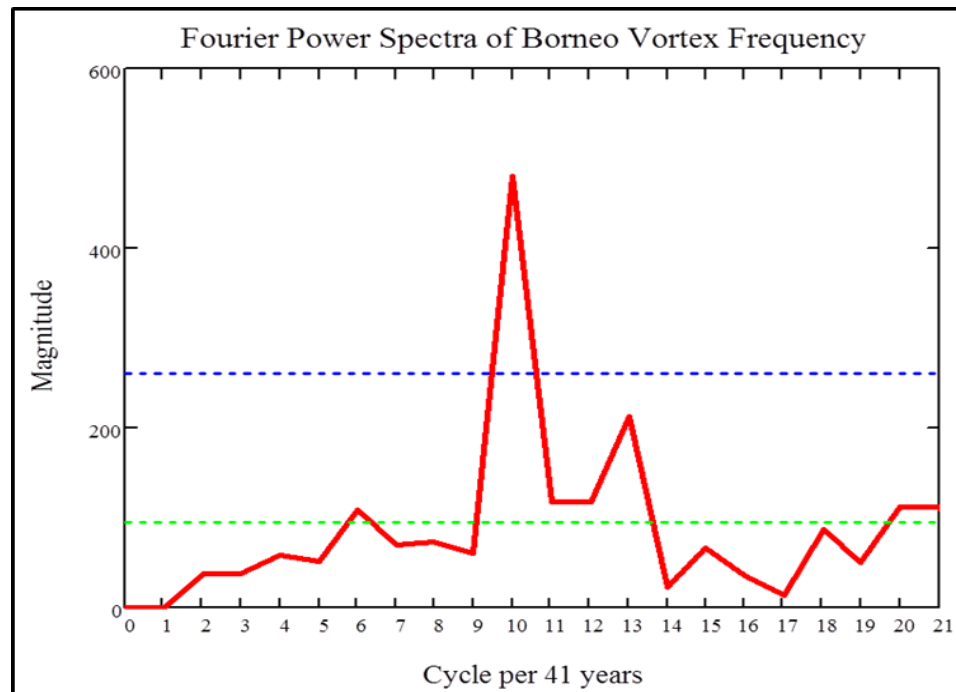


Fig. 3.1.4: The seasonal frequency of Borneo vortex for 41 winter monsoon seasons plotted as Fourier power spectra with the ordinate displaying the magnitude of the Fourier coefficient and the abscissa displaying the period of cycles per 41 years. The blue- and green-dashed lines indicate the 95% and 80% confidence level against the white-noise background, respectively.

The relationship between ENSO and the seasonal frequency of the Borneo vortex was determined by replicating the same techniques as in previous analyses except that the seasonal data in Table 3.1.1 were sorted according to respective ENSO years listed in Table 2.4.2. The final outcomes were summarized as in Table 3.1.5 below.

	All	EN	LN	NEU
No. of seasons	41	10	10	21
Total vortices	2,278	508	619	1151
Vortices per season	55.6	50.8	61.9*	54.8

Table 3.1.5: The seasonal averages of the Borneo vortex frequency stratified by ENSO years. "*" denotes the value is statistically significant at 90% confidence level.

Seasonally, more Borneo vortices are spawned during LN years with an average of 61.9, while the quantity is low in EN periods with 50.8 vortices. During NEU years, the seasonal average is 54.8, which is comparable with the long-term mean. LN events have been observed to enhance the Malaysian winter monsoon season by turning it more active while the impact is overturned for the case of EN. Such impacts have been discussed by numerous researchers such as Hendon (2003), Chang et al. (2004a), Tangang and Juneng (2004) based on the rainfall amount produced over the study domain.

Recent findings by Lin et al. (2011) indicate that as EN reaches its peak towards the end of the year, the winter monsoon weakens due to a spin down of the South China Sea circulation and a deceleration of its western boundary current, which cause the SST to decrease. It is believed that the impact caused by LN should be opposite over this area. As a consequence of all these, the atmospheric conditions in this region perhaps become more conducive for the formation of more convective weather systems, like the Borneo vortex, during LN years than any other ENSO periods. This feedback has also been examined by

Zuki and Lupo (2008) who found that there are strong correlations between the SST and the convergence activity, as well as the convergence and the cyclonic circulation over this region.

On a large scale analysis, this region, which is part of the Maritime Continent, has been recognized as one of the major convective region that drives the global atmospheric circulation, i.e. the Hadley cell and the Walker circulation. Plentiful works, such as by Krishnamurti et al. (1985), Oort and Yienger (1996) and Wang (2002) had shown that during the LN years the convective activities over this region get enhanced, while the center of action shifts from its regular position, which is further away from the study domain, during EN periods.

As a consequence to all these mechanisms, more Borneo vortices are likely to be triggered during LN years and fewer in EN years, which strongly agrees with the results gained here as presented in Table 3.1.5. From the statistical tests, it is shown that the mean vortex frequency during these events is significantly different than the long-term quantity, which supports the influence of EN and LN toward the variability of the vortex frequency in this region. However, only the mean value of LN years exceeds the 90% confidence level, as shown in Appendix A.

Zhang et al. (1997a), Gershunov and Barnett (1998), and Birk et al. (2010) discovered that PDO has a modulating effect on the climate patterns with regard to the ENSO events. The climate signal of EN is likely to be stronger during PDO1; conversely the climate signal of LN is stronger during PDO2. In order to

scrutinize such impacts on Borneo vortex variability over the studied region, the same steps are repeated as in the previous analyses by stratifying the data in Table 3.1.1 with PDO and ENSO phases following the respective years listed in Table 2.4.1 and Table 2.4.2. The final outcomes of these analyses were presented in Table 3.1.6 below.

	PDO1			PDO2		
	EN	LN	NEU	EN	LN	NEU
No. of seasons	5	2	15	5	8	6
Total vortices	228	106	834	280	513	317
Vortices per season	45.6	53.0	55.6	56.0	64.1	52.8

Table 3.1.6: The seasonal averages of the Borneo vortex frequency stratified by ENSO in PDO phases.

Comparing with the results gained in Table 3.1.5 and here, they clearly show that within PDO1 period, the seasonal mean quantity of the Borneo vortices during EN and LN years has reduced significantly. Contrariwise, the value increased when the PDO2 is in place. While, during NEU years, the vortex quantity does not differ that much with the former results. All these relationships imply that PDO1 has a tendency to reduce the number of Borneo vortices in this area, probably due to its influence in cooling down the SST, as mentioned by Gershunov and Barnett (1998) and Lin et al. (2011). On the other hand, the impact caused by the PDO2 is found to be the opposite.

Excluding the NEU years, the results obtained here probably suggest that PDO1 is able to suppress the ENSO events, which further depressed the atmospheric condition of EN years. While, PDO2 tends to boost the ENSO phases, which further enhanced the atmosphere of LN years. All these seem to coincide with the assertion made by some scholars as mentioned earlier. Statistically, the values listed in Appendix A indicate that some of the relationships identified here are relatively strong. However, none of them exceeds the 90% confidence level.

On top of the vortex frequency variations that are similar to PDO and ENSO oscillations, the Fourier power spectral analyses from the periodogram in Fig. 3.1.4 also signifies other notable peak at cycle number 20, which could be associated with Tropospheric Biennial Oscillation (TBO) or Quasi Biennial Oscillation (QBO), or both, with periodicity of about 2 to 2.5 years. Further information of both events could be found in previous chapter. In order to determine the similarity between QBO variability and seasonal periodicity of Borneo vortex frequency, the same methods prior to these analyses are applied by segregating the seasonal data in Table 3.1.1 according to the appropriate seasons listed in Table 2.4.3. The final outcomes are presented as in Table 3.1.7.

The analyses show that, seasonally, 57.1 vortices are generated within the study domain during the west QBO periods while 54.1 vortices are formed when the phases reversed. Both of these values do not look much of a difference

as compared to their long-term mean. This is supported by the insignificant results reveal in the statistical tests as shown in the Appendix A, which tells that QBO event may not exert any influence towards the 2-year variability of the Borneo vortex frequency in this region.

	All	West QBO	East QBO
No. of seasons	41	20	21
Total vortices	2,278	1,142	1,136
Vortices per season	55.6	57.1	54.1

Table 3.1.7: The seasonal averages of Borneo vortex frequency stratified by QBO phases.

For the case of TBO, the same procedure was done as in the earlier analyses by stratifying the seasonal data from Table 3.1.1 according to its respective phases listed in Table 2.4.4. The seasonal vortex frequencies for each phase were then averaged before tabulated in Table 3.1.8. The figures indicate that more Borneo vortices are formed during strong TBO phases with an average of 58.5 cases per season compared to 52.5 vortices in weak TBO periods.

All these outcomes suggest that during strong TBO phases, which are associated with active winter monsoon season (e.g. Meehl (1997); Meehl and Arblaster (2002)), the atmospheric condition is more favorable for convection to develop compared to the weak phase. This is not something unforeseen since the TBO involves with the land-atmosphere-sea interaction. The enhancement of the background potential would lead to more convective activities, and hence

increase the number of Borneo vortices. The impact is probably reversed when dealing with weak TBO. However, the vortex variation showed here is not as substantial as in the case of ENSO years discussed earlier. The statistical tests also show that both means are statistically insignificant (see Appendix A) compared to the vortex long-term average.

	All	Strong TBO	Weak TBO
No. of seasons	41	21	20
Total vortices	2,278	1,229	1,049
Vortices per season	55.6	58.5	52.5

Table 3.1.8: The seasonal averages of Borneo vortex frequency stratified by TBO phases.

The relation between TBO and ENSO has also been studied by many researchers, such as Yasunari (1990), Fasullo (2004), Wu and Kirtman (2004), and Meehl and Arblaster (2002, 2011). TBO is involved in monsoon–ENSO coupling through the large-scale east–west tropical circulation, tropical and mid-latitude interaction, and impacts of the land–sea thermal contrast on the monsoon (Wu and Kirtman, 2004), which make them connected to one another. However, the effect of TBO is just localized, whereas the ENSO is more globalized. Therefore, it was found that the TBO is modulated by ENSO, as in the case of ENSO by PDO. In order to determine their influence towards the fluctuation of seasonal Borneo vortex frequencies, the same technique as in

previous analyses is being utilized. All the values are summed up and averaged before being displayed in Table 3.1.9 below.

	Strong TBO			Weak TBO		
	EN	LN	NEU	EN	LN	NEU
No. of seasons	5	7	9	5	3	12
Total vortices	281	425	523	227	194	628
Vortices per season	56.2	60.7	58.1	45.4*	64.7	52.3

Table 3.1.9: The seasonal averages of the Borneo vortex frequency stratified by ENSO in TBO phases. "*" denotes the value is statistically significant at 90% confidence level.

The results show that, the number of Borneo vortices is further varied under this new background climate when compared to the climate condition set in Table 3.1.8. The influence of ENSO is found to be more significant toward the variability of the mean vortex frequency during weak TBO than in the phase of strong TBO. Within strong TBO, there is only a small reduction in vortex quantity during EN and slight increment in LN years. While, under weak TBO, the vortex quantity is reduced and increased tremendously during EN and LN events, respectively. As for NEU years, there is no variation revealed between both climate conditions either during strong or weak TBO.

As discussed before, strong TBO and LN events have a tendency to enhance the atmospheric condition in this region, and hence more Borneo vortices should be generated. On the other hand, less number of vortices is expected under the weak TBO and EN phase. Since the ENSO is known to

modulate the TBO, the vortex quantity should be increased significantly when the climate condition is in LN and strong TBO phases. The situation should be reversed when the background climate is supported by weak and EN events. Based on the understanding of the impact of ENSO over this region, all the mean values found here seem to be consistent with the expected outcomes. However, from statistical tests, only the case of EN in weak TBO passes the 90% confidence, while the rest are statistically insignificant.

3.2 Borneo vortex center

The center of the Borneo vortex is the bull's eye of a closed cyclonic circulation of a wind field that is formed within the study domain. Once identified, all the latitudes and longitudes of the vortex centers were documented. Due to the Coriolis force, the winds over the Northern Hemisphere are supposed to rotate in counterclockwise direction in order for the cyclonic circulation to develop, and clockwise in Southern Hemisphere. However, in some cases throughout this work, the winds were observed to flow in counterclockwise direction in the Southern Hemisphere, which is against the norm of the wind flow, as exhibited in Fig 3.2.1. Chang and Maas (1976) considered this kind of phenomena as a cross-equatorial displacement of the vortex.

Through the analysis of the wind field, such phenomena could only transpire in the presence of a strong northeasterly cold surge. The strong force of the surge either pushes the Northern Hemisphere Borneo vortex into the other

side of the equator or transports the auspicious environment from Northern into Southern Hemispheres for a new counterclockwise vortex to spawn there. According to Chang and Maas (1976), this special event can only take place as long as the vortex is not displaced too far away from the equator. At this locality, the Coriolis parameter is too weak or totally vanished, thus making it possible for any vortex to rotate in either direction.

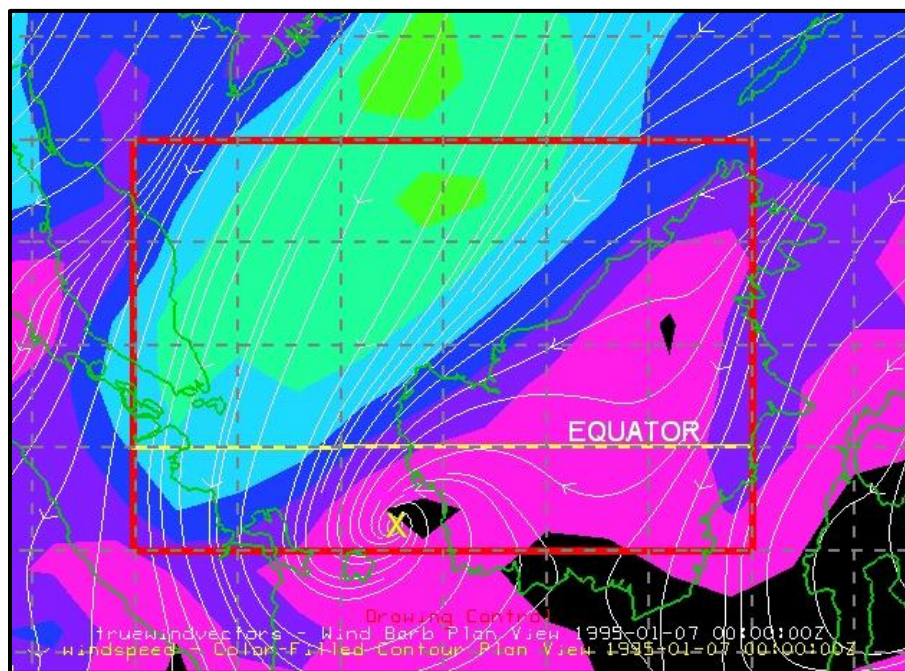


Fig. 3.2.1: One of the Borneo vortices that was observed to rotate in the counterclockwise direction in the Southern Hemisphere, which formed at 0000 UTC on 7 January 1995. The center is marked as yellow "X". The color-shaded area indicates the wind speed of 2 ms^{-1} or greater.

By acknowledging this kind of irregular circulation as being part of the Borneo vortices studied here, the information on the latitudinal and longitudinal positions of all the vortex centers were then documented according to their respective month and season. Since the study domain covers both the

hemispheres, the latitudinal position of the vortex centers over northern hemisphere had been assigned of having positive value, while the value was negative for Borneo vortices found in southern hemisphere.

The study domain consists of land areas that are surrounded by large water body of South China Sea. Therefore, the positions of each vortex center had also been analyzed based on whether it was formed over the land or water as summarized in Table 3.2.1. Throughout the study period, the outcomes reveal that 1,409 of the vortex centers are observed over the water body, which represents 62% of the total vortices while the remaining 38% was found over the land. Seasonally, the majority of the cases show that more vortices form over the water than land. However, there are seven seasons where more vortices are monitored over land than water, such as 1970/71, 1972/73 and 1973/74, as displayed in Table 3.2.1. This means that there is variability in term of the distribution of the vortices over land and water within the study period.

As discussed in section 3.1, on average, 55.6 vortices were calculated in each season throughout the study period. Out of that number, 34.4 vortices were generated over the water and the balance was formed over the land. However, the vortices were not uniformly distributed between the water and land from month to month as shown in Table 3.2.1. Fewer numbers of vortices were monitored over the land in November, which represents only about 11% of the total vortices of that month. As the winter monsoon progressed, the percentage increased and exceeded more than 50% in January and February. The situation

Year	Nov		Dec		Jan		Feb		Seasonal	
	Land	Water	Land	Water	Land	Water	Land	Water	Land	Water
2010/11	0	9	1	19	5	7	3	4	9	39
2009/10	0	18	5	13	2	6	3	1	10	38
2008/09	0	17	10	19	11	8	4	4	25	48
2007/08	0	5	9	13	10	3	4	6	23	27
2006/07	0	8	9	14	9	16	5	4	23	42
2005/06	0	11	0	11	6	14	13	3	19	39
2004/05	1	9	6	11	3	7	5	1	15	28
2003/04	0	13	6	10	8	5	0	2	14	30
2002/03	0	13	2	7	5	9	1	4	8	33
2001/02	0	11	2	15	5	5	7	2	14	33
2000/02	7	3	1	13	8	11	3	6	19	33
1999/00	1	12	5	17	8	6	6	12	20	47
1998/99	0	10	1	14	8	9	7	4	16	37
1997/98	5	7	3	7	3	2	1	4	12	20
1996/97	1	5	1	19	10	0	8	6	20	30
1995/96	2	14	1	14	8	9	12	4	23	41
1994/95	2	6	7	13	3	5	1	1	13	25
1993/94	1	13	3	9	9	4	4	3	17	29
1992/93	2	24	3	11	5	1	2	3	12	39
1991/92	1	21	2	20	1	3	1	1	5	45
1990/91	0	4	9	6	8	0	3	4	20	14
1989/90	3	17	2	11	6	7	1	0	12	35
1988/89	2	11	8	5	3	9	15	0	28	25
1987/88	0	9	7	19	10	9	6	2	23	39
1986/87	1	10	5	7	9	1	4	2	19	20
1985/86	2	14	5	17	8	4	6	3	21	38
1984/85	5	5	5	21	8	8	6	7	24	41
1983/84	0	9	5	19	12	9	10	10	27	47
1982/83	1	7	10	11	5	6	5	0	21	24
1981/82	3	8	7	12	12	2	8	2	30	24
1980/81	2	10	7	19	1	12	8	6	18	47
1979/80	0	24	8	9	11	5	6	7	25	45
1978/79	0	19	17	6	6	4	7	3	30	32
1977/78	1	12	11	10	9	4	8	0	29	26
1976/77	2	22	5	15	15	0	12	1	34	38
1975/76	1	20	4	15	15	3	9	1	29	39
1974/75	5	8	2	16	12	11	11	7	30	42
1973/74	3	11	10	14	10	2	15	3	38	30
1972/73	3	11	8	7	17	1	6	1	34	20
1971/72	1	18	3	24	11	6	8	3	23	51
1970/71	0	14	7	8	18	4	12	3	37	29
Average	58	492	222	540	333	237	256	140	869	1,409

Table 3.2.1: Monthly and seasonal locations of Borneo vortex centers during 41 winter monsoon seasons.

reversed for the case of vortices over the water. This implies that most of the Borneo vortices are generated over the water body of South China Sea during the early stage of the winter monsoon and shift southward into the land area of Borneo Island and others as the season progresses.

The transition of the Borneo vortex centers seems to coincide with the migration of monsoon trough. As discussed by Sadler and Harris (1970), the trough moves southward from its October position along 10°N latitude and begins to affect Malaysian region by November. In December, the trough mean position lies at the middle of the study domain. By January and February, it migrates further south close to the equator. Since the Borneo vortices are formed and embedded within this trough (Cheang, 1977 and 1987), therefore the southward migration of the monsoon trough during the northern hemisphere winter season has caused the vortex centers to also move southward.

In order to further investigate the transition of these vortices, the latitudinal and longitudinal positions of the vortex centers were analyzed according to their respective month and season. All the data were summarized as in Table 3.2.2. From 41 winter monsoon seasons studied here, the position of the vortex center was averaged at 2.4°N latitude and 110.6°E longitude, which is just off coast of west Borneo, depicted as a yellow star in Fig. 3.2.2. This spot is found to be within the region of maximum occurrence of the vortices of Chang et al. (2005b), even though their study only involved 21 winter monsoon seasons between 1980/81 and 2000/01 and covered the months of December, January and

Season	Nov		Dec		Jan		Feb		Seasonal Mean	
	Lat	Long	Lat	Long	Lat	Long	Lat	Long	Lat	Long
2010/11	4.8	108.9	4.0	110.5	3.4	112.4	2.7	111.7	3.7	110.9
2009/10	4.2	108.7	2.2	110.3	3.0	111.3	2.1	112.2	2.9	110.6
2008/09	4.4	108.1	3.8	111.0	3.3	112.3	2.3	112.1	3.5	110.9
2007/08	6.5	111.7	3.3	111.7	1.8	112.0	2.9	111.3	3.6	111.7
2006/07	3.2	109.9	2.2	110.2	2.3	110.4	0.9	110.7	2.2	110.3
2005/06	4.8	109.4	4.4	107.5	2.2	110.9	0.7	110.6	3.0	109.6
2004/05	3.8	110.8	2.0	110.0	-0.4	108.7	2.1	112.7	1.9	110.6
2003/04	3.8	109.7	2.5	111.2	-0.1	109.9	1.9	109.6	2.0	110.1
2002/03	5.5	110.0	1.7	109.0	0.6	110.4	-1.0	109.3	1.7	109.7
2001/02	4.4	109.8	2.6	109.1	-1.2	110.2	-0.3	111.3	1.4	110.1
2000/02	1.2	109.8	3.8	108.8	2.1	109.9	3.4	111.3	2.6	110.0
1999/00	2.2	107.7	4.5	110.9	0.7	110.3	3.8	111.5	2.8	110.1
1998/99	4.5	106.9	3.8	109.8	3.1	111.1	2.0	112.0	3.4	110.0
1997/98	3.7	111.4	1.4	109.0	-0.9	111.0	1.4	111.0	1.4	110.6
1996/97	2.5	107.8	4.4	110.4	0.7	112.5	3.3	112.0	2.7	110.7
1995/96	4.0	108.8	3.9	110.3	2.8	111.4	0.7	111.1	2.9	110.4
1994/95	1.0	108.8	2.0	109.5	1.2	110.6	-1.5	109.2	0.7	109.5
1993/94	3.1	109.1	4.3	110.7	1.9	111.2	1.0	110.8	2.6	110.5
1992/93	4.1	109.2	2.0	107.9	1.5	111.2	-0.6	109.9	1.8	109.6
1991/92	3.2	109.4	1.3	107.6	-0.4	110.6	0.2	110.9	1.1	109.6
1990/91	2.6	106.2	0.9	109.5	0.5	110.8	2.0	111.7	1.5	109.6
1989/90	3.0	110.2	-0.1	108.9	1.0	110.1	2.3	112.5	1.6	110.4
1988/89	3.2	109.4	3.0	111.3	1.5	110.4	1.8	113.8	2.5	111.2
1987/88	5.9	109.0	3.1	110.6	1.9	112.0	2.4	111.3	3.3	110.7
1986/87	3.2	109.0	0.7	109.7	-0.1	110.8	3.0	113.0	1.8	110.6
1985/86	4.3	110.7	3.6	110.3	1.3	111.2	2.2	112.6	2.9	111.2
1984/85	3.3	109.9	3.2	109.8	2.5	112.2	2.6	111.4	2.9	110.8
1983/84	5.9	110.3	2.5	110.1	2.7	111.6	0.8	110.2	3.0	110.6
1982/83	3.9	107.1	1.9	110.2	-0.2	110.0	-0.2	111.6	1.4	109.7
1981/82	3.8	110.6	2.3	110.3	2.3	113.0	1.2	111.8	2.4	111.4
1980/81	4.1	109.5	3.9	110.9	4.4	112.5	1.0	111.8	3.4	111.2
1979/80	4.5	110.7	2.7	111.7	1.3	110.7	-0.2	109.9	2.1	110.8
1978/79	5.9	109.2	1.4	111.5	0.4	109.5	-0.1	110.0	1.9	110.1
1977/78	3.8	110.5	2.4	111.1	1.5	111.9	0.7	112.8	2.1	111.6
1976/77	5.1	109.2	3.4	110.0	2.1	113.4	1.4	112.7	3.0	111.3
1975/76	3.9	108.8	4.0	110.1	3.1	114.6	1.5	113.0	3.1	111.6
1974/75	3.2	110.4	4.5	111.2	1.6	110.8	0.6	110.7	2.6	110.8
1973/74	5.2	110.1	3.4	111.0	3.2	113.6	1.3	111.3	3.3	111.5
1972/73	4.1	110.6	2.6	110.3	0.3	111.6	0.3	111.4	1.8	111.0
1971/72	5.3	109.9	3.4	109.3	2.6	112.1	2.2	112.0	3.4	110.8
1970/71	4.8	110.9	3.2	110.2	1.5	111.9	2.4	112.1	3.1	111.3
Average	4.0	109.5	2.8	110.1	1.5	111.3	1.4	111.5	2.4	110.6

Table 3.2.2: Monthly and seasonal averages of Borneo vortex centers based on latitude (Lat)-longitude (Long) positions (degree) during 41 winter monsoon seasons.

February. This implies that the Borneo vortex mean position is almost stationary despite the fact that the dataset comprised of different number of seasons, timespans and domains.

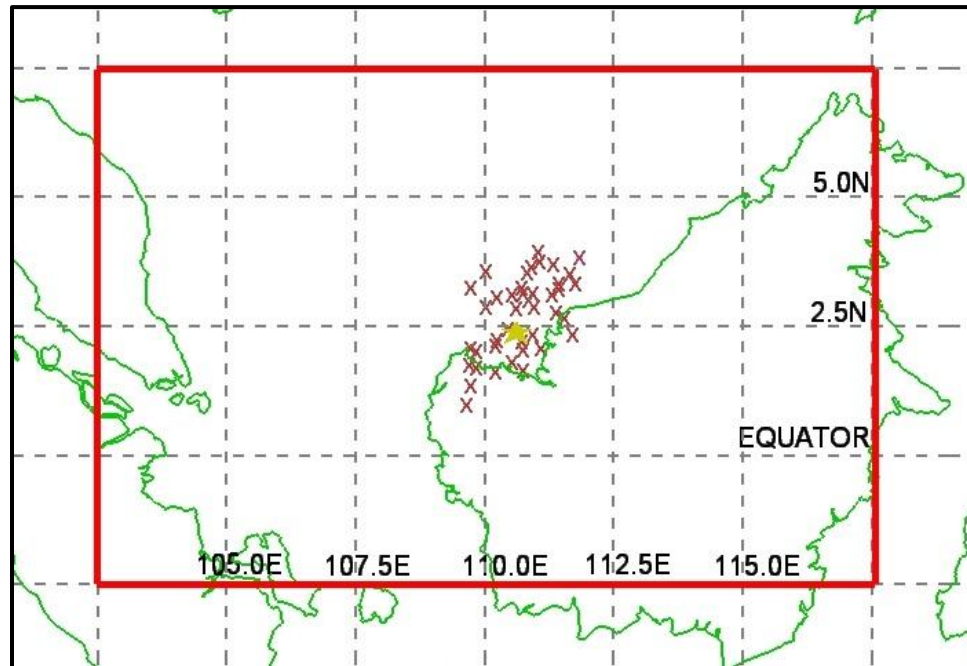


Fig. 3.2.2: Red “X”s are the position of the seasonal averages of Borneo vortex centers for 41 winter monsoon between 1970/71 and 2010/2011 seasons and the yellow star is the long-term average position of all the vortex centers throughout the study period.

The seasonal vortex centers in Table 3.2.2 were also placed on the map, as portrayed in Fig. 3.2.2, according to their latitudinal and longitudinal positions to provide a better picture on the location of all the centers. It is clearly shown that all the centers are located close to each other over the western part of the Borneo Island in a northeast-southwest orientation. Although the vortices had been observed to form anywhere within the domain throughout the study period, their seasonal mean positions are found to confine within a small area, which

probably indicates that the Borneo vortices are uniformly distributed from one season to another.

Out of 41 seasons, 30 had their vortex mean centers located over the water body, which encompasses about 73% of the study period. This again means that the majority of the Borneo vortices were established over water rather than the land. Since the Borneo vortices were observed to form and embed within the monsoon trough, this outcome also implies that most of the time the trough was laid over the water of southern part of South China Sea during the winter monsoon period in the study region.

To determine the long-term trend of the vortex centers, time-series graphs were plotted with respect to the latitudinal and longitudinal positions of the Borneo vortex centers in each season using their mean values from Table 3.2.2. The outcomes are shown in Fig 3.2.3. Both graphs demonstrate a significant fluctuation throughout the study period, which could probably be linked to certain interannual and/or interdecadal climate variability. Yet, their long-term linear trend shows opposite behaviors as follows.

The vortex longitudinal position had a steeper downward trend, which indicates that the seasonal Borneo vortex center has propagated westward from longitude 111.0°E to 110.1°E between 1970/71 and 2010/11 winter monsoon seasons. On the other hand, the latitudinal position exhibited almost no trend throughout the same period. When both results are combined, it suggests that there is a westward shift of the vortex centers over the 41-year study period,

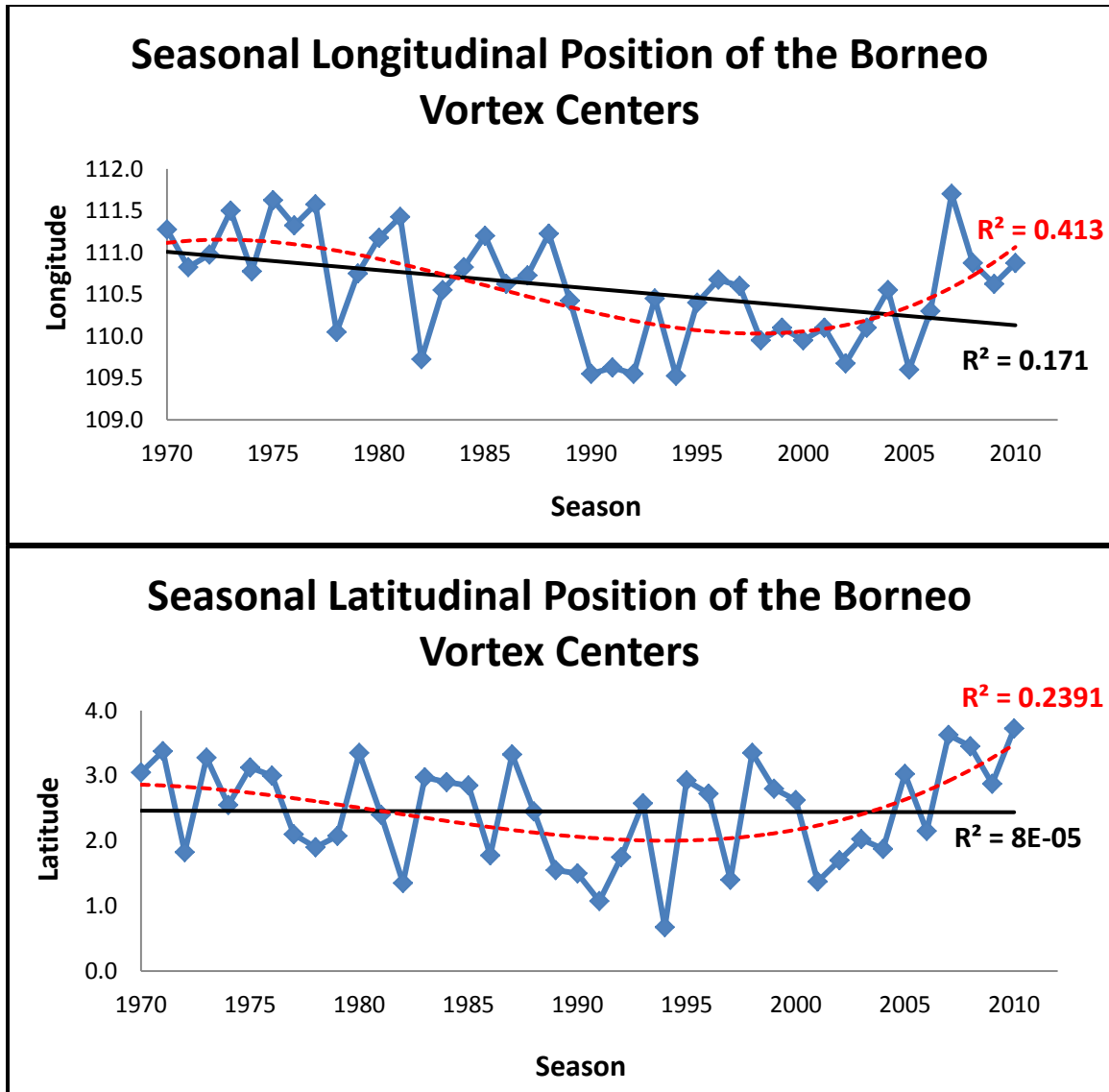


Fig. 3.2.3: The seasonal longitudinal (top) and latitudinal (bottom) positions of the Borneo vortex centers for 41 winter monsoon between 1970/71 and 2010/11 seasons. The red-dashed line is the 3rd order polynomial trendline and the black line is the linear trendline of the vortex positions.

which also implies that the vortex centers have slowly moved away from the Borneo coast. This outcome agrees with Juneng and Tangang (2010) but their center was found to move northwestward rather than just westward in here.

However, both linear regression lines displayed in Fig. 3.2.3 were insignificant owing to their small R^2 values, which indicate a weak correlation between the trendline and the seasonal positions of the vortex centers. The correlation increased tremendously when the analyses were done by applying the polynomial type of trendline. The R^2 values increased extensively from 8×10^{-5} to 0.239 for the case of the vortex latitudinal position and triple from 0.171 to 0.413 for longitudinal event when they were analyzed using the third order polynomial trendline. This shows that the long-term trend of the seasonal position of the Borneo vortex center is not linear, but tends to follow a curve similar to PDO periodicity as discussed in section 3.1.

Both polynomial trendlines demonstrate that the seasonal mean vortex centers tend to form relatively at higher latitudes and eastern side of its long-term mean position during cold PDO phase that take place prior to 1976 and from 1999 onward. On the contrary, during warm PDO phase, the vortices show a tendency to stay further southward and westward of the long-term mean vortex latitude and longitude, respectively. Further analyses on the relationship between the vortex position and PDO phases will be discussed later in this section.

The bar chart of the monthly variation of the mean latitudinal position of the vortex centers shown in Fig. 3.2.4 reveal that it shifts southward closer to the equator as the winter monsoon season progressed. The vortex center moves from 4.0°N in November to 2.8°N , 1.5°N and 1.4°N in December, January and February, respectively. While the monthly mean longitudinal position indicates

that the vortex center propagates eastward. The longitude was at 109.5°E in November, then shifted to 110.1°E in December, 111.3°E in January and finally reached the utmost eastern longitude position at 111.5°E in February.

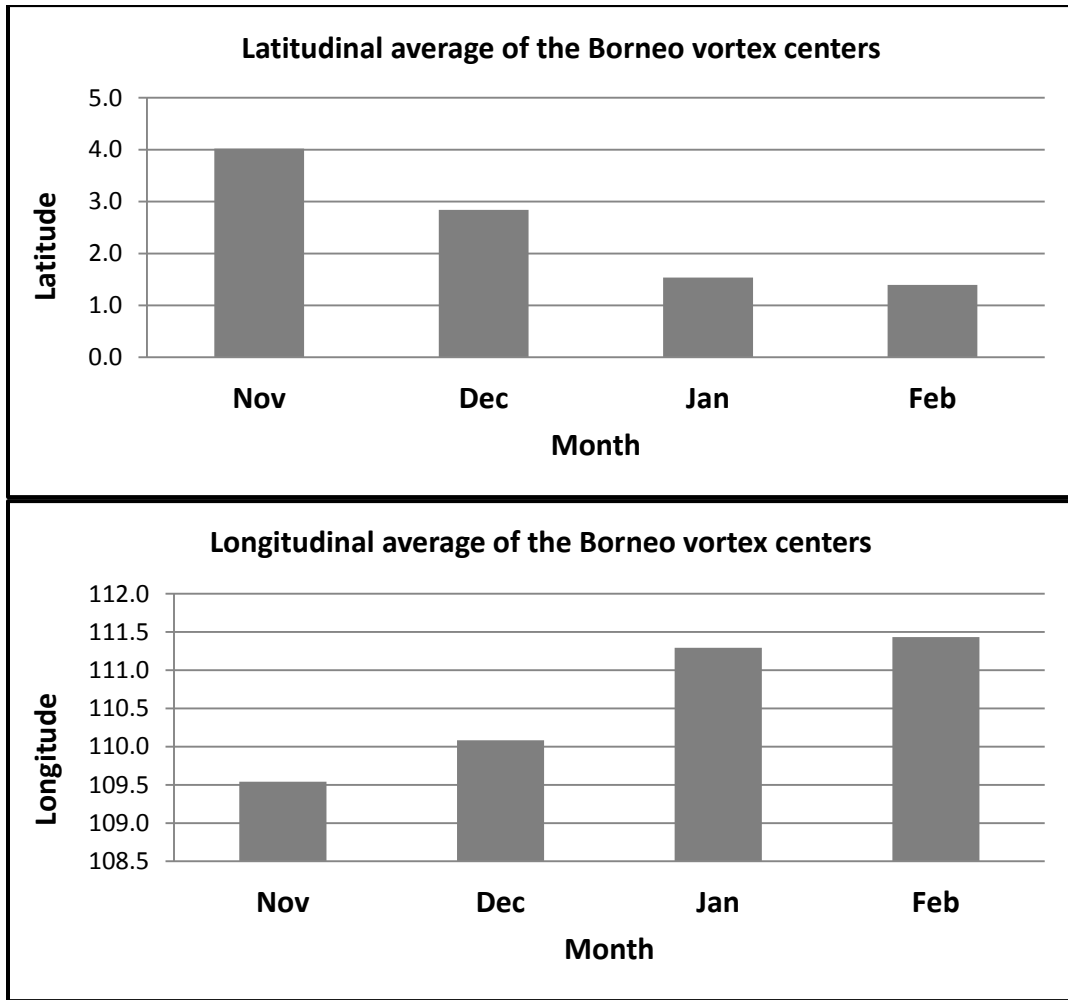


Fig 3.2.4: Monthly averages of latitudinal (top) and longitudinal (bottom) position of the Borneo vortex centers throughout 41 winter monsoon seasons.

When both dimensions are combined, it turns out that the mean monthly position of the Borneo vortex center propagates southeastward as the winter monsoon advanced from November to February. The results could be understood more easily by placing all the latitude and longitude values together

on the map as seen in Fig 3.2.5. It demonstrates that the mean vortex center is located over the water body in November and December, and moves inland in January and February.

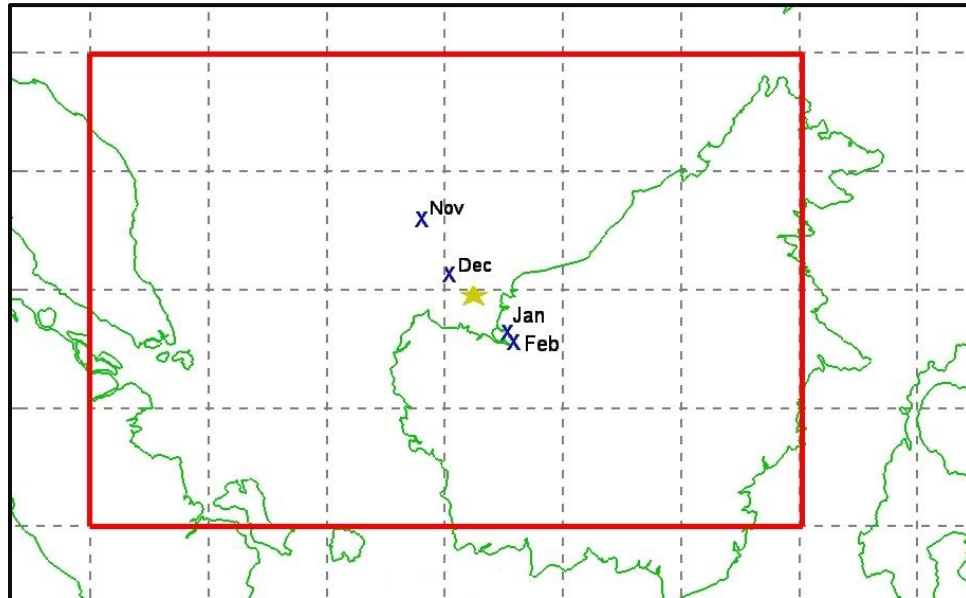


Fig. 3.2.5: Monthly position of the Borneo vortex centers (blue “X”s) based on the latitude-longitude average for 41 winter monsoon seasons. The yellow star is the long-term average and the red box is the study domain.

The results match the transition of monsoon trough as discussed by Sadler and Harris (1970) since the vortices are formed and embedded within it (Cheang, 1977 and 1987). Therefore the southward migration of the monsoon trough during the boreal winter has caused the mean position of the vortex centers to shift southeastward. The migration of the vortex centers also seem to agree pretty well with the advancement of the winter monsoon season based on the seasonal migration of the monsoon diabatic heating (Lau and Chan, 1983) and the transition of large amount of high clouds during the winter monsoon season (Tanaka, 1994).

As mentioned earlier, both graphs in Fig. 3.2.3 probably emulate a long-term trend pattern of PDO variability. In order to see the potential impact of this event to the position of the vortex centers, the compositing analysis technique was again applied here by segregating the seasonal latitudinal and longitudinal average values from Table 3.2.2 and matching them with the seasons that took place in respective PDO phase listed in Table 2.4.1. The corresponding centers were placed on the map as in Fig. 3.2.6. The outcomes reveal that during the PDO2 period, majority of the seasonal mean vortex centers (marked with blue “+”) are located over the water body. While most of the vortex centers that are found on the land are dominated by the brown “X” marks, i.e. the seasonal vortices that are formed during PDO1 phase.

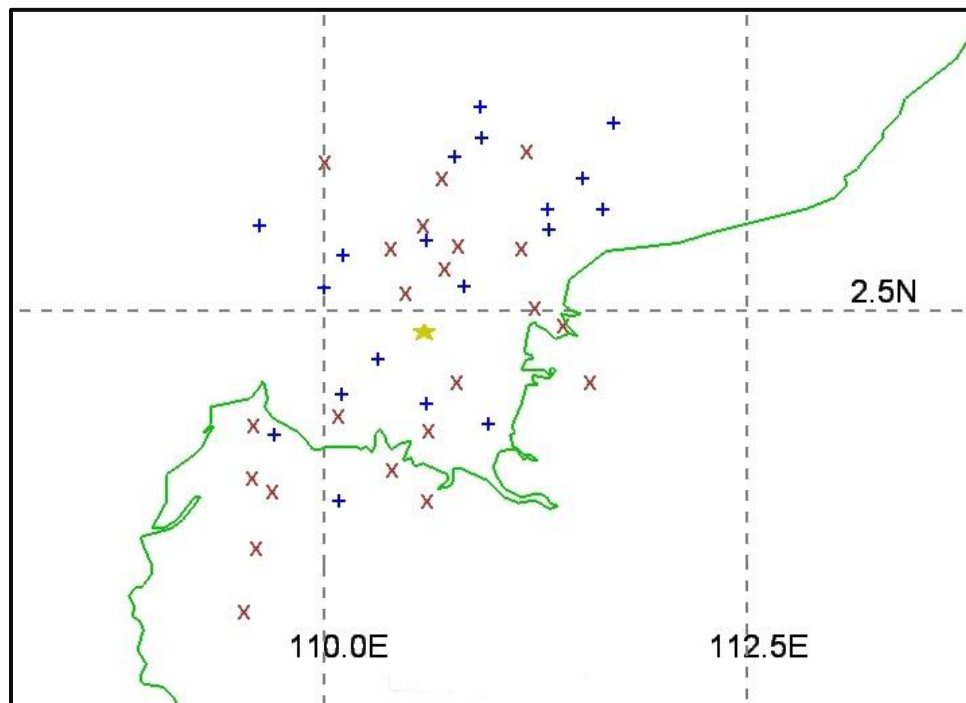


Fig. 3.2.6: The position of the seasonal Borneo vortex centers for 41 winter monsoon between 1970/71 and 2010/2011 seasons. The brown “X” indicates the vortex center during the PDO1 period while the blue “+” during PDO2. The yellow star is the long-term average position of the vortex center throughout the study period.

By separately averaging all the latitudinal and longitudinal values of the seasonal vortex centers in PDO1 and PDO2 periods, it was found that both seasonal mean centers are located not significantly far from each other as indicated in Table 3.2.3. Located at 2.7°N latitude and 110.7°E longitude, the mean PDO2 vortex center is placed slightly over the northeast of the long-term average position. The center is situated relatively further from the land mass as compared to long-term mean. On the other hand, at 2.2°N and 110.5°E, the average PDO1 vortex position is situated southwestward of the long-term average center, which is closer to the land mass.

	All	PDO1	PDO2
No. of seasons	41	22	19
Latitudinal average	2.4°N	2.2°N	2.7°N*
Longitudinal average	110.6°E	110.5°E	110.7°E

Table 3.2.3: The average positions of the Borneo vortex centers stratified by PDO phases. "*" denotes the value is statistically significant at 90% confidence level.

Studies by Gershunov and Barnett (1998) and Lin et al. (2011) claim that the SST over this study region is likely to be warmer during PDO2 and cooler in the course of the opposite period. A warm water body is known to be one of the main ingredients for the formation of any synoptic cyclonic circulation systems in the tropics, such as the Borneo vortex. This factor has been emphasized in many publications and textbooks, such as Gray (1975), Ahrens (2009) and Lupo (2011). On the other hand, PDO1 phase has a tendency to force the SST to stay

below its normal value in this region, which relatively reduces the convective activity during winter monsoon season, as demonstrated in Zuki and Lupo (2008).

Therefore, the consequence to this has possibly caused more vortices to develop over the warmer water body during PDO2 period and over or close to the land mass during PDO1, as was demonstrated in this analysis. Applying the same statistical tests to all the means like in previous section using the 2-tailed p-value from t-test, the results indicate that none of the values pass the 90% confidence level except for the case of vortex seasonal latitudinal position during PDO2 phase (see Appendix A).

In order to identify the influence of other natural climate oscillations toward the variability of the Borneo vortex positions, the same technique explained in section 2.3 was again applied here by transforming the time-series data of Fig. 3.2.3 into a function of cycle using the Fourier power-spectral method. The final outcomes were plotted on periodograms as shown in Fig. 3.2.7 below after filtered out the first and the last peaks of the spectrum. Next, the significance of the power-spectral for both cases was tested against the white-noise background.

At 95% and 80% confidence levels, both periodograms have significant peaks at cycle number 9 and 11, which indicates the position of the seasonal Borneo vortex centers has variability with a recurrence time of about 4 to 5 years. This could be associated with the influence of the ENSO event, which is the only

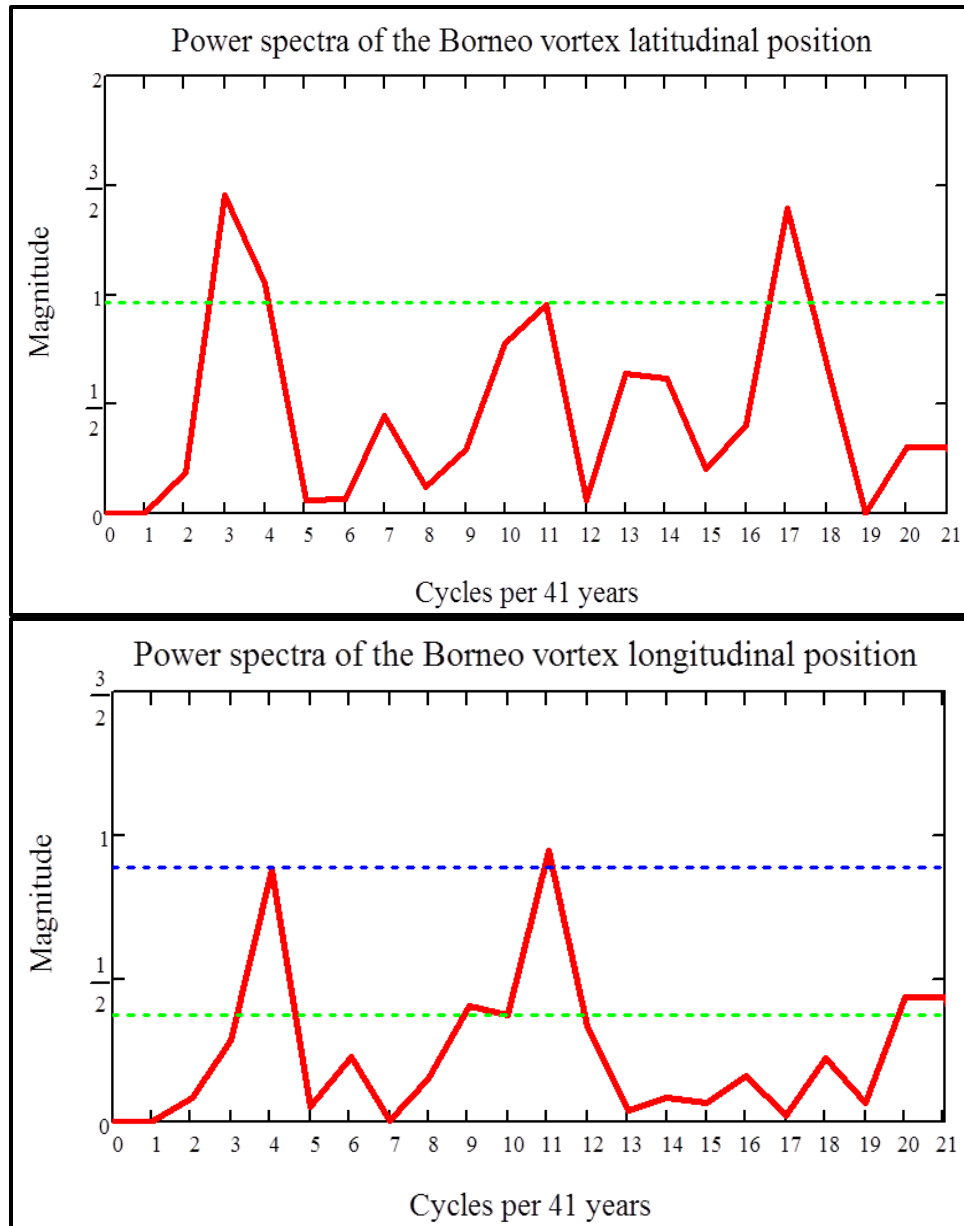


Fig. 3.2.7: The seasonal latitudinal (top) and longitudinal (bottom) positions of the Borneo vortex centers for 41 winter monsoon seasons plotted as power spectra with the ordinate displaying the magnitude of the Fourier coefficient and the abscissa displaying the period of cycles per 41 years. The blue- and green-dashed lines indicate the 95% and 80% confidence level against the white-noise background, respectively.

known natural event that has an oscillation with such periodicity. In addition, both periodograms also reveal other notable peaks at cycle number 17 and 20, correspond with the recurrence period between 2.5 and 2 years, which are

possibly owing to the influence of QBO or TBO, or both events. Other than that, the periodograms also demonstrated other peculiar peaks at cycle number 3 and 4, which probably emulate the variability of ENSO-PDO interaction with 13 to 10 years periodicity, similar to what was found in Enfield and Mestas-Nuñez (1999) and Birk et al. (2010). Descriptions of ENSO, TBO and QBO phenomena were already discussed in section 2.4

To investigate the association of the Borneo vortex positions with the ENSO events, again the compositing analysis technique was applied here by sorting the seasonal latitudinal and longitudinal average values from Table 3.2.2 according to the ENSO years listed in Table 3.1.6. The corresponding vortex centers were then placed on the map and shown as in Fig. 3.2.8. The results demonstrate that all the vortex centers are situated northward of the long-term average center during LN years (marked by blue "+"). On the contrary, majority of the vortex centers are located southward of the long-term position in EN years (marked by brown "X").

The findings by Trenberth (1976) on the correlation between the ITCZ and ENSO events reveal that the trough moves southward from its mean position during EN years and northward in LN years, which later were supported by Chen and Lin (2005) based on the analysis of water vapor quantity measured from the satellite. Since the vortex is known to be embedded in the ITCZ (Cheang, 1977 and 1987), it appears that the outcome from these analyses matches Trenberth's (1976) assertion and could be used to reinforce their claim.

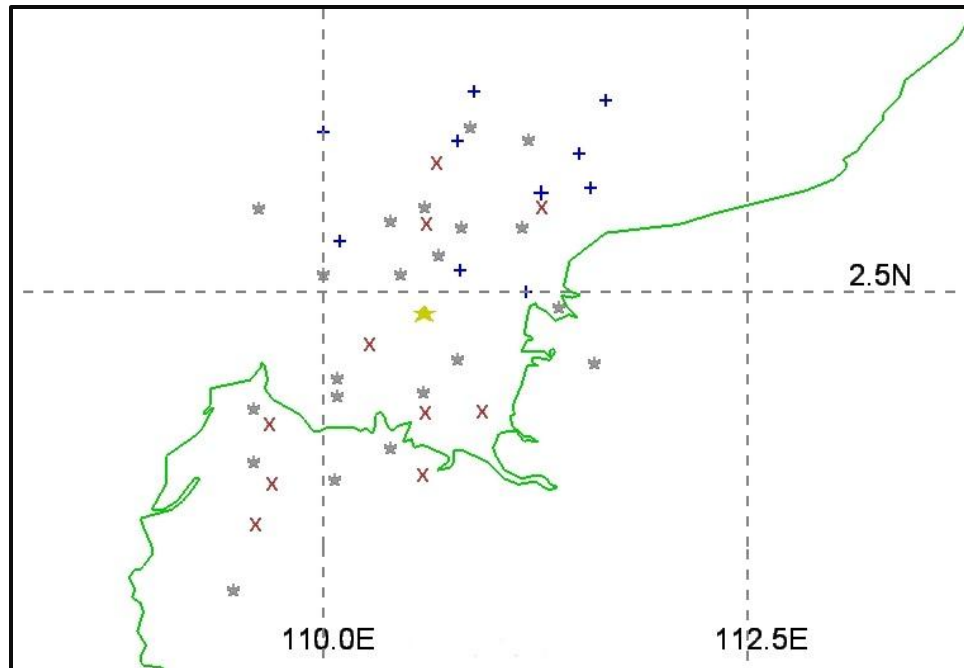


Fig. 3.2.8: The position of the seasonal Borneo vortex centers for 41 winter monsoon between 1970/71 and 2010/2011 seasons. The brown “X” indicates the vortex center during the EN years, the blue “+” is LN and the grey “*” is NEU year. The yellow star is the long-term average position of the vortex center throughout the study period.

Further analysis on the latitudinal and longitudinal values of the vortex centers as calculated in Table 3.2.4 shows that the mean center of all the vortices formed during NEU years is about the same as the long-term average throughout the study period. For the case of LN years, the mean vortex position is at 3.0°N and 111.0°E, which is over the northeast of the long-term average center. While during the EN years, the mean center is located at 2.0°N and 110.4°E, which is southwest of the long-term average position. These seasonal mean centers were then tested statistically against the vortex long-term mean position. The results reveal that only the vortex means latitudinal position during LN years exceed 95% confidence level, while the rest are below 90% as shown in Appendix A.

	All	EN	LN	NEU
No. of seasons	41	10	10	21
Latitudinal average	2.4	2.0	3.1*	2.3
Longitudinal average	110.6	110.4	111.0	110.5

Table 3.2.4: The average positions (degree) of the Borneo vortex centers stratified by ENSO years. "*" denotes the value is statistically significant at 99% confidence level.

The northeast and southwest orientation of the vortex centers associated with LN and EN years, respectively, tends to match the previous analyses of PDO events. Such behavior is not an unexpected outcome because PDO1 has been described as a long-lived EN pattern of Pacific climate variability and PDO2 for the case of LN, since both events have similar relationships regarding deviations in SST (Zhang et al., 1997a). Therefore, it is essential to examine the influence of the combination of both events towards the variability of the seasonal latitudinal and longitudinal positions of the Borneo vortex centers within the study domain.

The analyses were established the same way as in previous work, except that the data from Table 3.2.2 were sorted according to season of both events listed in Table 2.4.1 and Table 2.4.2. The final outputs were presented in Table 3.2.5. The results reveal that, within PDO1 phase, the Borneo vortex seasonal mean centers have been shifted southwestward of their EN and LN mean location shown in Table 3.2.4. Conversely, they move northeastward when PDO2 is in command.

	PDO1			PDO2		
	EN	LN	NEU	EN	LN	NEU
No. of seasons	5	2	15	5	8	6
Latitudinal average	1.8	2.9	2.3	2.3	3.2 ⁺	2.4
Longitudinal average	110.3	110.6	110.5	110.6	111.1 [*]	110.3

Table 3.2.5: The average positions (degree) of the Borneo vortex centers stratified by ENSO in PDO phases. “+” and “*” denotes the value is statistically significant at 95% and 90% confidence level, respectively.

These outcomes established here could probably imply that PDO1 has further depressed the atmospheric condition in this region under different ENSO phases, except in NEU years, which cause the vortex center to shift its position and move closer to the mainland as a result of cooler than normal SST (Gershunov and Barnett (1998) and Lin et al. (2011)). While, PDO2 is known to force the SST over this region to increase, which probably has allowed more vortices to form in the water body, thus cause the mean vortex center to shift away from the land, except for the case of NEU years. All these connections seem to match the work of Zhang et al. (1997a), and Gershunov and Barnett (1998) mentioned earlier with regard to the influence of PDO to ENSO events. However, the statistical tests results shown in Appendix A reveal that only the variability position of seasonal mean vortex center of LN in PDO2 period is found to be significant.

Besides PDO and ENSO, QBO is likely to be another natural event in the tropics that could contribute to the interannual variation of the Borneo vortex

position based on the Fourier power spectra analysis depicted in Fig. 3.2.7. The analyses were done similar to the previous method by separating the latitudinal and longitudinal positions of the Borneo vortex centers from Table 3.2.2 according to the seasons and QBO phases listed in Table 3.1.10. Finally, the respective vortex centers were plotted on the map as displayed in Fig. 3.2.9 below.

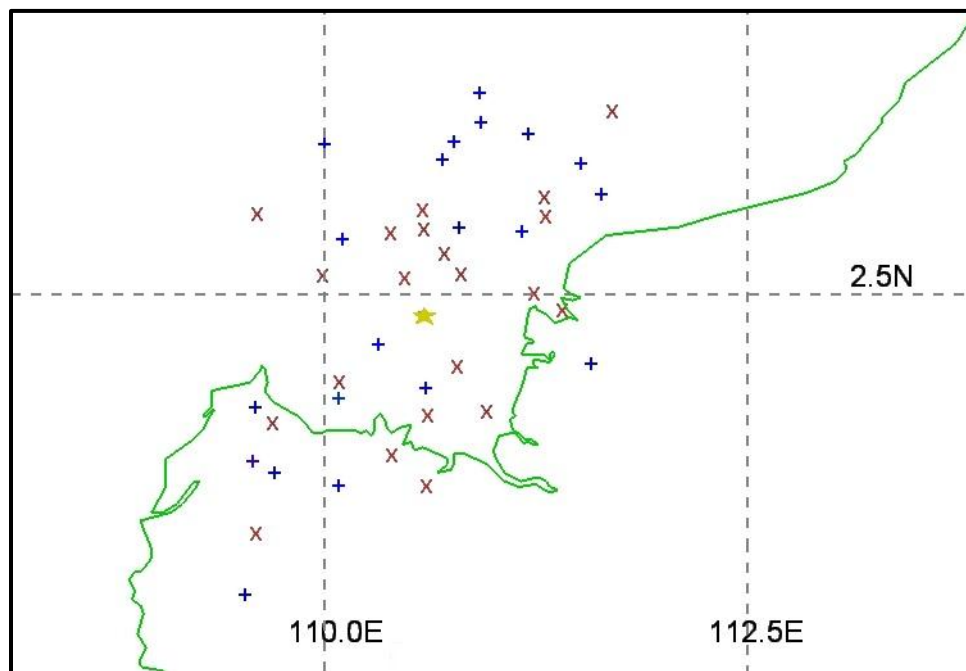


Fig. 3.2.9: The position of the seasonal Borneo vortex centers for 41 winter monsoon between 1970/71 and 2010/2011 seasons. The brown “X” indicates the vortex center during the east QBO mode and the blue “+” is west QBO. The yellow star is the long-term average position of the vortex center throughout the study period.

The outcomes demonstrate that during the west phase of the QBO (marked by blue “+”), the vortex centers tend to form further northward or southward from the long-term average position compared to the position of the east phase (marked by brown “X”). If we consider that the equator in this study is

the trough line that crosses the vortex long-term mean center, then the variability of the vortex seasonal mean here seems to agree with Gray et al.'s (1992) claim that the QBO east phase tends to enhance deep convective activity close to the equator while the west phase shows a tendency to enhance it away from the equator due to the thermal wind effects of QBO.

By computing the average of the seasonal latitudinal and longitudinal position of the vortex centers of both phases, it was found that the values were almost the same as the long-term seasonal average as shown in Table 3.2.6, which made them statistically insignificant (see Appendix A). However, this could probably also imply as if all the 41 seasonal average centers are mirrored to one another with the long-term average location acts as a reflection point.

	All	West QBO	East QBO
No. of seasons	41	20	21
Latitudinal average	2.4	2.5	2.4
Longitudinal average	110.6	110.5	110.6

Table 3.2.6: The average positions (degree) of the Borneo vortex centers stratified by QBO phases.

Over long-term period, the fluctuation of the vortex seasonal average positions for both phases seems to be in balance with respect to its mean position, which is also the mean position of the monsoon trough or ITCZ throughout the study period. Therefore, by taking into account the findings of

Gray et al. (1992), it can be proposed that for the case of west QBO mode, Borneo vortices that are formed further north of the mean monsoon trough, will be equipoised by the vortices located far to the south after sometime or vice versa, while those in east mode are generally found close to the trough.

Since the vortex did not demonstrate much variation under the influence of QBO, the variability reveals by the periodogram in Fig. 3.2.7 is likely to follow the TBO phases, i.e. another climate system that has a similar return period as the QBO. Applying the same method as in previous analysis, the average position for each seasonal vortex center from Table 3.2.2 were plotted according to its respective TBO phases listed in Table 2.4.4. The outcomes from Fig. 3.2.10 show that the distribution of the vortex centers has no distinctive pattern to distinguish between the phases. Thus, no definite conclusion could be made on this analysis.

Further analysis was done by comparing the mean of seasonal latitudinal and longitudinal positions of the vortex center during each TBO phases. The seasonal vortex centers from Table 3.2.2 were totaled and averaged accordingly, and then tabulated in Table 3.2.7. The results demonstrate that there is no significant difference for both cases as well. The latitude and longitude values not only show a small variation with each other, they also display only a slight difference with the vortex long-term averages. All these analyses could imply that TBO event does not play a major role in governing the climatology of the Borneo

vortex in this region. This is also supported but insignificant outcome of their statistical tests as revealed in Appendix A.

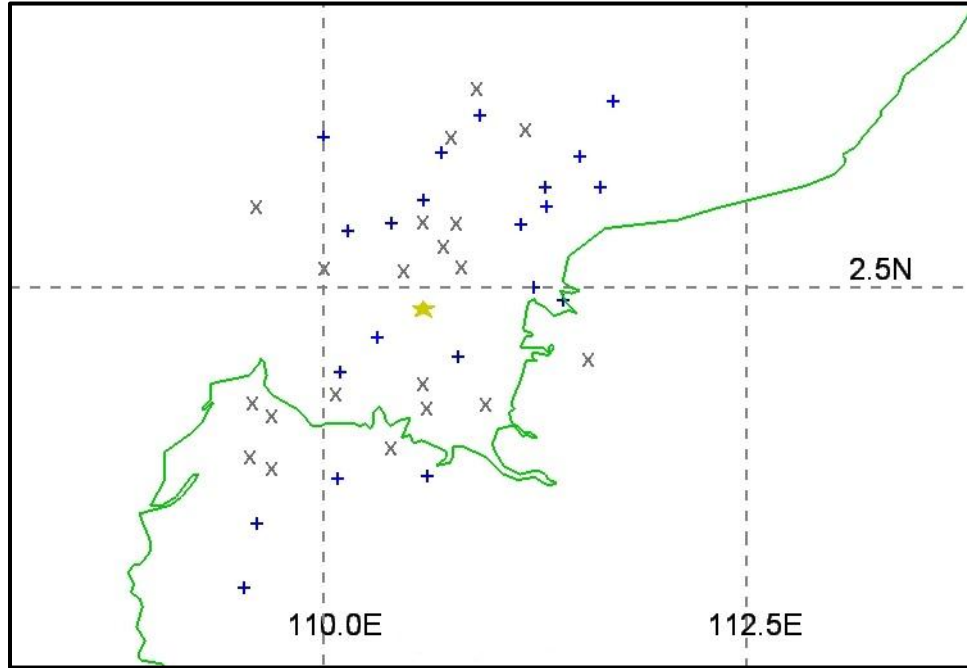


Fig. 3.2.10: The position of the seasonal Borneo vortex centers for 41 winter monsoon between 1970/71 and 2010/2011 seasons. The grey “X” indicates the vortex center during the weak TBO mode and the blue “+” is strong TBO. The yellow star is the long-term average position of the vortex center throughout the study period.

	All	Strong TBO	Weak TBO
No. of seasons	41	21	20
Latitudinal average	2.4	2.5	2.4
Longitudinal average	110.6	110.7	110.4

Table 3.2.7: The average positions (degree) of the Borneo vortex center stratified by TBO phases.

However, the results of the analyses changed when the seasonal mean position of the Borneo vortex was determined based on the stratification of ENSO years in TBO phases since some earlier studies had shown that TBO and ENSO are related (Meehl (1994), Wu and Kirtman (2004), Meehl and Arblaster (2011), etc.). The analyses were done by segregating the seasonal vortex positions in Table 3.2.2 and matched them with respective seasons listed in Table 2.4.1 and Table 2.4.4. The final outcomes were summarized as in Table 3.2.8.

	Strong TBO			Weak TBO		
	EN	LN	NEU	EN	LN	NEU
No. of seasons	5	7	9	5	3	12
Latitudinal average	2.2	3.1*	2.3	1.9	2.4	2.3
Longitudinal average	110.5	111.1	110.6	110.3	110.8*	110.4

Table 3.2.8: The average positions (degree) of the Borneo vortex center stratified by ENSO in TBO phases. "*" denotes the value is statistically significant at 99% confidence level.

Compared to the results in Table 3.2.7, the outcomes here reveal that the seasonal Borneo vortex center has been forced to move away from its normal mean center in both TBO phases under the influence of different ENSO periods. Within strong and weak TBO phase, the EN events tend to push the vortex mean center southwestward of its normal position found in Table 3.2.7, while the mean center was forced to shift northeastward under the influence of LN years. As in NEU events, the vortex mean center remains unchanged.

As mentioned before, the TBO is just the tendency for a relatively strong monsoon to be followed by a relatively weak one, and vice versa (Meehl, 1997). Based on the earlier findings, the vortex seasonal mean center did not change much under its influence, which likely suggests that the intensity of winter monsoon has no impact on the Borneo vortex seasonal position. On the other hand, EN and LN events have always been associated with the warming and cooling of the SST including over this region, as shown in many works such as by Tangang and Juneng (2004), Zuki and Lupo (2008) and Lin. et al. (2011). From the results found earlier, the vortices probably prefer to stay over warm location, which cause them to form more over the water body in LN years and move close to or on the inland during EN phase as a result of relatively cooler SST.

Therefore, within the background climate of ENSO in TBO, the behavior of the seasonal Borneo vortex center tends to follow the orientation of the mean vortex position of ENSO climate, which suggest the role of ENSO in modulating the TBO events. Statistically, some of these behaviors indicate that there are strong associations between them, as shown in Appendix A. However, only the events of the vortex latitudinal position during the stratification of LN years in both the strong and weak TBO phases pass the statistical tests at 99% confidence level.

Throughout the entire analyses, they show that the Borneo vortex position has the inclination to get pushed northward and northeastward of the long-term

mean center when the atmospheric background was favorable while it moved southward and southwestward under less conducive condition. This implies that the longitude and latitude values tend to be large during active condition and low when it is less active. These relationships were tested and it was found that they were quite strongly correlated with the correlation coefficient of 0.56, which was statistically significant at 99% confidence level.

3.3 Borneo vortex system and lifespan

In section 3.1, we discussed the climatology of the Borneo vortices according to their monthly and seasonal frequencies throughout 41 winter monsoon seasons, wherein every Borneo vortex was treated as a separate entity and not related to each other. However, in this section, the study involved the analyses of number of vortices that combined together into a group, which is termed as Borneo vortex system. This system was determined depending upon the lifespan of the Borneo vortex, i.e. from the time when the vortex was first identified within the study domain until it finally decayed or moved out from the area based on day to day analysis of 0000 UTC wind field data at 925 hPa level. Therefore, this kind of analyses not only would assist in understanding the climatological behaviors of the vortex systems, but it could also help in determining the duration or lifespan of each system.

The vortex systems were identified based on the time of their genesis. Therefore, for the case where the vortex system lifespan stretched between two

different months, it would be considered to belong to the month where the system was first originated. By taking this into consideration, the Borneo vortex systems were documented according to their respective month and season, as summarized in Table 3.3.1. A total of 641 Borneo vortex systems were established throughout the study period with a wide range of variation between 9 and 21 systems per season, where the highest quantity was recorded in 1993/94 and 1977/78 while the lowest during 1991/92 winter monsoon season.

The number of vortex systems averaged 15.6 events per season, which was an average of about 3.9 systems per month throughout the 4 months of winter monsoon season. Looking at the actual monthly distribution listed in Table 3.3.2, the variation is considered insignificant. On the other hand, the analyses done in earlier section demonstrate that the vortex mean monthly frequency shown in Table 3.1.2 is highly seasonal. This indicates that, over the long-term period, the monthly number of vortex systems over this region is almost constant throughout the monsoon period but not its lifespan.

This implies that, each vortex system has different duration throughout its life cycle. If the system has a shorter lifespan, the impact towards the winter monsoon activity could not be as substantial as the one that persists longer. Therefore, the analyses of the vortex system lifespan are found to be more meaningful than examined the systems quantity. Basically, the lifespan information could be obtained by dividing the number of vortices or days in Table

Season	Nov	Dec	Jan	Feb	Total
2010/11	5	3	4	5	17
2009/10	2	5	2	3	12
2008/09	7	4	2	4	17
2007/08	2	6	5	5	18
2006/07	3	6	2	7	18
2005/06	4	2	4	4	14
2004/05	5	5	1	3	14
2003/04	6	6	5	2	19
2002/03	4	3	3	2	12
2001/02	5	4	5	3	17
2000/02	3	3	5	3	14
1999/00	4	4	7	4	19
1998/99	1	4	3	3	11
1997/98	7	4	4	4	19
1996/97	1	3	3	3	10
1995/96	5	2	4	4	15
1994/95	5	2	3	2	12
1993/94	7	5	4	5	21
1992/93	5	2	5	3	15
1991/92	6	4	2	2	14
1990/91	2	3	1	3	9
1989/90	5	3	7	1	16
1988/89	3	2	6	3	14
1987/88	3	5	9	2	19
1986/87	4	4	2	3	13
1985/86	5	4	2	7	18
1984/85	4	4	4	5	17
1983/84	3	4	5	5	17
1982/83	5	5	5	4	19
1981/82	3	4	4	5	16
1980/81	4	2	2	7	15
1979/80	4	3	4	5	16
1978/79	3	5	4	4	16
1977/78	6	4	5	6	21
1976/77	6	3	3	3	15
1975/76	4	3	3	3	13
1974/75	4	3	5	4	16
1973/74	4	6	4	4	18
1972/73	6	5	5	2	18
1971/72	3	4	4	3	14
1970/71	2	3	4	4	13
Total:	170	156	161	154	641

Table 3.3.1: The monthly and seasonal number of Borneo vortex systems.

	All	Nov	Dec	Jan	Feb
No. of seasons	41	41	41	41	41
Total systems	641	170	156	161	154
System per season	15.6	4.1	3.8	3.9	3.8

Table 3.3.2: The seasonal and monthly average number of Borneo vortex systems.

3.1.1 by the number of vortex systems found here. The final outcomes were then tabulated in Table 3.3.3.

Seasonally, the mean vortex system lifespan varies between 1.7 and 5.2 days. The shortest average period was found in the winter monsoon season of 1997/98 where the background climate was driven by EN, warm PDO, east QBO and strong TBO phases, as listed in section 2.4. On the other hand, the longest average lifespan was recorded in 1971/72 season, where the climate condition was driven by LN, cold PDO, west QBO and weak TBO phases.

As shown in Table 3.3.4, each vortex system has a long-term average lifespan of 3.6 days, which is within a timescale of synoptic type of weather systems. With such timescale, a lot of scholars, such as Cheang (1977 and 1978), Johnson and Priegnitz (1981) and Chang et al. (2003 and 2005), have considered the Borneo vortex as a synoptic scale weather system. However, based on the actual lifespan of each of the vortex systems found here, more than half did not reach the lifespan of at least 3 days or greater, which makes them more likely to be treated as mesoscale type of weather systems. Hence, through

Season	Nov	Dec	Jan	Feb	Seasonal Average
2010/11	2.0	6.0	3.0	1.4	2.8
2009/10	9.0	3.6	3.0	1.3	3.8
2008/09	2.4	10.3	3.5	2.0	4.3
2007/08	2.5	4.7	1.4	2.8	3.0
2006/07	2.7	5.2	8.5	1.3	3.6
2005/06	3.3	4.5	5.0	4.0	4.1
2004/05	2.0	4.4	5.0	2.0	3.1
2003/04	3.0	1.7	2.4	1.0	2.2
2002/03	3.5	3.0	4.7	2.5	3.5
2001/02	2.2	4.3	2.0	3.0	2.8
2000/02	3.7	4.3	4.8	2.0	3.9
1999/00	4.0	5.0	2.0	4.5	3.6
1998/99	9.0	5.3	3.7	3.7	4.7
1997/98	1.7	2.5	1.3	1.3	1.7
1996/97	6.0	6.7	3.3	4.7	5.0
1995/96	6.0	3.0	4.5	3.8	4.6
1994/95	3.2	6.0	2.7	1.0	3.2
1993/94	2.0	2.4	3.3	1.4	2.2
1992/93	5.2	7.0	1.2	1.7	3.4
1991/92	5.7	2.5	2.0	1.0	3.6
1990/91	2.0	5.0	9.0	2.3	3.9
1989/90	4.2	4.0	1.9	1.0	2.9
1988/89	4.3	5.5	2.0	6.0	3.9
1987/88	3.0	5.2	2.4	2.5	3.3
1986/87	3.5	2.0	5.0	2.0	2.9
1985/86	5.6	2.8	5.5	1.9	3.5
1984/85	2.5	8.8	1.8	2.6	3.8
1983/84	7.3	3.8	3.4	4.2	4.4
1982/83	1.6	4.4	2.0	1.3	2.4
1981/82	4.3	4.3	3.5	2.0	3.4
1980/81	4.8	13.5	3.0	1.7	4.3
1979/80	6.0	5.0	3.8	2.6	4.2
1978/79	8.0	4.4	1.5	2.5	3.9
1977/78	2.2	5.3	2.6	1.3	2.6
1976/77	4.7	5.7	5.3	4.7	5.0
1975/76	5.5	6.3	5.0	3.3	5.1
1974/75	3.3	7.3	4.2	4.0	4.5
1973/74	3.3	3.8	2.5	6.0	3.9
1972/73	2.7	2.4	4.4	2.0	3.0
1971/72	6.7	7.5	3.3	3.3	5.2
1970/71	7.0	6.3	4.5	3.8	5.1

Table 3.3.3: The monthly and seasonal average lifespan of the Borneo vortex systems.

these analyses, it could be deduced that the vortex can be classified of having both the mesoscale and synoptic type of weather system scale.

There is a slight difference between the total number of vortices or days with vortices in Table 3.1.1 and the one shown in Table 3.3.4. This is happening due to the way the vortex quantity was counted in both sections. In section 3.1, only the one formed within the study domain was acknowledged as a Borneo vortex. While, in here, the days with vortices were determined throughout the entire life of the vortex system, even though the vortex sometimes moves out from the study domain and re-enter again. Due to that, more vortices were observed here than in earlier section.

	All	Nov	Dec	Jan	Feb
No. of seasons	41	41	41	41	41
Total systems	641	170	156	161	154
Total vortices or days	2,289	646	740	503	400
Average lifespan	3.6	3.8	4.7	3.1	2.6

Table 3.3.4: The seasonal and monthly average lifespans (days) of the Borneo vortex systems.

Looking at the monthly mean vortex system lifespan in Table 3.3.4, December has the longest period, followed by November, January and February. The order seems to match the active period of winter monsoon season based on the studies of the atmospheric backgrounds over the region revealed by Chang et al. (2005b), and Zuki and Lupo (2008). Hence, it implies that the longer the

timespan of each vortex system, the active the winter monsoon could become, which leads by December, followed by November, January and February. The extensive vortex system lifespan in December has also been linked to the formation of two unusual tropical cyclones over the study domain, namely Tropical Storm Greg in 1996 and Typhoon Vamei in 2001.

Through the analyses of the wind field data used for this study, the genesis of Typhoon Vamei was first detected as a Borneo vortex on 20th December near the equator at 0.3°N latitude and 110.6°E longitude and remained in the study domain until 28th December of 2001. While Tropical Storm Greg was first formed as a Borneo vortex on 11th December at 3.0°N latitude and 112.1°E longitude and remained within the region for 16 days before decaying on 26th December of 1996. However, the actual observations from the Typhoon Warning Center considered this event as two separate cyclonic systems. The first portion was considered as tropical depression “41W” that lived between 12th and 21st December, and the remaining part was Tropical Storm Greg that existed from 21st to 27th December of 1996 (Lander et al., 1999).

Using the data listed in Table 3.3.3, the seasonal means of the vortex system lifespan were transformed into a time-series graph depicted as Fig. 3.3.1. The outcomes show that the graph line runs quite vigorously throughout the study period, which possibly following certain interannual and/or interdecadal variations of the atmospheric oscillations. The long-term linear trend shows a downward tendency, which suggests that the seasonal mean vortex system

lifespan basically decreasing throughout the study period from about 4.1 days in 1970/71 winter monsoon season to 3.2 days in 2010/11. However, this linear trendline has a very small R^2 value of only 0.1086, which indicates a weak correlation between the trendline and the seasonal vortex system lifespan.

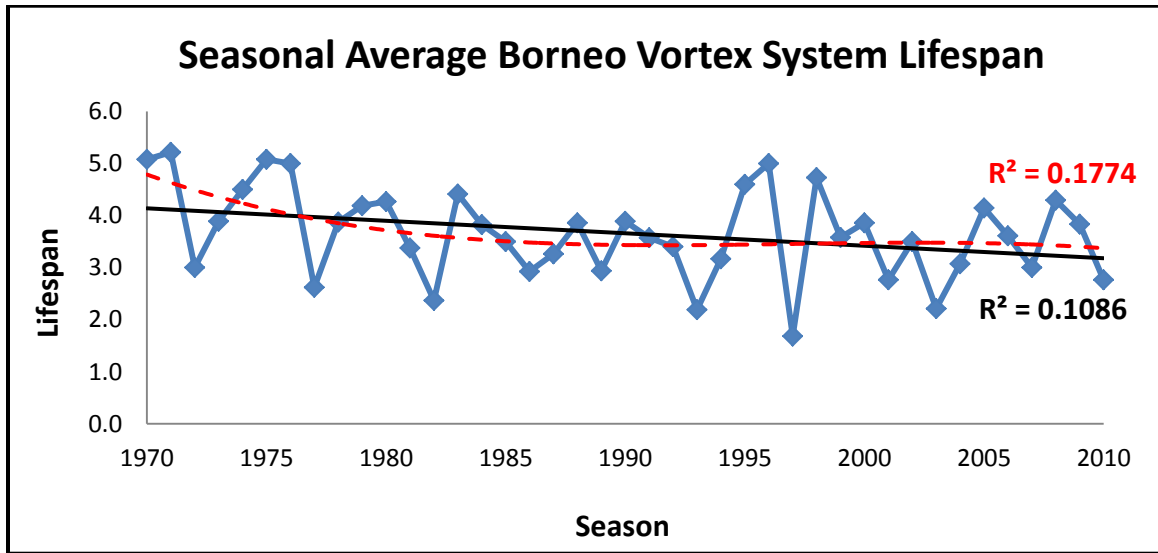


Fig. 3.3.1: Seasonal mean of Borneo vortex system lifespan between 1970/71 and 2010/11 winter monsoon seasons. The black line indicates the linear trendline and red-dashed line is the 3rd order polynomial trendline.

The R^2 value increases by about 70% to 0.1774 when the 3rd order polynomial regression line is applied to the graph. Even though the value is still small but it shows that the correlation has turned stronger than the linear trend analysis. This trend demonstrates that the vortex system lifespan decreases is tremendously at the early part of the study period. By mid-80's, the vortex lifespan reaches the bottom of the curve line and since then it remains the same through the entire study course. One of the reasons the curve line decreases probably due to the shift of PDO phases from cold to warm periods. However, as

the PDO shifts back to cold phase toward the end of the 20th century, the curve slope does not change, which means that the PDO may not play any role in the variation of the seasonal mean of the vortex lifespan here.

There are possibly other types of natural events that might influence the vortex lifespan variation throughout the study period. In order to identify that, the Fourier power-spectral method was again applied as in previous sections. The outcomes were presented in a form of cyclical series on the periodogram in Fig. 3.3.2 by filtering out the first and the last peaks of the spectrum. It was then tested against the white-noise background, which reveals that the seasonal mean vortex lifespan has certain number of significant return periods that emulate common interannual variability of tropical climate oscillations.

At 95% confidence level, the peaks are considered significant only at cycle number 8 and 10, which indicate that the vortex lifespan has a periodicity of 5 and 4 years, respectively. The only natural event that is known of having such return periods is the ENSO. At 80% confidence level, more peaks are found to be significant. The peaks at number 12 and 13 have similar recurrence period to ENSO, while the peaks between cycle number 16 and 21 are potentially related to TBO or QBO, or combination of both phases, which indicate 2 to 2.5 years of oscillation periods. Further information about ENSO, QBO and TBO events was already discussed in section 2.4.2.

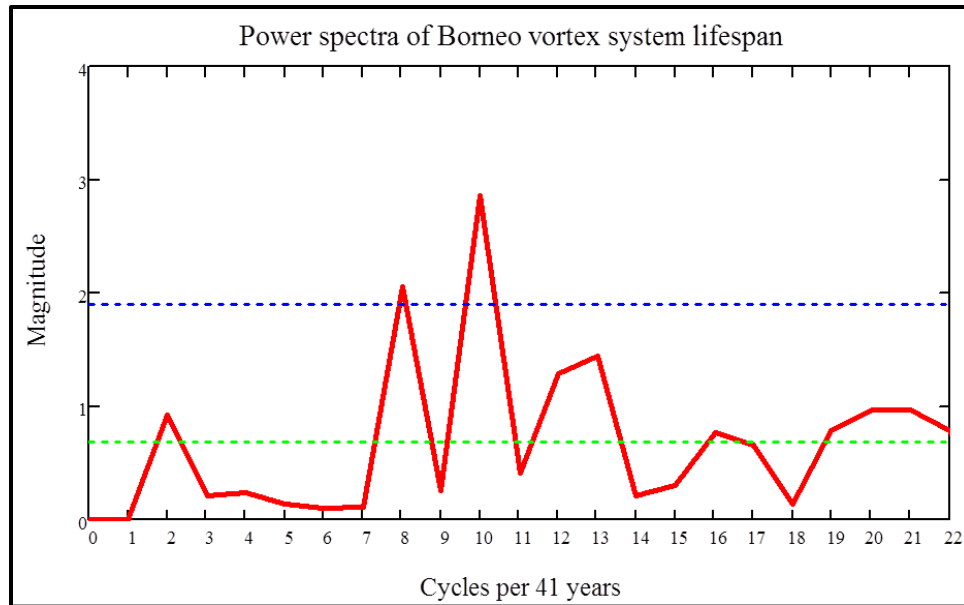


Fig. 3.3.2: The seasonal lifespan of Borneo vortex systems for 41 winter monsoon seasons plotted as Fourier power spectra with the ordinate displaying the magnitude of the Fourier coefficient and the abscissa displaying the period of cycles per 41 years. The blue- and green-dashed lines indicate the 95% and 80% confidence level against the white-noise background, respectively.

To investigate the relationship between the ENSO phases and the seasonal vortex systems lifespan, the compositing analysis technique was again applied here by isolating the number of days with Borneo vortex and the vortex systems quantity listed in Table 3.3.1 according to seasons of respective ENSO years listed in Table 2.4.2. Both data were totaled before being divided accordingly in order to determine the vortex system lifespan. The final output was shown in Table 3.3.5.

The results show that the seasonal mean vortex system lifespan stays much longer during LN years and shorter in EN periods compared to their long-term mean, while it does not change much with respect to NEU years. This suggests that during LN phase, the atmospheric backgrounds are probably very

favorable and that makes it conducive for the vortex systems to remain longer in the study domain. In contrast, the atmosphere perhaps has turned slightly passive in EN years, which then shorten the vortex system lifespan.

	All	EN	LN	NEU
No. of seasons	41	10	10	21
Total systems	641	159	153	329
Total days	2,289	509	622	1,158
Average Lifespan	3.6	3.2	4.1	3.5

Table 3.3.5: The seasonal mean of Borneo vortex lifespan (days) stratified by ENSO years

These outcomes seem to match the works of Chang et al. (2004a), Tangang and Juneng (2004), and Zuki and Lupo (2008). They found that LN events tend to enhance the background potential for convective activities in this region and turn them weak during EN period. However, statistically, all the mean values shown in Table 3.3.6 are insignificant compared to the vortex lifespan long-term mean, as shown in Appendix A. It almost reaches the 90% confidence level for the case of LN event, but the rest are all below 80% level.

Another event that is believed to influence the seasonal variability of the Borneo vortex system lifespan over the study domain is the QBO. This is based on the power-spectra signal detected by the periodogram in Fig. 3.3.2, which shows that the vortex systems have a return period of about 2.5 to 2 years. In order to examine it, the same methods were applied as in previous analyses,

only that the data were segregated according to season of different QBO phases listed in Table 2.4.3. The number of vortex days was then divided by the vortex system quantity accordingly before being tabulated in Table 3.3.6.

	All	West QBO	East QBO
No. of seasons	41	20	21
Total systems	641	319	322
Total days	2,289	1,144	1,145
Average Lifespan	3.6	3.6	3.6

Table 3.3.6: The seasonal mean of Borneo vortex lifespan (days) stratified by QBO phases.

The outcomes reveal that the seasonal average of the Borneo vortex system lifespan remains the same in both QBO phases as compared to the long-term mean, which supports Baldwin et al. (2001) claim that the impact of QBO towards the climate variability in the tropics is almost nothing. Therefore, one could possibly deduce that the QBO does not play any role in governing the variability of the vortex lifespan over this region.

In addition to QBO, there is also another natural event that has a similar periodicity pattern, known as TBO. The seasonal variation of the vortex systems lifespan was determined following the same technique used in previous analyses, except that the data were stratified conforming to season of strong and weak modes of TBO from Table 2.4.4. The final outputs were summarized as in Table 3.3.7 below.

	All	Strong TBO	Weak TBO
No. of seasons	41	21	20
Total systems	641	338	303
Total days	2,289	1,242	1,047
Average Lifespan	3.6	3.7	3.5

Table 3.3.7: The seasonal mean of Borneo vortex lifespan (days) stratified by TBO phases.

The results reveal that the seasonal average of the Borneo vortex systems lifespan does not vary significantly with respect to the long-term mean. They are supported by statistical tests where both means fail to pass any significant levels, as shown in Appendix A. All these outcomes suggest that the influence of TBO towards the variability of the seasonal vortex lifespan in the study region is negligible, which follows the same results discovered in QBO event.

As discussed in the previous section, TBO and ENSO are strongly connected due to the monsoon-ENSO coupling that governs the TBO phases (Wu and Kirtman, 2004). In order to investigate such relationship, the same methods were used as in earlier analyses. The outcomes in Table 3.3.8 show that the seasonal means of the vortex systems lifespan vary greatly by the stratification of ENSO events in TBO phase as compared to the condition shown in Table 3.3.7.

The results reveal that, under the influence of EN years, the vortex seasonal mean lifespan is getting shorter in both TBO events than in condition

showed in Table 3.3.7. On the other hand, the LN events seem to force the vortex lifespan to prolong further than its normal duration. As for the case of NEU years, its lifespan does not change much. These outcomes imply that both the EN and LN years have driven the TBO to follow their contrast behaviors, which strongly support the assertion of many scholars, such as Meehl and Arblaster (2002 and 2011), and Wu and Kirtman (2004).

	Strong TBO			Weak TBO		
	EN	LN	NEU	EN	LN	NEU
No. of seasons	5	7	9	5	3	12
Total systems	85	106	147	74	47	182
Total days	284	430	528	225	192	630
Average Lifespan	3.3	4.1	3.6	3.0	4.1	3.5

Table 3.3.8: The seasonal mean of Borneo vortex lifespan (days) stratified by ENSO in TBO phases.

As discussed in previous analyses, LN event has a tendency to enhance the atmospheric background, thus stretches the vortex lifespan, while the impact is the opposite during the EN years. Since both of them are more dominant than the TBO phases, the results found here clearly reveal of these claims. Even though the statistical tests reveal that several of these relationships are relatively strong, none of them passes the 90% confidence interval, as shown in Appendix A.

As mentioned earlier, the extensive lifespan of Borneo vortex systems over this study domain has been associated with the active monsoon periods and also could become one of the main mechanisms in the formation of tropical cyclones, as revealed by Chang et al. (2003). The study on the tropical cyclones activities in this area by Zuki and Lupo (2008) had shown that their variability tended to follow the ENSO events. More tropical cyclones were formed during LN years and less in EN periods, which agree with the variation of the vortex system lifespan found in Table 3.3.5.

Furthermore, Zuki and Lupo (2008) had divided the tropical cyclone activity into sample groups of active and non-active years in order to determine the contribution of SST, wind shear, divergence and relative vorticity in the formation and maintenance of the tropical cyclone in this region. Using the years chosen by them, the seasonal mean lifespan of the Borneo vortex systems was calculated so as to find if any association that could probably exist, which can be used to support this study. The outputs were summarized in Table 3.3.9.

The results show that during the active periods, which coincide with 1998/98, 1996/97, 1995/96 and 1970/71 winter monsoon seasons of this study, the seasonal mean lifespan of the Borneo vortex systems tend to be lengthier than two other non-active groups. Additionally, this mean value is the longest among the climatic conditions that has been set throughout this study. The p-value from the t-test indicates that it is statistically significant at 99% confidence

level, which implies that the long seasonal mean vortex lifespan corresponds well with tropical cyclone activity during the active periods.

	Active	Non-active (Warmest SSTs)	Non-active (Coldest SSTs)
No. of seasons	4	3	5
Total systems	49	44	81
Total days	237	142	299
Average Lifespan	4.8*	3.2	3.7

Table 3.3.9: The seasonal mean of Borneo vortex lifespan (days) based on the sample groups of tropical cyclone activity from Zuki and Lupo (2008). “*” denotes the value is statistically significant at 99% confidence level.

Since the study domain used here and in their work are almost the same, whatever findings they found could reflect the outcome of these analyses. Zuki and Lupo (2008) showed that the climate were driven by LN and cold NEU years during active periods, while both non-active periods were under the influence of EN and warm NEU events. In addition, the mean environment of the main atmospheric backgrounds during active period was very conducive, while it was less favorable for the case of non-active period.

The warmest SSTs were found to be less helpful in having lengthy vortex lifespan since the coldest SSTs managed to generate longer vortex lifespan than the warmest one, as demonstrated in Table 3.3.9. However, all the coldest SSTs shown in Zuki and Lupo (2008) were greater than 27°C, which is above the

threshold value for the development of any tropical cyclone. All these outcomes suggest that the Borneo vortex systems lifespan able to persist longer in this region owing to the support of favorable atmospheric ingredients, which include the warm SST, strong convergence and cyclonic circulation. As for the case of short vortex lifespan, the effect should be the opposite.

3.4 Borneo vortex intensity

In this section, we further examine the behavior of the Borneo vortex within the study domain by categorizing each of them into different type of intensities. The stronger the intensity, the more active and severe the winter monsoon could become, since the Borneo vortex is considered as one of the synoptic weather systems that control the winter monsoon in this region (Cheang (1987), Chang et al. (2005) and Tangang et al. (2008)). The vortex intensity was determined based on the method explained in chapter 2. The Borneo vortices are considered as weak if all the speeds of the wind field in the $2.5^\circ \times 2.5^\circ$ grid square around the vortex center are 5 ms^{-1} or less. If any portion of the grid square has wind speeds greater than 5 ms^{-1} but less than or equal to 10 ms^{-1} , the vortices are classified as moderate while strong intensity is for those vortices that are supported by the wind speeds greater than 10 ms^{-1} .

After completing the classification of all the vortices, they were summarized and tabulated according to their respective seasons and months as shown in Table 3.4.1. The outcomes reveal that the majority of the vortices are

fallen under weak intensity category, which occupied almost 77% (1757/2278) of the total number of the Borneo vortex, followed by moderate intensity at about 17% (396/2278) and strong vortex with slightly above 5% (125/2278). Based on the analyses of the 925 hPa wind field, strong and moderate vortices were formed mainly due to their interaction with cold surge winds that come all the way from Siberia in central Asia as discussed by many scholars, such as Ramage (1971), Krishnamurti et al. (1973), Cheang (1987) and Chang et al. (2005b). The surge not only able to enhance the Borneo vortex but it also can cause the winter monsoon in this region to become more active and vigorous.

From Table 3.4.1, the figures clearly show that there is a wide range variation in term of the numbers of Borneo vortex occurrences for each category of intensity from one season to another throughout the study period. The weak one is ranging between 28 and 59 cases, where the maximum quantity was observed during 1979/80 and 1983/84 winter monsoon periods while the minimum value was found in 1990/91 season. For the case of moderate intensity, the maximum frequency was 22, which were observed during 2008/09 season while the lowest number of appearances was spotted in 1997/98 with only 2 occasions.

As for the case of strong vortex intensity, the occurrence was not as frequent as other categories. The maximum number of such intensity took place in 1976/77 with 11 cases while 12 seasons did not record any vortex of such category throughout the study period. This indicates that the vortex with strong

Season	Nov			Dec			Jan			Feb			Annual Total		
	W	M	S	W	M	S	W	M	S	W	M	S	W	M	S
2010/11	8	1	0	18	2	0	12	0	0	7	0	0	45	3	0
2009/10	8	6	4	15	3	0	3	3	2	4	0	0	30	12	6
2008/09	12	3	2	15	12	2	9	7	3	8	0	0	44	22	7
2007/08	4	1	0	13	5	4	12	1	0	8	1	1	37	8	5
2006/07	7	1	0	20	3	0	13	9	3	9	0	0	49	13	3
2005/06	8	3	0	10	1	0	20	0	0	12	4	0	50	8	0
2004/05	10	0	0	13	4	0	6	4	0	6	0	0	35	8	0
2003/04	11	2	0	9	6	1	13	0	0	2	0	0	35	8	1
2002/03	9	4	0	9	0	0	7	7	0	5	0	0	30	11	0
2001/02	5	3	3	7	8	2	10	0	0	9	0	0	31	11	5
2000/01	10	0	0	9	3	2	19	0	0	6	3	0	44	6	2
1999/00	12	1	0	7	10	5	14	0	0	12	4	2	45	15	7
1998/99	10	0	0	11	1	3	14	2	1	10	1	0	45	4	4
1997/98	10	2	0	10	0	0	5	0	0	5	0	0	30	2	0
1996/97	6	0	0	3	11	6	10	0	0	12	1	1	31	12	7
1995/96	12	1	3	5	7	3	16	1	0	15	1	0	48	10	6
1994/95	8	0	0	15	5	0	8	0	0	2	0	0	33	5	0
1993/94	14	0	0	8	4	0	10	3	0	7	0	0	39	7	0
1992/93	17	9	0	9	5	0	5	1	0	5	0	0	36	15	0
1991/92	18	4	0	12	9	1	4	0	0	2	0	0	36	13	1
1990/91	3	1	0	13	2	0	6	2	0	6	1	0	28	6	0
1989/90	15	5	0	13	0	0	13	0	0	1	0	0	42	5	0

1988/89	4	6	3	11	2	0	11	1	0	15	0	0	41	9	3
1987/88	8	1	0	19	6	1	18	1	0	8	0	0	53	8	1
1986/87	6	4	1	11	1	0	10	0	0	6	0	0	33	5	1
1985/86	15	1	0	15	4	3	10	2	0	9	0	0	49	7	3
1984/85	9	1	0	14	11	1	13	3	0	13	0	0	49	15	1
1983/84	5	2	2	17	6	1	17	4	0	20	0	0	59	12	3
1982/83	8	0	0	18	3	0	11	0	0	5	0	0	42	3	0
1981/82	7	2	2	12	3	4	11	3	0	10	0	0	40	8	6
1980/81	11	1	0	16	10	0	7	3	3	14	0	0	48	14	3
1979/80	18	6	0	13	4	0	16	0	0	12	1	0	59	11	0
1978/79	8	8	3	18	5	0	10	0	0	10	0	0	46	13	3
1977/78	11	2	0	15	5	1	11	2	0	8	0	0	45	9	1
1976/77	7	10	7	13	3	4	15	0	0	13	0	0	48	13	11
1975/76	15	3	3	8	4	7	18	0	0	10	0	0	51	7	10
1974/75	11	2	0	9	4	5	16	7	0	15	3	0	51	16	5
1973/74	10	3	1	9	8	7	12	0	0	17	1	0	48	12	8
1972/73	12	1	1	12	0	3	16	2	0	6	1	0	46	4	4
1971/72	7	7	5	21	6	0	14	3	0	11	0	0	53	16	5
1970/71	9	5	0	13	2	0	16	3	3	15	0	0	53	10	3
Total	398	112	40	508	188	66	481	74	15	370	22	4	1757	396	125

Table 3.4.1: Monthly and seasonal frequencies of Borneo vortices based on their intensity. Weak (W), moderate (M) and strong (S) intensities correspond to the wind speed around the vortex within 2.5° X 2.5° grid square with at least 2-5 ms⁻¹, 5-10 ms⁻¹ and greater than 10 ms⁻¹, respectively.

intensity is not a regular episode during winter monsoon season in the study region. However, once it is generated, it can turn into more powerful weather system, such as a tropical cyclone.

In some cases, the winds that wrap around the strong intensity vortex exceeded 17 ms^{-1} , i.e. attained the strength of a tropical storm. With the right ingredients, some of them reached the tropical cyclone intensity, which is considered unusual over this region due to its location close to the equator. On 24th December, 1996, a strong Borneo vortex with maximum wind speed of 23 ms^{-1} had transformed into Tropical Storm Greg and made a landfall over the northern tip of Borneo Island (Lander et al., 1999). 238 people got killed in this event together with US\$ 52 million worth of economic loss (Ooi and Ling, 1996).

In another event, the wind around the vortex had been reported to reach 39 ms^{-1} and gust up to 54 ms^{-1} after it evolved into Typhoon Vamei on 27th December, 2001 (Chang et al., 2003). The typhoon caused severe flooding and mudslides in the southern part of Malaysian peninsula with more than 17,000 people evacuated and five reported deaths (Tangang et al., 2007). Besides, of these two events, there were 18 other cases where the tropical cyclones have been documented to form within this region throughout the study period, as documented by Zuki and Lupo (2008). All these systems were probably come from any of 125 Borneo vortices of strong intensity identified here.

Looking at Fig. 3.4.1, the monthly variation shows by the weak vortex intensity basically coincide with the variation found earlier in Fig. 3.1.2 when the

analyses were first done on the entire Borneo vortices quantity. The most number of Borneo vortices with weak intensity were documented in December, and then followed by January, November and February. However, when dealing with the vortex quantity of moderate and strong intensities, the sequence changes a bit with November occurrences being greater than January, while during December and February the most and the least number of vortices occurred, respectively.

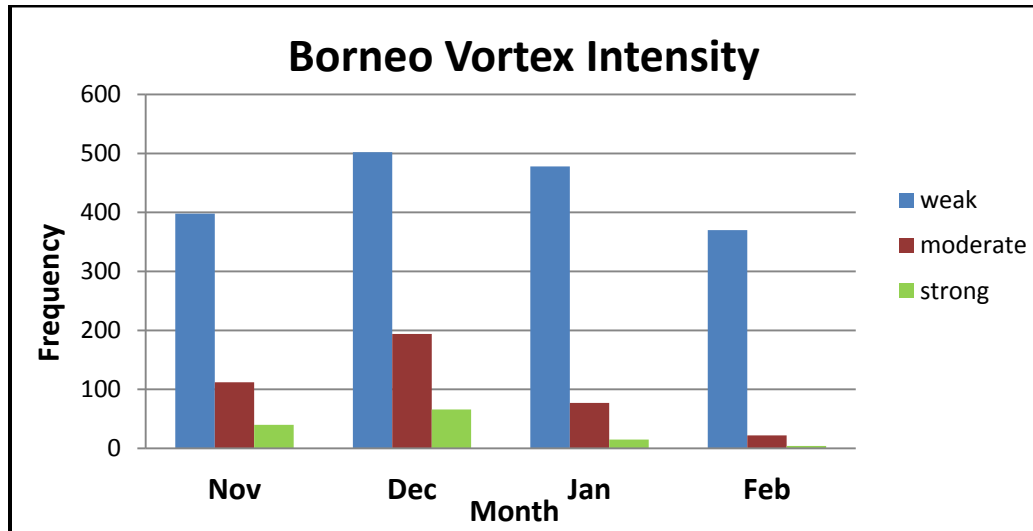


Fig.3.4.1: Monthly distribution of Borneo vortex frequency of different intensities.

If we consider that the winter monsoon in this region is driven by moderate and strong Borneo vortices, therefore based on Fig. 3.4.1, December should be the most active period, followed by November, January and February. These outcomes agree well with most studies, such as Cheang (1977), Chang et al. (2005b) and Wang et al. (2009) that December is the most active month within winter monsoon period.

Based on the long-term average value summarized in Table 3.4.2, the region experienced only 3.0 strong intensity vortices per season. The moderate category is slightly below 10 vortices, while weak intensity has with an average of 42.9 vortices, seasonally. However, looking at the monthly distribution of the Borneo vortex in Table 3.4.1 and the bar chart in Fig. 3.4.1, they show that most of the strong and moderate vortices are detected in the month of November and December, which suggests that both months have greater chances for the Borneo vortex to turn into tropical cyclone. Zuki and Lupo (2008) also found that the majority of the tropical cyclones in this region were formed within these two months. On average, about 1.0 of strong and 2.7 of moderate vortices were generated during November, while the number was greater in December with 1.6 and 4.7 of strong and moderate vortices, respectively.

	Seasonal	November	December	January	February
Weak	42.9	11.7	12.4	9.7	9.0
Moderate	9.7	2.7	4.6	1.9	0.5
Strong	3.0	1.0	1.6	0.4	0.0

Table 3.4.2: The long-term seasonal and monthly mean of Borneo vortex frequency with different intensities.

On the contrary, January and February only experience a small number of such events, which suggests a slim chance of encountering any tropical cyclone phenomena in those months. Their monthly average show that only about 0.4 of strong and 1.9 of moderate vortices were formed during the month of January,

while it was almost none for strong vortex and 0.5 for the moderate case in February. All these monthly variations are probably due to the atmospheric conditions that are favorable for the formation of active and strong convective systems in November and December, while they are less conducive in January and February as observed and studied by Chang et al. (2005b), Zuki and Lupo (2008) and Wang et al. (2009).

The total numbers of seasonal Borneo vortices in every category were then plotted on time-series graph, as displayed in Fig. 3.4.2. All the graph lines demonstrate considerable fluctuation, which is most likely could be associated with certain interannual and/or interdecadal variability of common climate oscillations. The trend of each graph was determined, and it was found that the 3rd order polynomial regression line fitted well with most of the data based on their R^2 values as compared to the linear type trendline (not shown).

The highest correlation was shown by the weak intensity vortex, followed by strong and moderate, respectively. The trend of seasonal quantity of the moderate and strong vortices is almost parallel with slight downslope curve at the middle of the study period and two upslopes at the beginning and the end of it, which generally does not change much over long-term period. While the trend of weak vortices is more significant with steep downslope, which reaches the minimum value around the year of 2000 before it increases back until the end of the study period. It is actually about the same as the pattern of the seasonal Borneo vortex frequency shown in Fig.3.1.1. Indeed, all these patterns seem to

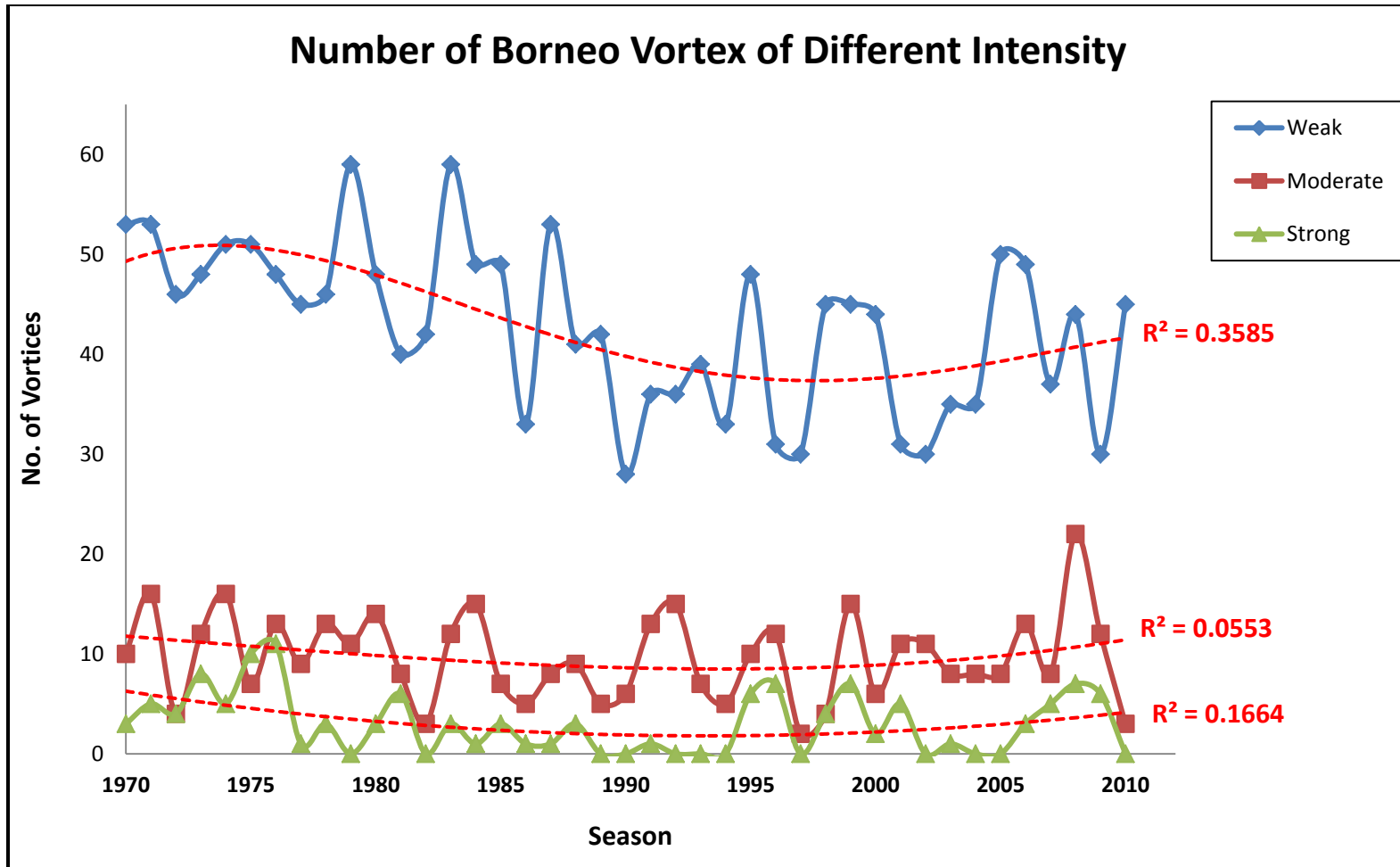


Fig. 3.4.2: The seasonal Borneo vortex frequency for weak (blue line), moderate (brown line) and strong (green line) intensities throughout 41 winter monsoon between 1970/71 and 2010/11 seasons. The red-dashed lines are the 3rd order polynomial trendlines.

coincide with PDO phases, which had also been demonstrated by other Borneo vortex aspects analyzed prior to this section.

To further analyze the influence of PDO event on this Borneo vortex aspect, the same processes as in previous analyses were engaged by separating the seasonal data in Table 3.4.1 according to the seasons in PDO phases listed in Table 2.4.1. The frequency of each vortex category were then summed up and averaged accordingly before being displayed in Table 3.4.3. The results show that there are significant variations in term of the seasonal mean of vortex occurrences for the case of moderate and strong intensities between the two PDO phases. The number of moderate and strong vortices tends to be more during PDO2 period and less in PDO1 when compared to the long-term average, while there is almost no variation to show in the case of weak vortex.

	All	PDO1	PDO2
Weak	42.9	42.4	43.4
Moderate	9.7	8.8	10.7
Strong	3.0	2.0*	4.3

Table 3.4.3: The Borneo vortex seasonal average frequency of different intensities stratified by PDO phases. "*" denotes the value is statistically significant at 95% confidence level.

From the analyses in section 3.1, it was discovered that the seasonal vortex frequency was greater than the long-term mean during PDO2 period, as shown in Table 3.1.4. Since the average number of weak vortices was almost

similar in both PDO phases, therefore, the difference in the seasonal mean vortex frequency that was identified in previous section was mostly due to the presence of moderate and strong vortex intensities. Hence, combining both results from these analyses and the one in section 3.1, it can be suggested that under the influence of PDO phases, the long-term variation of the vortex frequency over the study domain depends on the moderate and strong type Borneo vortices, while the weak vortex remains constant.

As pointed out earlier, the higher number of Borneo vortices formed during PDO2 period was due to the availability of the conducive atmospheric conditions for the development of any convective systems in this region as a result of warmer than normal SST (Gershunov and Barnett (1998) and Lin et al. (2011)). However, through this analysis, it demonstrates that PDO2 not only able to increase the number of Borneo vortices, but it also capable of enhancing their intensity by spawning more moderate and strong vortices, as revealed in Table 3.4.3. Statistically, the variability of moderate and strong vortices demonstrates very strong confidence level as shown in Appendix A. However, only strong vortex during PDO1 reaches 95% significance level, while it is slightly below 90% for the case of PDO2.

Besides the PDO event, there should also possibly be other natural climate oscillations that might influence the distribution of seasonal vortex frequency of different intensities in this region. One way to detect them is via Fourier power-spectral method, which had been used in every analysis prior to

this. The procedure to apply it had been described in chapter 2, in which the time series data were transformed into a function of oscillation in order to capture the return period of each Borneo vortex category. The final outputs were plotted on three separate periodograms as displayed in Fig. 3.4.4.

At 95% and 80% confidence levels, the significant peaks between cycle number 5 and 13 suggest that the seasonal number of Borneo vortices of each category throughout the study period have recurrence time ranging from 8 to 3 years, which are likely due to strong link to ENSO events. While, the peaks for cycle number 16 to 20 indicate the periodicity of about 2.5 to 2 years, are probably associated with the influence of the QBO or TBO, or both. The peaks at number 2 to 4, i.e. 20 to 10 years oscillation, which were also observed in Enfield and Mestas-Nuñez (1999) and Birk et al. (2010), could possibly succeeding the variability of ENSO-PDO interaction event.

The relationship between ENSO and the seasonal frequency of the Borneo vortex of different intensities was determined by replicating the same techniques as in previous, only that the seasonal data in Table 3.4.1 were segregated following the seasons of different ENSO phases listed in Table 2.4.2. The final outputs were summarized in Table 3.4.4. As discovered in section 3.1, the seasonal average of Borneo vortex quantity was higher during LN years and lower in EN periods compared to their long-term average value. However, through these analyses, the outcomes reveal that the Borneo vortex frequency behaves differently for different type of intensities.

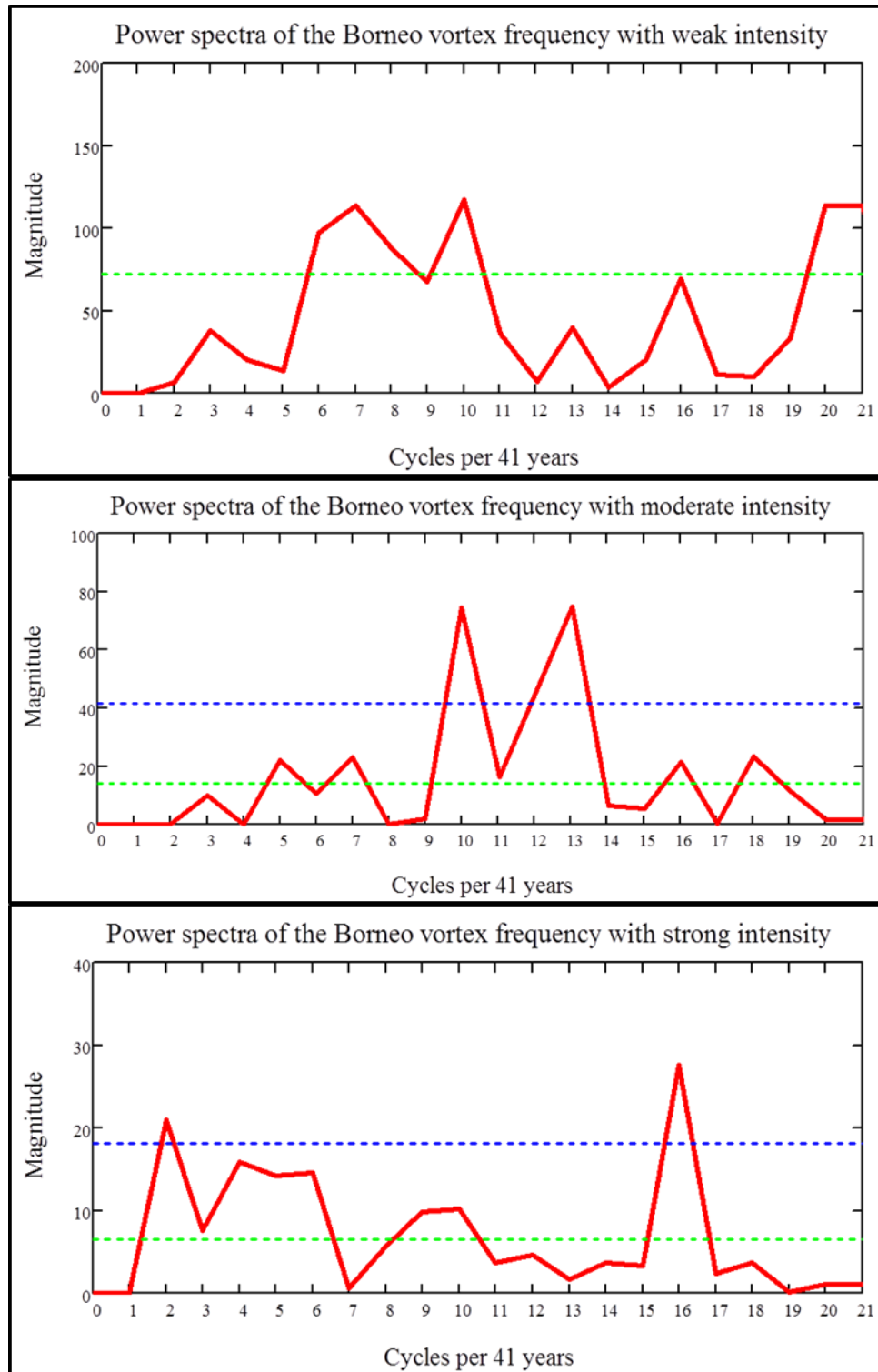


Fig. 3.4.3: The seasonal Borneo vortex frequency for weak (top), moderate (middle) and strong (bottom) intensities plotted as Fourier power spectra with the ordinate displaying the magnitude of the Fourier coefficient and the abscissa displaying the period of cycles per 41 years. Blue-dashed lines are significant interval at 95% level for weak event, and 99% for moderate and strong.

As disclosed in Table 3.4.4, the number of moderate vortices during EN, LN and NEU years is almost unchanged compared to the long-term average. However, the difference turns significant in the case of weak and strong vortex intensities for different ENSO events. Compared to the long-term mean, the occurrence of weak and strong vortices over this region is slightly lower in EN years but much higher during LN periods, which exceed the 90% confidence level of the statistical tests (see Appendix A).

	All	EN	LN	NEU
Weak	42.9	39.7	46.9*	42.4
Moderate	9.7	8.4	10.0	10.1
Strong	3.0	2.7	5.0*	2.3

Table 3.4.4: The Borneo vortex seasonal average frequency of different intensities stratified by ENSO years. "*" denotes the value is statistically significant at 90% confidence level.

From earlier discussion, it was mentioned that the impact of EN and LN over this region is very contradicting. A lot of studies have shown that the EN periods tend to suppress the environment (Chang et al. (2004a), Tangang and Juneng (2004), and Zuki and Lupo (2008)), while the LN turns it into a favorable condition for the development of active convective weather system, such as Borneo vortex. Therefore, the results attained here possibly imply that the influence of ENSO events on the Borneo vortex not only on its quantity, but it also being specific to certain type of vortices, which comprises of weak and strong intensities.

Since the PDO event is known to modulate ENSO behavior, the analyses on the simultaneous influence of both events towards the variation of the seasonal mean of vortex quantity of different intensity had also been made. The same method was repeated here as in previous analyses by segregating the data in Table 3.4.1 and matched them with the seasons listed in Table 2.4.1 and Table 2.4.2 before being tabulated in Table 3.4.5 below.

	PDO1			PDO2		
	EN	LN	NEU	EN	LN	NEU
Weak	38.8	42.0	43.5	40.6	47.9*	39.8
Moderate	6.2	6.5	9.9	10.6	10.9	10.5
Strong	0.6 ⁺	3.5	2.2	4.8	5.3	2.5

Table 3.4.5: The Borneo vortex seasonal average frequency of different intensities stratified by PDO periods and ENSO years. “+” and “*” denotes the value is statistically significant at 99% and 90% confidence level, respectively.

The results show that, within PDO1 phase, the majority of the seasonal average numbers of Borneo vortices of different intensities decrease in every ENSO phase compared to their normal mean values displayed in Table 3.4.4. However, the variances are not uniformly distributed on each vortex category. The difference is very small for the case of weak and moderate vortices, which are found to be statistically insignificant (see Appendix A). On the other hand, the impact of PDO1 on ENSO looks substantial for the case of a strong vortex. This kind of variability has also been observed by Lupo et al. (2008) and Lupo (2011) in the tropical cyclone activities. The statistical tests show very high confidence in

their mean values, but only the association of EN in PDO1 period is considered significant, i.e. reaches the 99% confidence level.

On the other hand, within PDO2 period, the vortex seasonal mean quantity for different intensity seems to increase throughout the ENSO events compared to their normal means listed in Fig. 3.4.4. However, most of the differences are relatively small, except in the case of strong vortex in EN years. The seasonal mean value during this event increase almost 75% than its normal figure, but it is found to be not statistically significant as shown in Appendix A. The only mean value in these analyses that pass 95% confidence level is on the impact of PDO2 on LN years over weak Borneo vortex.

Most of the results found here basically well agreed with the claim made by Zhang et al. (1997a), Gershunov and Barnett (1998), and Birk et al. (2010) regarding the influence of PDO periods on ENSO events. PDO1 has a tendency to dampen the atmospheric background over this region, as discussed before, thus permits the convective activity to be less conducive. Meanwhile, PDO2 able to enhance the environment and make it more conducive for the formation of convective system like Borneo vortex. However, the effect is significant mainly on the vortex of weak and strong intensities, and not that much on the moderate case, which is similar to previous results found in Table 3.3.4.

In the past three sections, none of the analyses had shown that the QBO had played a significant role on the variation of any Borneo vortex behaviors even though all the power spectral periodograms had detected a strong signal,

which could be associated with QBO event. The same thing happened in this section where the signal from periodogram in Fig. 3.4.3 still exhibits a similar periodicity as QBO variability. In order to investigate this indication, the same methods were applied by separating the seasonal data in Table 3.4.1 corresponding to the QBO phases listed in Table 2.4.3. The final figures were summarized and shown in Table 3.4.6.

	All	West QBO	East QBO
Weak	42.9	43.8	42.0
Moderate	9.7	10.3	9.0
Strong	3.0	3.1	3.0

Table 3.4.6: The Borneo vortex seasonal average frequency of different intensities stratified by QBO phases.

As expected, the outcomes reveal that there is not much variation between both phases as well as with the long-term means that were calculated before as in Table 3.4.2. The only difference that was noticed is for the case of moderate vortex during the east QBO phase. It shows that the seasonal occurrence of the moderate vortex is slightly less than the long-term average but it is statistically insignificant (see Appendix A). Therefore, over the 41 winter monsoon seasons between 1970/71 and 2010/2011, one can imply that the QBO does not have any influence to the seasonal variability of the number of Borneo vortex of different intensities over the study region.

In addition to QBO, there is also another natural event in the tropics, known as TBO that has a similar periodicity of 2 to 2.5 years as deduced from the periodogram in Fig. 3.4.3. To identify the impact of TBO towards the intensity of the Borneo vortex, the same techniques were used as in previous analyses, except that the data were stratified according to the seasons of each TBO phase itemized in Table 2.4.4. The final outcomes were revealed in Table 3.4.7 after all the number of vortices for each category were totaled and averaged.

	All	Strong TBO	Weak TBO
Weak	42.9	44.5	41.1
Moderate	9.7	9.9	9.4
Strong	3.0	4.1	1.9*

Table 3.4.7: The Borneo vortex seasonal average frequency of different intensities stratified by TBO phases. "*" denotes the value is statistically significant at 95% confidence level.

The results show that the seasonal mean values of the Borneo vortex frequency of different intensities are comparable with the seasonal long-term average, except for the category of strong vortices. More strong vortices are observed during strong TBO phase than in the weak period. From earlier analyses in section 3.1, we discovered that the number of Borneo vortices were greater during strong TBO phase. However, through this analysis, it demonstrates that the disparity in the seasonal vortex frequency between those phases only exists in the category of strong intensity.

When both results are combined, one may suggest that during the strong TBO phase, which is associated with strong monsoon activity, the increase in the seasonal vortex occurrences in the study region are mainly because of the presence of more vortices with strong intensity. Therefore, for winter monsoon to be considered as strong in any of the season, the Borneo vortex quantity not only need to be large, but it also has to come with vortices that have more strong intensity. The statistical tests reveal that the variation of the seasonal mean of strong vortex with respect to its long-term average is relative strong in both TBO conditions, but only the case of weak TBO passes the 95% confidence level.

As discussed in previous section, TBO and ENSO events are found to be strongly related (Meehl and Arblaster (2002, 2011), and Wu and Kirtman (2004)). Therefore, for this section, the relationship between these two events was also being investigated in order to find the connection that might exist when both events were layered on one another, as in the case of PDO and ENSO. The analyses were done using the same approaches as in previous works by isolating the seasonal data in Table 3.4.1 based on the seasons listed in Table 2.4.2 and Table 2.4.4 for different ENSO years and TBO phases. The final outputs were summarized as in Table 3.4.8.

Under the influence of ENSO, the outcomes clearly reveal that there is a strong variability of Borneo vortex quantity, particularly on the category of strong and weak intensities, in TBO phases. Compared to their normal average values showed in Table 3.4.7, the EN tend to reduce the number of vortices in both TBO

events, while the quantity increases when LN years occurred. As in NEU years, the means do not differ that much.

	Strong TBO			Weak TBO		
	EN	LN	NEU	EN	LN	NEU
Weak	43.2	45.7	44.2	36.2	49.7*	41.1
Moderate	9.8	10.3	9.9	7.0	11.7	9.8
Strong	3.2	5.5	3.4	2.2	3.3	1.4

Table 3.4.8: The Borneo vortex seasonal average frequency of different intensities stratified by TBO and ENSO phases. "*" denotes the value is statistically significant at 90% confidence level.

The results gained here simply imply that EN and LN are the main players in regulating the vortex variability of different categories over this area during winter monsoon period. They also match with the findings of other works related to these events, such as Meehl and Arblaster (2002 and 2011), and Wu and Kirtman (2004). As discussed in section 2.4.4, strong TBO is believed to be associated with strong monsoon activity (Meehl, 1997). Under this condition, the convection activities could become more active, which probably allows more Borneo vortex to form.

However, when the EN arrives, the atmosphere in this region is likely to get dampened, and hence makes it less favorable for vortex generation. This kind of impacts has been discussed by many researchers such as Chang et al. (2004a), Tangang and Juneng (2004), and Zuki and Lupo (2008). Since TBO is

controlled by the EN, therefore the number of Borneo vortex gets reduced, which involves all categories of Borneo vortex. The impact is reversed under the influence of LN. Anyhow, based on the statistical tests, most of these variations are insignificant except in the case of weak vortex of weak TBO in LN years, where it passes the 90% confidence level.

In the early part of this section, it was mentioned that the Borneo vortex distribution under the strong intensity might have been strongly correlated with the tropical cyclone activity in this region. In order to verify this statement, the study of Zuki and Lupo (2008) was referred, as done in the previous section. If the claim is true, whatever results found in their study could also be applied here. Based on their sample groups of active and non-active years of tropical cyclone activity, the findings were tested against the seasonal number of Borneo vortex of strong intensity. The years of active and non-active condition were matched with respect to the winter monsoon seasons studied here. The final outputs were displayed in Table 3.4.9 below.

	Active	Non-active (Warmest SSTs)	Non-active (Coldest SSTs)
No. of years/seasons	4	3	5
Total vortices	20	2	6
Vortices per season	5.0*	0.7 ⁺	1.2 ⁺

Table 3.4.9: The seasonal mean quantity of Borneo vortex with strong intensity based on the sample groups of tropical cyclone activity from Zuki and Lupo (2008). "*" and "+" denote the value is statistically significant at 90% and 95% confidence levels, respectively.

The outcomes clearly show that on average, large number of Borneo vortex with strong intensities is found during the active years of tropical cyclone activity determined in Zuki and Lupo (2008), while the quantity is relatively small in the non-active periods. They also demonstrate that the warmest SST is not always set up the best conducive environment for the development of convective system in this region compared to the relatively cold SST, which had also been identified in earlier analyses. Statistically, all these mean values exceed the 90% confidence level, which implies that the seasonal number of strong Borneo vortices corresponds well with tropical cyclone activity in this region.

Therefore, based on all these results, it can be suggested that for the winter monsoon in this region to gain more Borneo vortex of strong intensity, the atmospheric background needs to be as favorable as in the active years set by Zuki and Lupo (2008), which generally presence under the climatic condition of LN years. Besides LN, the climatological analyses done in this section also show that the number of strong vortex tends to be large under the influence of PDO2 and strong TBO, while the quantity could turn less when the background climate is supported by EN, PDO1 and weak TBO events.

3.5 The onset and retreat dates of the Borneo vortex

The final climatological aspect of the Borneo vortices that will be analyzed here were the dates of their commencement as well as departure for each and every winter monsoon season throughout the study period. The dates were

determined based on the first and the last Borneo vortex observed within the domain set for this study as depicted in Fig. 2.1.1. Furthermore, the location of each vortex was also documented as to further analyze its first and final positions of the season. All this information was then tabulated as in Table 3.5.1.

The records indicate that all of the first Borneo vortices of the seasons occur in November, where most of them appear during the first 10 days of the month. Of these, 13 events occur as early as 1st November, and it is possible the first one might appear earlier than that. However, since the study only considered the period of winter monsoon season between November and February, thus the first vortex that developed prior to the month of November was documented as 1st November. For the remaining of the study period, five seasons did not have a first vortex occurs until the middle of November while only one case appeared within the last 10 days of the month. On average, the date for the first Borneo vortex of winter monsoon to be seen in this region was roughly on the 5th of November.

The majority of these dates stay within the onset period of winter monsoon season defined by Malaysian Meteorological Department (MMD), i.e. between early and middle of November (MMD, 2012). Based on the analyses of the daily 925 hPa wind field throughout the study period, it was found that most of the time the first vortex tends to develop as soon the first northeasterly winds penetrate into the study domain. The arrival of these winds is generally followed by the beginning of the winter monsoon season over this region. Therefore, the

Season	First date (Nov)	First Location		Last date (Feb)	Last Location	
		Lat	Long		Lat	Long
2010/11	1	5.6N	103.3E	24	4.7N	112.7E
2009/10	1	4.1N	107.0E	20	0.0N	109.5E
2008/09	6	4.7N	105.6E	26	3.4N	112.1E
2007/08	3	7.5N	112.8E	29	5.2N	111.9E
2006/07	6	4.5N	113.2E	26	1.8N	111.8E
2005/06	9	7.1N	114.9E	26	1.1N	111.0E
2004/05	4	2.9N	111.1E	24	0.9N	108.8E
2003/04	1	2.4N	108.6E	28	0.6N	108.5E
2002/03	5	4.6N	112.3E	15	1.2S	108.2E
2001/02	4	6.7N	111.7E	27	2.0S	108.4E
2000/02	13	1.9N	111.6E	24	2.1N	117.1E
1999/00	15	3.0N	107.4E	28	1.8N	110.4E
1998/99	1	7.0N	112.5E	27	2.0N	114.1E
1997/98	5	2.9N	112.7E	21	5.3N	114.6E
1996/97	18	0.3N	111.4E	25	3.0N	113.3E
1995/96	10	4.8N	105.9E	22	2.2S	109.2E
1994/95	2	1.1N	110.3E	20	2.0S	107.8E
1993/94	2	3.8N	110.5E	28	1.3N	112.7E
1992/93	1	6.7N	114.9E	25	1.2S	107.6E
1991/92	3	4.7N	110.7E	11	2.2N	114.0E
1990/91	21	6.0N	110.2E	28	1.6S	106.2E
1989/90	6	6.3N	114.4E	3	2.3N	112.5E
1988/89	1	5.1N	111.6E	28	5.0N	115.7E
1987/88	2	4.9N	113.0E	19	1.4N	109.8E
1986/87	1	5.2N	102.6E	27	1.3S	110.8E
1985/86	4	3.9N	108.4E	28	1.8S	112.2E
1984/85	10	5.3N	114.2E	21	5.3N	111.2E
1983/84	4	5.5N	104.3E	29	1.6S	111.5E
1982/83	4	2.9N	106.0E	22	0.3S	112.3E
1981/82	3	2.7N	116.4E	24	0.5N	116.7E
1980/81	19	5.1N	114.2E	26	3.0N	113.4E
1979/80	1	6.0N	113.4E	26	0.5S	106.6E
1978/79	6	5.9N	114.2E	19	0.1N	110.5E
1977/78	1	2.8N	110.9E	27	1.0S	109.8E
1976/77	2	5.6N	116.3E	28	5.3N	110.6E
1975/76	1	3.3N	106.9E	26	1.2N	108.0E
1974/75	11	6.9N	107.5E	28	0.9S	108.1E
1973/74	1	4.9N	107.9E	28	1.9N	115.5E
1972/73	1	7.0N	109.5E	20	0.3S	109.5E
1971/72	1	4.1N	108.8E	24	3.8N	108.3E
1970/71	5	6.4N	114.5E	25	5.1N	107.0E
Average:	5.2	4.7N	110.6E	24.0	2.2N	111.0E

Table 3.5.1: The seasonal dates and locations of the first and last Borneo vortex observed over 41 winter monsoon between 1970/71 and 2010/11 seasons.

presence of first Borneo vortex perhaps can be used as an indicator for the onset of winter monsoon season in this region since both the wind and first vortex could possibly arrive and occur just about the same time.

As for the departure of the last vortex of the season shown in Table 3.5.1, the outcomes reveal that all the events appear in February. The earliest date was recorded on 3rd February while the majority of the last vortex was found toward the end of the month, which includes 10 cases that occur on the last day of February or possibly later. However, since the study only considered the winter monsoon period that ends in February, thus, any last vortex that occurred after that month would be logged as 28th or 29th of February. On average, the long-term mean date for the last Borneo vortex of the season to retreat from this region was on 24th of February.

The winter monsoon in Malaysian region ends when the northeasterly wind begins to fade and later be replaced by southwesterly winds. Based on the persistence of the wind steadiness, Cheang (1987) found that the dates of retreat of the winter monsoon in this area vary considerably, which could happen as early as 5th February and as late as in late March. This date variation well-matched with the results found here. Therefore, similar to the case of the first vortex, the departure date of the last Borneo vortex could also probably be used to determine the end of the winter monsoon season over the study domain. Both these dates could be used to determine the mean duration of the winter monsoon

period over this region, which in this case stretched for almost 112 days, seasonally.

In addition to these dates, the location of each vortex center for respective case had also been documented as in Table 3.5.1. All the centers were then placed on the map, as depicted in Fig. 3.5.1, in order to get a better picture of the vortex position with regard to its first and final appearances of the season. The outcomes clearly show that majority of the first vortex of the season (marked by blue “X”) tend to occur within the top half portion of the study area, mainly northward of 2.5°N latitude line.

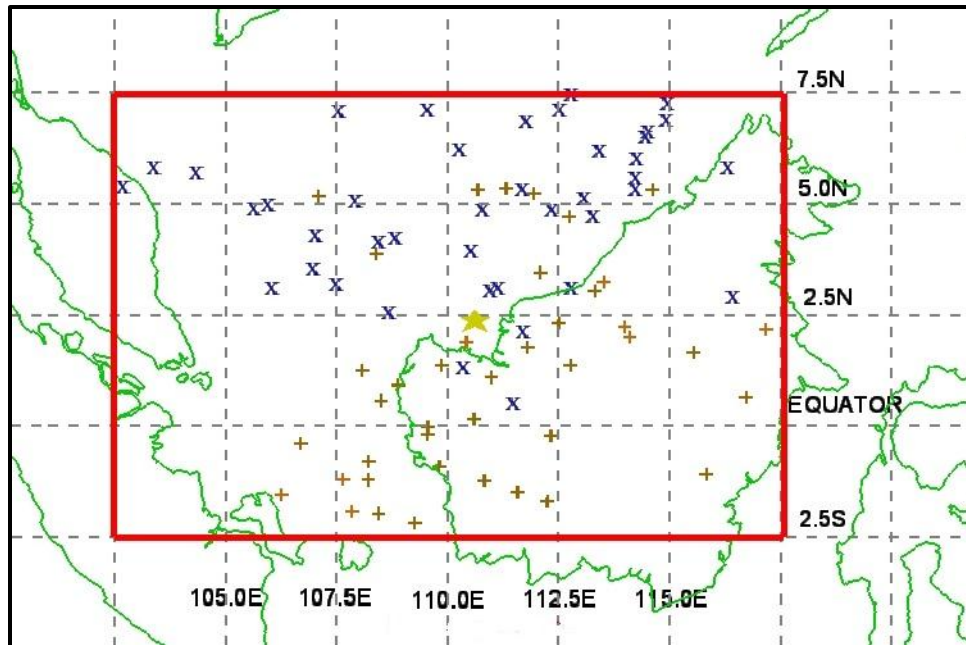


Fig. 3.5.1: The location of the first and last Borneo vortex centers that had been detected in each winter monsoon between 1970/71 and 2010/11 seasons. The blue “X” indicates the first vortex and brown “+” is the last vortex of the season. Yellow ‘star’ is the long-term mean Borneo vortex position as analyzed in section 3.2.

The vortex center was averaged at 4.7°N latitude and 110.6°E longitude, which is located over the water body and directly north of the long-term average Borneo vortex position at 2.4°N and 110.6°E, as analyzed in section 3.2. On the contrary, most of the last vortex centers (marked as brown "+") are seen at the bottom half of the domain with its mean position at 1.1°N and 111.0°E. This center is located over the inland of Borneo Island, which is over the south-southeast of the vortex long-term average position.

The results found here agreed well with the outcomes in section 3.2. Cheang (1977) in his study has stated that the Borneo vortex is a synoptic weather system that embeds in the monsoon trough. The trough had been observed to migrate southward from East Asia into this region and move close to the equator as the winter monsoon season progresses (Sadler and Harris, 1970). Therefore, at the beginning stage of the winter monsoon season, the first vortex has a high tendency to form over the upper half of the study domain since the trough has just entered the region from the north. As the season advanced and come to an end, the trough shifts further south before lying close to the equator. As a result, the last vortex has a greater chance to be found at the lower half of the domain, which is covered by more land area rather than water.

To determine the long-term trend of the seasonal date of the first and last Borneo vortex appearances throughout the study period, time-series graph was plotted for each case between the date of the first and last vortex occurrences, and its respective season as listed in Table 3.5.1. The final outputs were

depicted as in Fig. 3.5.2. Both graphs exhibit vigorous fluctuation, which suggest that there is possible interannual and/or interdecadal variability on the seasonal first and last dates of Borneo vortex occurrences in this domain throughout the study period, probably due to the influence of certain common tropical climate oscillations.

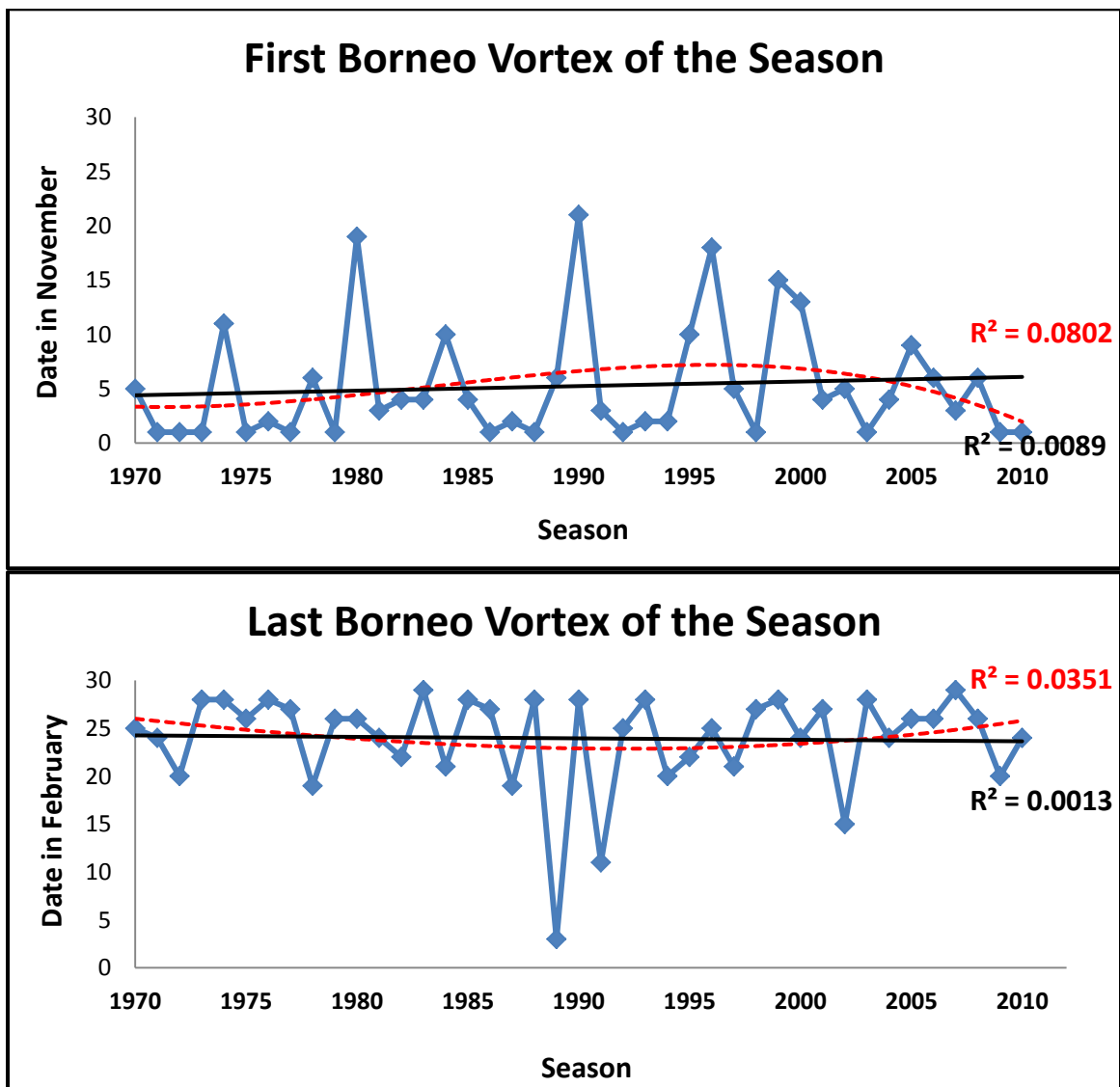


Fig. 3.5.2: The date of the first (Top) and last (Bottom) Borneo vortex observed in each winter monsoon between 1970/71 and 2010/11 seasons over the study region. The black line indicates the linear trendline and red-dashed line is the 3rd order polynomial trendline.

The linear trend for both cases indicates that there is almost no change on the date tendency, which tells that the date for the first and last Borneo vortex to appear in every winter monsoon season over the study region has remained similar throughout the study period. If the occurrence of the first and last Borneo vortex is going to be considered as the onset and retreat date of the winter monsoon in this region, this trend could probably suggests that the winter monsoon duration has not changed that much throughout the study period. The relationships exhibit by both linear trendlines here are very weak based on their small R^2 value, i.e. 0.0089 and 0.0013, respectively.

The correlations become a bit stronger by applying the 3rd order polynomial regression line on both time-series graphs, but not strong enough to be considered as significant. The seasonal first vortex polynomial trendline with R^2 value of 0.0802 exhibits one concave curve at the middle of study period and two partially-convex curves at both ends, which mean that the first vortex was set a bit late at the middle of the study period while it appeared much early at the beginning and toward the end of the study duration.

On the other hand, the seasonal last vortex with R^2 value of 0.0351 has one convex curve at the middle and two partly-concaves curves at both ends of the study period. These indicate that the last date the seasonal vortex retreated from this region was slightly early at the middle of the study period, while it was a bit late during the start and end of the study stretch. Both trends demonstrate here tend to follow the PDO variability, where during warm PDO phase, the first

and the last vortex of the season has a tendency to appear late and leave early, respectively, and vice-versa in the case of cold PDO.

If the event of the first and last Borneo vortex would have been considered as the onset and retreat date of the winter monsoon season, then these trends could probably suggests that the duration of this monsoon has become longer during PDO2 period and short in PDO1 over this region. To further examine the influence of PDO toward the interdecadal variation of this Borneo vortex aspect, the compositing analysis technique was again used here by sorting the dates in Table 3.5.1 in accordance to the seasons of respective PDO phase listed in Table 2.4.1. Afterward, the dates of each case were totaled and averaged accordingly before being summarized and tabulated as in Table 3.5.2.

	All	PDO1	PDO2
First date (November)	5.2	5.7	4.7
Last date (February)	24.0	23.0	25.1
Monsoon duration (days)	111.8	110.3	113.4

Table 3.5.2: The seasonal mean dates of the first and last Borneo vortex detected over the study domain as stratified by PDO phases.

The results show that there are minor variations in term of the seasonal mean dates of the first and last vortex existence over this area. The first Borneo vortex of the season commenced half day earlier and the last one retreated one

day later, which made it to remain longer than the long-term average duration during cold PDO phase. On a contrary, the duration became shorter in warm PDO period. The outcomes found here are consistent with the results obtained from the analyses of the graph trendlines of Fig. 3.5.2.

As mentioned before, cold PDO tends to increase the SST over the study region and decrease it in the presence of warm PDO based on the studies made by Gershunov and Barnett (1998), and Lin et al. (2011). Warm SST has the ability to enhance the atmospheric conditions to enable more convective systems to be generated as compared to cold water. Zuki and Lupo (2008) showed that there is a strong correlation between the SST and the convergence activity in this region, as well as the convergence and the cyclonic circulation. As a result, it probably turns the winter monsoon to be more active and runs longer, which could be attained by having early onset and later retreat dates. While the effect is reversed as the warm PDO takes place. However, none of these mean values is statistically significant compared to the long term-mean as revealed in Appendix A.

Other than PDO, there might also be other natural climate oscillations that possibly responsible for the variability of the first and last dates of the Borneo vortex occurrences in this region. One way to detect those signals is by applying the Fourier power-spectral method, which has been used in every analysis prior to this. The procedure to apply it was described in chapter 2, in which the time-series data were transformed into cyclical series in order to capture the return

period of this event. The final outputs were plotted on two separate periodograms as depicted in Fig. 3.5.3.

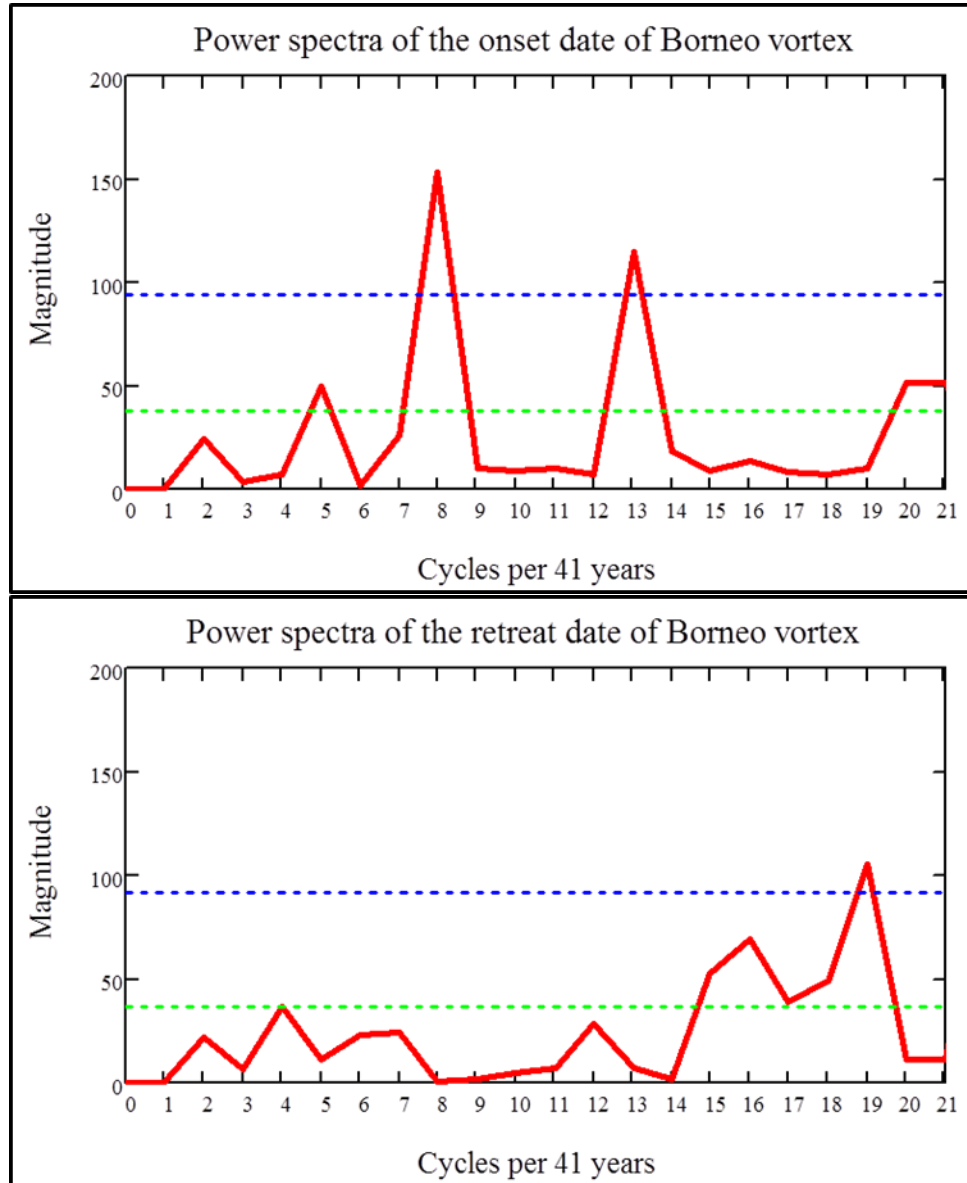


Fig. 3.5.3: The onset and retreat dates of the first (Top) and last (Bottom) Borneo vortex, respectively, observed in each winter monsoon between 1970/71 and 2010/11 seasons plotted as Fourier power spectra with the ordinate displaying the magnitude of the Fourier coefficient and the abscissa displaying the period of cycles per 41 years. Blue- and green-dashed lines indicate significant interval at 95% and 80% confidence levels against the white-noise background, respectively.

After filtered out the first and the last spectrum peaks, at 95% and 80% confidence levels, the peaks are considered significant only at cycle number 5, 8 and 13 for the vortex onset date, which indicate that the vortex lifespan has a periodicity of 8, 5 and 3 years, respectively. Typically, these periods are associated with the ENSO events. In addition to that, the significant peaks between numbers 15 to 20 found in both periodograms might potentially relate to TBO or QBO, or combination of both events, which are known of having recurrence periods of about 2 to 2.5 years. As for peak at cycle number 4, which was also found in Enfield and Mestas-Nuñez (1999) and Birk et al. (2010), the signal is likely due to the consequence of the interaction between PDO and ENSO events.

The impact of ENSO events toward the variability of the seasonal date of the first and last Borneo vortex over the study domain was determined by replicating the same process as in earlier analyses. The final outputs were summarized and tabulated as in Table 3.5.3. The results reveal that during EN years, the average date for the first vortex to appear is on 3rd of November, i.e. two days earlier than the long-term mean, while the last one to depart is on 21st of February, which is 3 days less than the long-term average. By considering both means as the onset and retreat dates of winter monsoon season here, the period stretches for about 111 days, one day short than the long-term mean.

As for the case of LN years, the first vortex to enter the region is averaged on 4th of November and the last one to leave is roughly on 27th of February,

which is one day earlier and three days later of the long-term average, respectively. With these dates, the winter monsoon mean duration is almost 116 days, which are far lengthier than the long-term mean period. Lastly, during NEU years, it turns out that the mean date for first vortex to form is on 7th of November and the last one to be seen is on 24th of February, i.e. two days later and about the same as the long-term average, correspondingly.

	All	EN	LN	NEU
First date (November)	5.2	3.0 ⁺	4.0	6.9
Last date (February)	24.0	20.9	26.7 ⁺	24.1
Monsoon duration (days)	111.8	110.9	115.7 [*]	110.2

Table 3.5.3: The seasonal mean dates of the first and last Borneo vortex detected over the study domain as stratified by ENSO years. “+” and “*” denotes the value is statistically significant at 99% and 95% confidence level, respectively.

These outcomes imply that the winter monsoon duration tends to be short during EN years and stays long under LN phase. They reach their mature stage during the winter monsoon season, which could maximize the impact to this region as discussed by many scholars, such as Chang et al. (2004a), Tangang and Juneng (2004), and Zuki and Lupo (2008). The atmospheric condition is generally less conducive during EN years, while it is the opposite in the case of LN event. As a feedback to these, the winter monsoon is likely to turn relatively short during EN years and long in LN.

In spite of having an early arrival vortex of the season, which is statistically significant (see Appendix A), the winter monsoon duration in EN years was cut short by quick departure of its last vortex. While during LN years, the first vortex was also observed to come early, even though not as early as in EN event, its last vortex tended to stay back and left the domain much later, which made its duration lengthy. Both the late departure and long monsoon period during LN years pass the statistical tests at 99% and 95% confidence level, respectively, as shown in Appendix A.

Both analyses done above revealed that the mean date of the first and last Borneo vortex appearances for every winter monsoon season throughout the study period fluctuate according to PDO and ENSO variability, even though some relationships were not statistically significant. Therefore, if the influence of both events is combined, perhaps the outcomes could turn out to be more significant since the PDO phases have been known to influence the ENSO years (Zhang et al. (1997b), Gershunov and Barnett (1998) and Birk et al. (2010)). In order to do so, the data from Table 3.4.1 were segregated and matched according to the seasons that follow ENSO and PDO periods listed in Table 2.4.1 and Table 2.4.2. The outputs were then summarized as in Table 3.5.4 below.

The results reveal that, within PDO1 period, the mean dates for the first and last vortex of EN years do not differ much with its normal average found earlier in Table 3.5.3. The monsoon duration is one day short but it is not statistically significant (see Appendix A), which suggests that the influence of

PDO1 toward this EN event is relatively weak. In the case of LN event, it is surprising to see that the first vortex tends to arrive early and the last one departs much later, which causes the monsoon period within this climate background to extend significantly. However, this outcome is a bit suspicious since the sample size is very small, which involve only two seasons. As for NEU years, the variation of their mean values is statistically insignificant, as shown in Appendix A.

	PDO1			PDO2		
	EN	LN	NEU	EN	LN	NEU
First date (November)	3.0*	1.0	7.2	3.0	4.8	6.2
Last date (February)	20.0	27.5*	25.1	21.8	26.5	25.8
Monsoon duration (days)	110.0	119.5 ⁺	110.9	111.8	114.7	112.6

Table 3.5.4: The seasonal mean dates of the first and last Borneo vortex detected over the study domain as stratified by PDO and ENSO phases. “⁺” and “*” denotes the value is statistically significant at 95% and 90% confidence level, respectively.

Within PDO2 period, in general, the outcomes reveal that the monsoon periods tend to be longer. Even though the mean onset date remains the same during EN years, its retreat date departs much later, which makes the monsoon period stays longer than the climate conditions analyzed in Fig. 3.5.3. The same thing takes place when dealing with NEU years. As for LN event, the PDO2 background seems to shorten the monsoon duration by one day compared to the condition set in Table 3.5.3, which is considered as unexpected result. However,

all the monsoon period mean values produced here are insignificant based on the statistical tests (see Appendix A). This implies that the influence of ENSO on the monsoon duration during PDO2 phase is relatively weak.

Besides the influence of PDO and ENSO, the periodograms in Fig. 3.5.3 also detected other significant signals, which indicate that both dates of the first and last Borneo vortex of the season have return periods of 2 to 2.5 years, which are similar to the periodicity of QBO and TBO events. The influence that possibly exhibits by them could be detected by applying the same analysis technique as done earlier. For the case of QBO, the final analysis outputs were shown in Table 3.5.5 below.

	All	West QBO	East QBO
First date (November)	5.2	5.5	5.0
Last date (February)	24.0	24.8	23.2
Monsoon duration (days)	111.8	112.3	111.2

Table 3.5.5: The seasonal mean dates of the first and last Borneo vortex detected over the study domain as stratified by QBO phases.

The results reveal that the mean dates of the first and last Borneo vortex of the winter monsoon season throughout the study period for both QBO phases do not differ much with the long-term average values shown in Table 3.5.2, which are also statistically insignificant (see Appendix A). This implies that QBO

possibly does not play any role in causing the first and last Borneo vortex of the season to fluctuate with a regularly recurrence period of 2 to 2.5 years over this region. The outcomes gain here is not something surprising because all the previous analyses that involve QBO have shown a similar behavior, which has also been demonstrated in other studies as well, such as Baldwin et al. (2009).

As for the case of TBO event, its final outputs were given in Table 3.5.6. The results indicate that during strong TBO phases, the mean onset date of the first Borneo vortex of the winter monsoon season falls on 4th November, which is about one day earlier than the long-term average. While the average retreat dates of the last vortex is one day later than the long-term mean date. As a result, the mean monsoon duration turns lengthy. Statistically, the tests reveal that the dissimilarity between these mean values and their population mean is significant. However, only the onset date and monsoon duration pass the 90% confidence level, as shown in Appendix A.

On the contrary, the mean monsoon period is cut short by almost 3 days in the event of weak TBO. The mean date for the first Borneo vortex of the season to be found within the domain here is on 7th November, which is two days later than the long-term average while its last vortex leaves the area on 23rd February, which is one day shorter than the long-term mean date. Even though, all these mean values show strong statistical probability, none of them exceeds 90% confidence level when compared to their long-term averages (see Appendix A).

	All	Strong TBO	Weak TBO
First date (November)	5.2	3.8*	6.8
Last Date (February)	24.0	25.0	22.8
Monsoon duration (days)	111.8	114.2*	109.0

Table 3.5.6: The seasonal mean dates of the first and last Borneo vortex detected over the study domain as stratified by TBO phases. "*" denotes the value is statistically significant at 90% confidence level.

All these results imply that during strong TBO phases, which are associated with active winter monsoon season (Meehl (1997); Meehl and Arblaster (2002)), the monsoon duration tends to be long. Since TBO involves the interaction of land, atmosphere and sea, therefore along the line, the strong one probably able to force the winter monsoon to stay long, which then allows this region to receive more rainfall as discussed in section 2.4.4. Meanwhile, the impact of weak TBO is probably reversed. As the land-atmosphere-sea interaction turns weak, the monsoon become less active, and hence cut the season short with lack of rainfall.

The variability of TBO event is strongly influenced by the presence of different ENSO phases as discussed by many scholars, such as Fasullo (2004), Wu and Kirtman (2004), and Meehl and Arblaster (2002, 2011). Therefore, in order to determine the variability of the seasonal date of the first and last Borneo vortex within this region under this climate condition, the data in Table 3.5.1 were

sorted accordingly with respect to the combination of ENSO and TBO periods listed in Table 2.4.2 and Table 2.4.4. They were then averaged before being summarized as in Table 3.5.7 below.

	Strong TBO			Weak TBO		
	EN	LN	NEU	EN	LN	NEU
First date (November)	3.4	3.9	4.0	2.4*	4.3	9.2
Last date (February)	21.0	27.3*	25.6	20.8	25.3	23.0
Monsoon duration (days)	110.6	116.4	114.6	111.4	114.0	106.8

Table 3.5.7: The seasonal mean dates of the first and last Borneo vortex detected over the study domain as stratified by TBO and ENSO phases. "*" denotes the value is statistically significant at 99% confidence level.

In these analyses, the results show that the winter monsoon duration in both TBO phases vary significantly under the influence of ENSO. The average period is shortened in EN years and lengthened during LN event when compared to their normal means listed in Table 3.5.6. While in NEU years, the value variability is minimal. The EN event was able to reduce the monsoon duration by 4 days owing to early departure of its last vortex during strong TBO. However, the period was slightly extended in weak TBO due to the vortex early onset. Statistically, only the seasonal mean date of early onset vortex during weak TBO phase was found to be significant that passed the 99% confidence (see Appendix A).

As for LN years, the mean monsoon duration was forced to stretch by 2 days in strong TBO and 5 days during the weak phase as a result of early onset and late departure of the vortex when compared to their normal values in Table 3.5.6. The vortex late departure during strong TBO probably caused by the LN event is revealed to be statistically significant at 99% confidence level as shown in Appendix A. All these outcomes imply that the vortex seasonal onset date tends to be early during weak TBO in EN years and have a late departure date during strong TBO in LN phase, which is a similar behavior as the background climate discussed in Table 3.5.4.

Therefore, the results gained here strongly indicate that the ENSO has played a major impact in influencing the monsoon period of different TBO phases, which support the assertion made by some scholars about the relationship between the ENSO and TBO, such as Meehl and Arblaster (2002, 2011), and Wu and Kirtman (2004). The results found prior to these analyses demonstrate that EN and weak TBO phases tend to shorten the monsoon duration while it lengthens the duration in the event of LN and strong TBO. Even though, all the seasonal monsoon period during TBO phase in EN and LN years shows a very strong confidence with respect to their normal values, none of them was able to reach the 90% significant level.

3.6 Discussions

The study of the variability of five seasonal aspects of the Borneo vortices over 41 winter monsoon seasons in Malaysian region reveals that most of them tend to follow the interdecadal oscillation of PDO, except for the case of the vortex system lifespan. However, it is difficult to acknowledge these findings since there is very limited number of studies related to the impact of PDO event over the study region. Zuki and Lupo (2008) found that the PDO variability did not play any role in the long-term trend of the tropical cyclone activity over this area. Anyway, they considered this outcome as questionable due to the small area included in the study, the small data set, or other real factors. Therefore, it is hoped that the findings discovered here could become a turning point for more fruitful studies on the effect of PDO oscillation to the climatology of Malaysia.

Besides the impact of this long-term climate variability, the results found here also revealed that the Borneo vortex aspects have a tendency to fluctuate according to the ENSO and TBO interannual oscillations, but not the QBO. The impact of ENSO over the Malaysian region has long been recognized, mainly in term of its rainfall distribution. Even though the relationship demonstrates considerable spatial and strong seasonal variation (Hendon (2003), Chang et al. (2004a), and Juneng and Tangang (2005)), in general, LN is likely to provide more rainfall, which is associated with active atmospheric background as shown in Zuki and Lupo (2008), while the effect is reversed in EN years.

Based on these feedbacks, some of the results gained here related to the ENSO events were something should have be expected, such as the seasonal number of vortices, the vortex system lifespan and the duration of the monsoon period. However, some portion of those outcomes could be considered as new discoveries, which include the seasonal position of the vortex center, and the onset and retreat of the first and the last vortex of the season, respectively.

As in the case of PDO event, no study related to the impact of ENSO in PDO period has ever been established over the Malaysian region before. Most of the results found here appear to be aligned with the findings of other studies, such as Zhang et al. (1997a), Gershunov and Barnett (1998), and Birk et al. (2010), where the signal of EN is strong in warm PDO period while LN signal is strong in cold PDO. This suggests that the climatological background of the study region not only is strongly influenced by the ENSO, but it is also affected by the presence of PDO event. This relationship should be taken into consideration by other researchers in the near future when conducting the studies involving the ENSO variability over this region.

The TBO oscillation could be considered as the least known interannual variation compared to the others. This is because the TBO event only limited between the Indian and Australian monsoon regions (Meehl, 1997). Furthermore, its impact is more localized, which makes it impossible to quantify as a whole. Since the TBO is associated with the monsoon intensity, some of the results

found here, like the number of vortices and the monsoon duration, should be straight forward. However, that is not the case in this study.

Most of the outcomes that are expected to be statistically significant were found to be less substantial. One of the reasons for this discrepancy is possibly due to the ad hoc technique used in quantifying the event. The method used here maybe too simplistic, which is not adequately representing the whole domain. Maybe, the best way to do it is by using the reanalysis or satellite data to estimate the total rainfall for the whole domain rather than getting it from a sole weather observation station.

Besides all these interannual and interdecadal variability, there is another type of climate background that is known to impact the winter monsoon intensity in the Malaysian region known as Indian Ocean Dipole (IOD) (Vinayachandran et al. (2007) and Tangang et al. (2008)). It is a coupled ocean-atmosphere phenomenon in the Indian Ocean. Positive IOD is characterized by anomalous cooling of SST in the southeastern equatorial Indian Ocean and anomalous warming of SST in the western equatorial Indian Ocean, while it is an opposite for the negative phase (Saji et al., 1999). This implies that the winter monsoon seasons in this study domain is likely to get enhanced in the negative IOD phase and depressed during positive period. Even though, this phenomenon is considered to have interannual variability, the periodicity is not as regular as ENSO, TBO and QBO oscillations; hence making it difficult to be detected by the power spectral method used in this study.

All the results found in this study are primarily based on statistical analyses. Therefore, any result that is found to be statistically significant and show a strong correlation should be used with cautious since they do not imply cause and effect. Conversely, relationships that are found to be strong, but not statistically significant may still have underlying causes due to some atmospheric forcing process or mechanism (Lupo and Johnston, 2000).

Through these extensive works, it is hoped that the findings could be used as additional tools by meteorologists at the regional as well as national weather authorities within the study domain in preparing better long-range seasonal weather forecasts related to winter monsoon. Over some part of the Malaysian region, this monsoon has been known to generate excessive amount of rainfall, which then follows by possible severe floods that lead to the damage of crops and properties, and loss of lives.

Due to that reason, it has been the responsibility of the Malaysian Meteorological Department to provide the country winter monsoon outlooks and pass them to other related agencies before further actions could be taken prior to the start of the season. Since the Borneo vortex and this monsoon are strongly connected, therefore, the variability found here could possibly turn the seasonal forecast of this region into more reliable and accurate one.

CHAPTER 4

Case Studies

In previous sections, it has been shown that most of the climatological patterns of Borneo vortices with regard to their frequencies, locations, intensities, lifespan, commencement and departure dates emulate the climate variability caused by ENSO, PDO and TBO events. Now, in this chapter, we select two specific cases in order to further explain the vortex of different intensities behaviors and characters, mainly concerning the convective parameters that support its existence and maintenance.

To begin with, the long-term seasonal means of typical atmospheric backgrounds within the study domain were first determined using only the latest version of ERA-Interim reanalysis data (Version 2.0), which become available on the ECMWF website at <http://data-portal.ecmwf.int> since Dec 2011. It has a resolution of $0.75^\circ \times 0.75^\circ$, which is much better than Version 1.0 that was used earlier in this study. The dataset includes the winter monsoon from November to February between 1979 and 2010 seasons, which is an extension of 10 more years of information than the previous version.

4.1 Background Mean Fields

The long-term seasonal mean of 925 hPa streamlines displayed in Fig 4.1.1 reveals that the position of the monsoon trough, which is also considered as part of the ITCZ, lies diagonally along the northern region of Borneo coast and southern tip of South China Sea. Comparing to the Borneo vortex long-term mean position located at 2.4°N latitude and 110.6°E longitude as discussed in section 3.2, it shows that the center is located within the trough belt, which strongly agrees with Cheang's (1977 and 1978) assertion that the vortices are formed and embedded within the monsoon trough. Therefore, from this finding, it can be inferred that the placement of monthly mean trough should lie northward of the long-term mean position in November and shift southward as the winter monsoon progresses till February based on the monthly mean position of the Borneo vortex centers plotted in Fig 3.2.6.

A region of strong convection has always been corresponded with area of active development of convective weather systems, such as this Borneo vortex. Looking at the analysis chart of long-term seasonal average of 925 hPa horizontal divergence depicted in Fig. 4.1.2, it shows that strong convergence zone, i.e. the least value of divergence, is located over the inland of Borneo Island owing to the effect of high mountain ranges, having heights greater than 1,000 meters above sea level. Apart from that, regions of strong convection have also been established over the water body of northeast and northwest side of the study area.

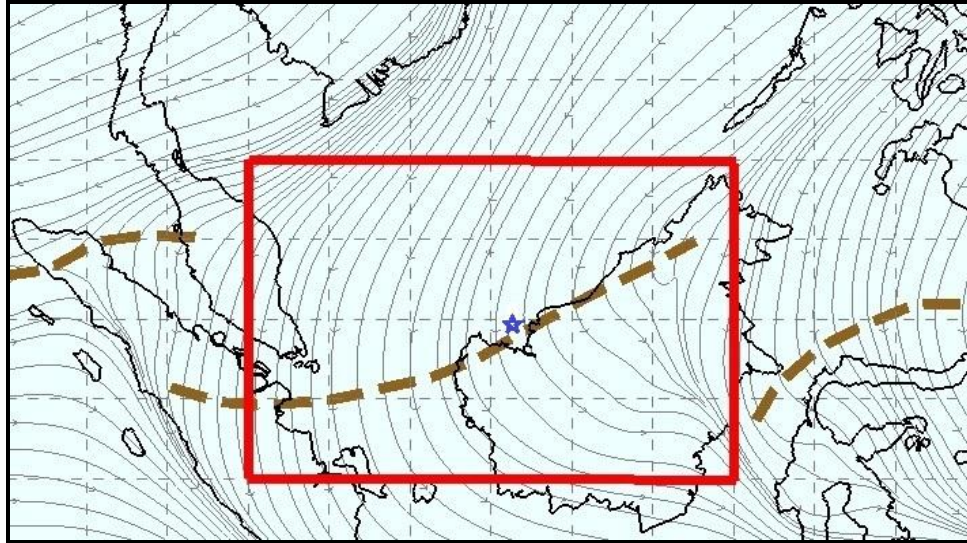


Fig 4.1.1: The 0000 UTC seasonal mean streamlines of 925 hPa wind field for winter monsoon between 1979/80 and 2010/11 seasons. Brown-dashed line is the trough and blue star is the center of Borneo vortex long-term mean position determined from section 3.2.

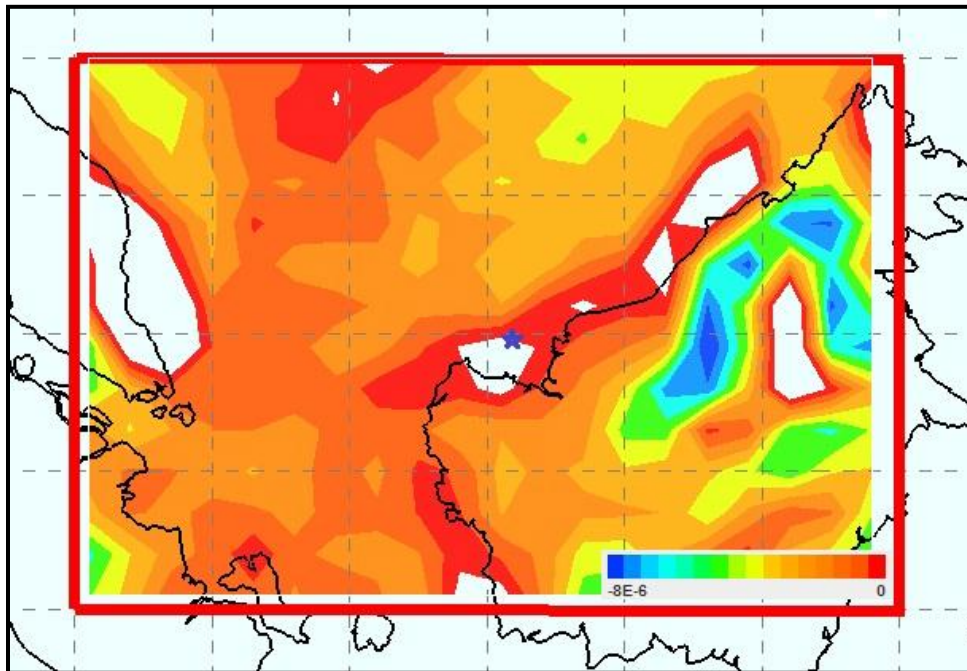


Fig. 4.1.2: The analysis of 0000 UTC seasonal mean divergence (s^{-1}) at 925 hPa chart throughout winter monsoon between 1979/80 and 2010/11 seasons. The blue star is the center of Borneo vortex long-term mean position determined from section 3.2.

However, it is unexpected to see that the location of the vortex seasonal mean center is embedded within weak convergence zone. This zone is formed probably due to strong influence of continuous land-sea breeze processes associated with the diurnal heating of the island as studied by Houze et al. (1981) or frictional effect on account of the interaction between the low-level northwesterlies and rough land mass during the early winter monsoon seasons, or both. The impact from these processes could turn the area of divergence into convergence, and vice versa. Therefore, on long-term run, it looks as if it is a neutral divergence region as analyzed in Fig. 4.1.2. Similarly, it might be the case over the east coast of Peninsular Malaysia.

Mathematically, horizontal divergence is given by $\nabla \cdot V = D = \frac{\partial u}{\partial x} + \frac{\partial v}{\partial y}$

(Holton, 1979), where V is the horizontal wind velocity, and u and v are the wind velocity in x and y directions, respectively. By adding all the 925 hPa monthly mean divergence within the study domain using pre-calculated gridded value from ERA-Interim data throughout winter monsoon period and averaging it accordingly, its long-term winter monsoon season average was determined. The value comes out as $-1.54 \times 10^{-6} \text{ s}^{-1}$, which implies that the atmospheric background of this area is in convective state.

On monthly basis, the domain experiences the strongest mean convection in December with an intensity value of $-2.28 \times 10^{-6} \text{ s}^{-1}$, followed by November, January and February with convergence intensity of $-2.06 \times 10^{-6} \text{ s}^{-1}$, $-1.37 \times 10^{-6} \text{ s}^{-1}$ and $-4.59 \times 10^{-7} \text{ s}^{-1}$, respectively. These sequences match the order of

monthly Borneo vortices lifespan duration and the number of vortex of moderate and strong intensities, which suggests that the length of the vortex lifespan and its intensity strongly depends on the convection intensity in this region.

Relative vorticity, i.e. a measure of the degree of wind cyclonicity, is another atmospheric ingredient that is normally applied in discussing the development and presence of any vortex systems in the atmosphere. The long-term mean vorticity at 925 hPa level charted in Fig. 4.1.3 reveals that the majority of the region is in positive phase, which indicates that the wind rotation basically is in cyclonic form.

This is taking place mainly because of the continuous shear between strong low level northeasterly wind and the weak equatorial westerlies during this winter monsoon season, which turns this region into conducive spot for the development of vortex systems. Indeed, large cyclonic low-level vorticity, like the Borneo vortex, could produce initially a frictionally forced low-level convergence of mass and water vapor, and consequently leading to upward vertical motion in favor of deep and strong convective systems (Gray, 1968).

When placing the long-term mean vortex center onto the chart, its position is located within intense vorticity band along the Borneo Island coast, which suggests the need of strong vorticity to support the vortex existence. In equation form, horizontal relative vorticity is defined as $\nabla \times V = \zeta = \frac{\partial v}{\partial x} - \frac{\partial u}{\partial y}$ (Holton, 1979). Taking the predetermined gridded value of monthly mean vorticity from ERA-Interim dataset and using the same method as in the previous analyses, the

long-term seasonal average vorticity was approximated. It turns out to be about $8.67 \times 10^{-6} \text{ s}^{-1}$, which indicates that the basic-state background of this area is in cyclonic state. It reaches the highest monthly mean intensity in January with a vorticity of $1.05 \times 10^{-5} \text{ s}^{-1}$ and closely followed by December with $1.04 \times 10^{-5} \text{ s}^{-1}$, while February and November experienced relatively weaker cyclonicity with vorticity of $8.8 \times 10^{-6} \text{ s}^{-1}$ and $4.96 \times 10^{-6} \text{ s}^{-1}$, respectively.

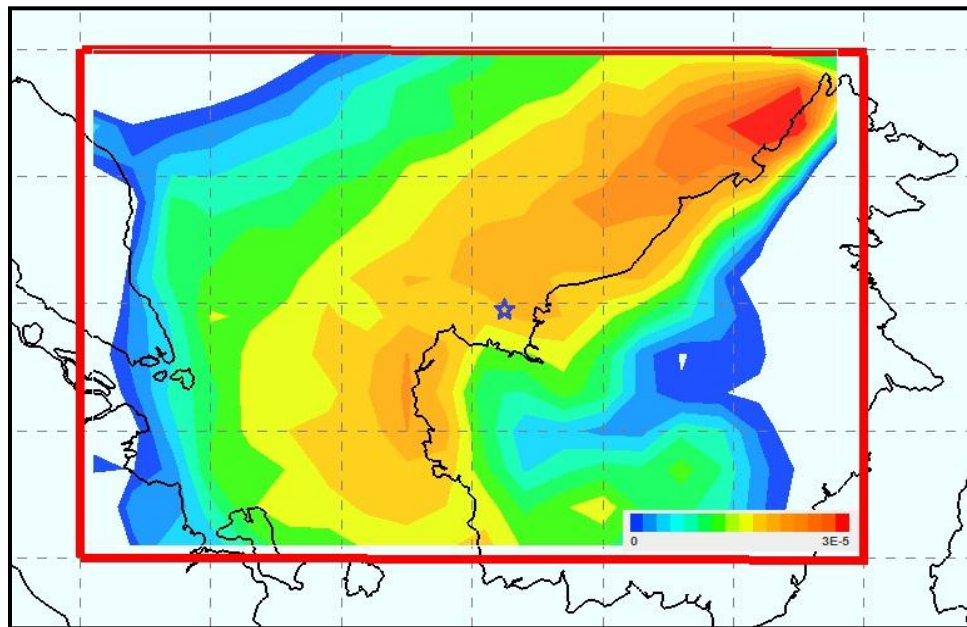


Fig. 4.1.3: The analysis of 0000 UTC seasonal mean vorticity (s^{-1}) at 925 hPa chart throughout winter monsoon between 1979/80 and 2010/11 seasons. The blue star is the center of Borneo vortex long-term mean position determined from section 3.2.

In addition to all the aforementioned parameters, the synoptic-dynamic elements of convective weather systems can also be measured through the mean vertical velocity in the atmosphere. Generally, a negative value of vertical velocity in an x-y-p coordinate system is associated with the rising of air, which can turn the atmosphere unstable and enhance the convection for Borneo vortex

to form. The long-term seasonal mean of vertical velocity in Fig. 4.1.4 shows that the vertical motion at 925 hPa level in most parts of the area is upward, which suggests that the area is favorable for the formation of convective systems. There is relatively strong rising air along Borneo coast where the long-term seasonal mean of Borneo vortex center is stood.

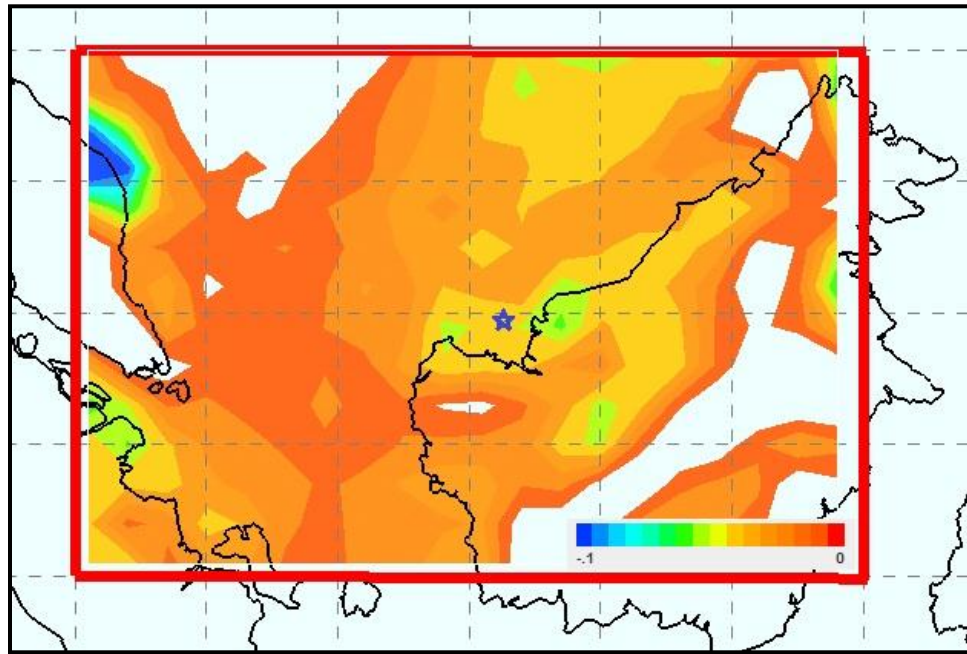


Fig. 4.1.4: The analysis of 0000 UTC seasonal mean vertical velocity (Pa s^{-1}) at 925 hPa chart throughout winter monsoon between 1979/80 and 2010/11 seasons. The blue star is the center of Borneo vortex long-term mean position determined from section 3.2.

The basic mathematical form of vertical velocity, which is also known as the kinematic omega, is normally written as $\frac{dp}{dt} = \omega_{p1} = \omega_{p0} - \int_{p0}^{p1} (\nabla \cdot V)_h dp$ (Holton, 1979), where p is the atmospheric pressure. Using pre-calculated monthly mean vertical velocity from ERA-Interim dataset, the seasonal mean within the region was estimated. The value is averaged at -0.016 Pa s^{-1} , which implies that the atmospheric basic-state during winter monsoon in this area is in

upward motion. For monthly mean, the rising motion is the strongest in December with vertical velocity of -0.022 Pa s^{-1} followed by November and January with -0.016 Pa s^{-1} , while February gained the weakest force with -0.008 Pa s^{-1} .

Another alternative way that can be used to describe the presence and development of convective and cyclonic weather systems in the atmosphere is through the analysis of potential vorticity field. Its long-term mean at 925 hPa level shown in Fig. 4.1.5 demonstrates that the region of greatest potential vorticity value is located over the northeast of Borneo above the water body area. The region agrees well with the zone of intense convection in Fig. 4.1.2 and strong vertical velocity in Fig. 4.1.4, which suggests that high potential vorticity value over that place is corresponded to the region of active convective weather development, such as the Borneo vortex.

Through various research works and observations, they verified that this kind of region is actually an area loaded with a diabatically produced potential vorticity as a result of latent heat release through rainfall activity within the troposphere. However, the position of the vortex long-term mean center is only slightly away from the core of maximum potential vorticity value. The sector over northeast of the domain has large amount of potential vorticity probably owing to strong influence of tropical cyclone activities. The outer side of that region is known to be one of the main origin and pathway location of those tropical

cyclones during winter monsoon period, as shown in Lin et al. (2009), and Lin and Lee (2011).

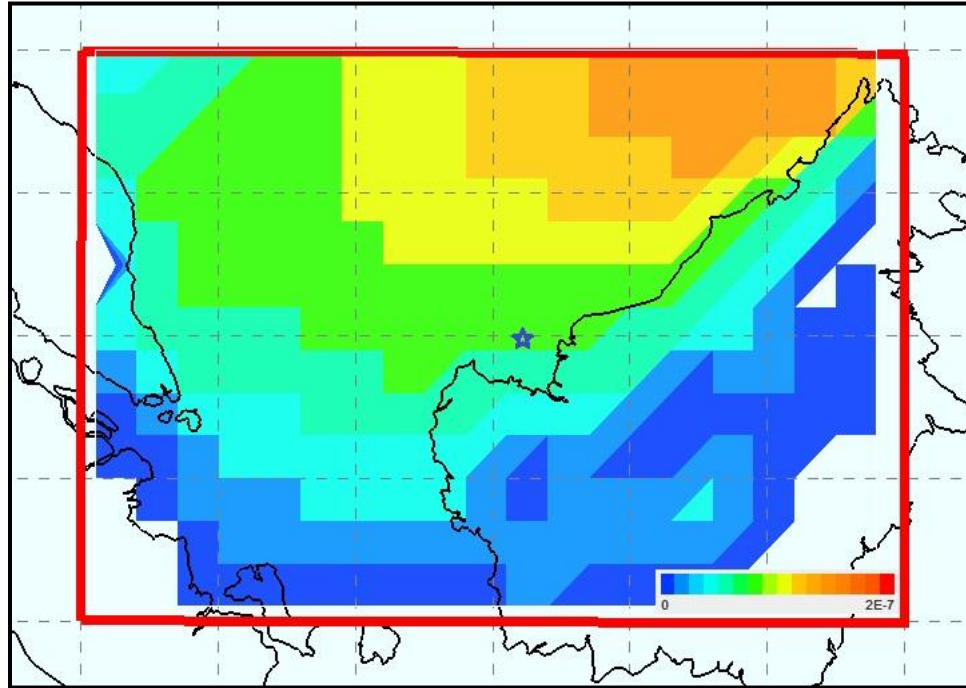


Fig. 4.1.5: The analysis of 0000 UTC seasonal mean potential vorticity ($\text{K m}^2 \text{Kg}^{-1} \text{s}^{-1}$) at 925 hPa chart throughout winter monsoon between 1979/80 and 2010/11 seasons. The blue star is the center of Borneo vortex long-term mean position determined from section 3.2.

The basic form of two dimensional (2-D) potential vorticity equation is generally written as $PV = -g\zeta_a \left(\frac{\partial \theta}{\partial p} \right)$ (Holton, 1979), where g is the gravitational acceleration, ζ_a is the absolute vorticity and θ is the potential temperature. Basically, PV is just a ratio of vorticity of certain vertical depth. In addition, PV is a quantity that is conserved in adiabatic and frictionless motion. Applying the same method as in previous analysis, the long-term seasonal mean of potential vorticity is approximated as $6.26 \times 10^{-8} \text{ K m}^2 \text{kg}^{-1} \text{ s}^{-1}$, which is equivalent to 0.0626 PVU (Potential Vorticity Unit). This value is relatively small compared to

the one found at higher latitude places since the tropics are known to possess weak absolute vorticity as a result of insignificant contribution of Earth vorticity. On monthly basis, the greatest mean was recorded in December and January with 0.07 PVU, followed by February with 0.06 PVU, while November experienced the weakest force of potential vorticity with only 0.05 PVU.

Based on the analyses of long-term seasonal mean of common background states, they obviously exhibit that throughout the winter monsoon, December is the most favorable period for Borneo vortex to form. Meanwhile, November and January atmospheric ingredients are generally having the same strength but relatively weaker than December, and February provides the least conducive condition for the occurrence of Borneo vortex. The sequence is well-matched with the climatological results attained in chapter 3. By taking all these basic-state backgrounds into consideration, detailed studies of two specific events out of 2,259 cases were chosen in order to better understand the synoptic and dynamic behaviors of Borneo vortex of different intensities.

4.2 Weak and moderate Borneo Vortices (3 December 1991)

This event was observed to include two vortices of different intensities at the same time as displayed in Fig. 4.2.1. According to the requirement set in section 2.3, the closed circulation wind centered at 4.3°N latitude and 112.2°E longitude was considered as weak vortex while the moderate one was found at 1.4°N and 108.0°E. The weak vortex was part of the vortex system that lived for

only 2 days, which appeared on the 925 hPa wind field charts on 3 and 4 December 1991 over the domain. For the case of moderate vortex, it came from a long-lived vortex system that last for 18 days, which started from 25 November and was last seen on 12 December 1991, encompassed of 9 vortices with weak intensity, 8 moderate and 1 strong.

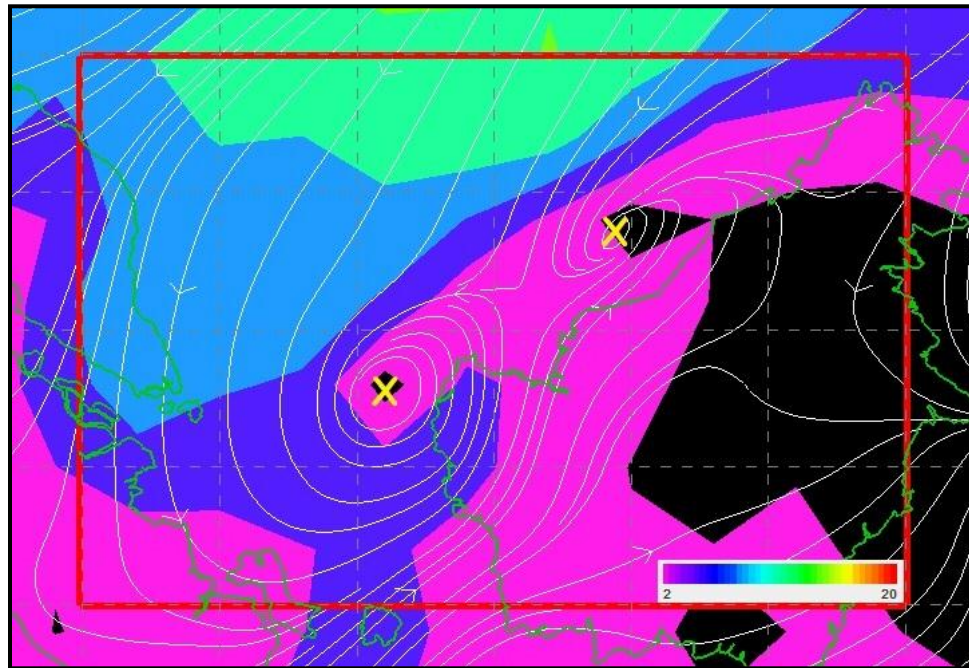


Fig 4.2.1: The analysis chart of 925 hPa wind direction (white lines) and speed (color-shaded area in ms^{-1}) at 0000 UTC on 3 Dec 1991. The yellow 'X' is the center of Borneo vortex.

During 1991/92 winter monsoon season, the climate was driven by El Nino (EN), warm PDO (PDO1) and strong PDO phases. Climatologically, from previous analyses, it was found that the EN event in PDO1 period could lead to the occurrence of less number of Borneo vortices over the study domain. While active winter monsoon associated with strong TBO would get dampened by the influence of EN phase, which also could probably reduce the seasonal vortex

quantity. From Table 3.1.1 and Table 3.4.1, 50 vortices were observed in 1991/92 winter monsoon in which 36 of them were categorized as weak, while 13 were moderate and 1 was strong. When comparing these numbers with Borneo vortex long-term mean in Table 3.4.2, it shows that most of the quantities are below normal except for the case of moderate vortex.

The 0000 UTC synoptic chart at 925 hPa in Fig. 4.2.2 clearly shows that both vortices, which are depicted by closed cyclonic circulation wind field, are embedded within the monsoon trough line that lies along the Borneo coast. The trough position seems to fit well with the location of December long-term mean center of the Borneo vortex analyzed in section 3.2. At 850 hPa level, which is about 750 meters higher than the previous altitude, both vortices are still visible on the chart and located almost at the same position as on earlier map.

However, as we move further up into 700 hPa level, the weak vortex dissipates from the map, which suggests that the presence of this type of vortex is only limited within lower atmospheric level. As for the case of moderate vortex, the center has shifted slightly to the left compared to its original position at 925 hPa level, which implies that the vertical structure of this vortex is tilted westward likely owing to strong vertical wind shear. At 600 hPa chart, about 1,000 meter higher than the previous level, the moderate vortex disappears together with the monsoon trough, which indicates that the vertical extent of this type of vortex only manages to stay between the lower and middle tropospheric levels.

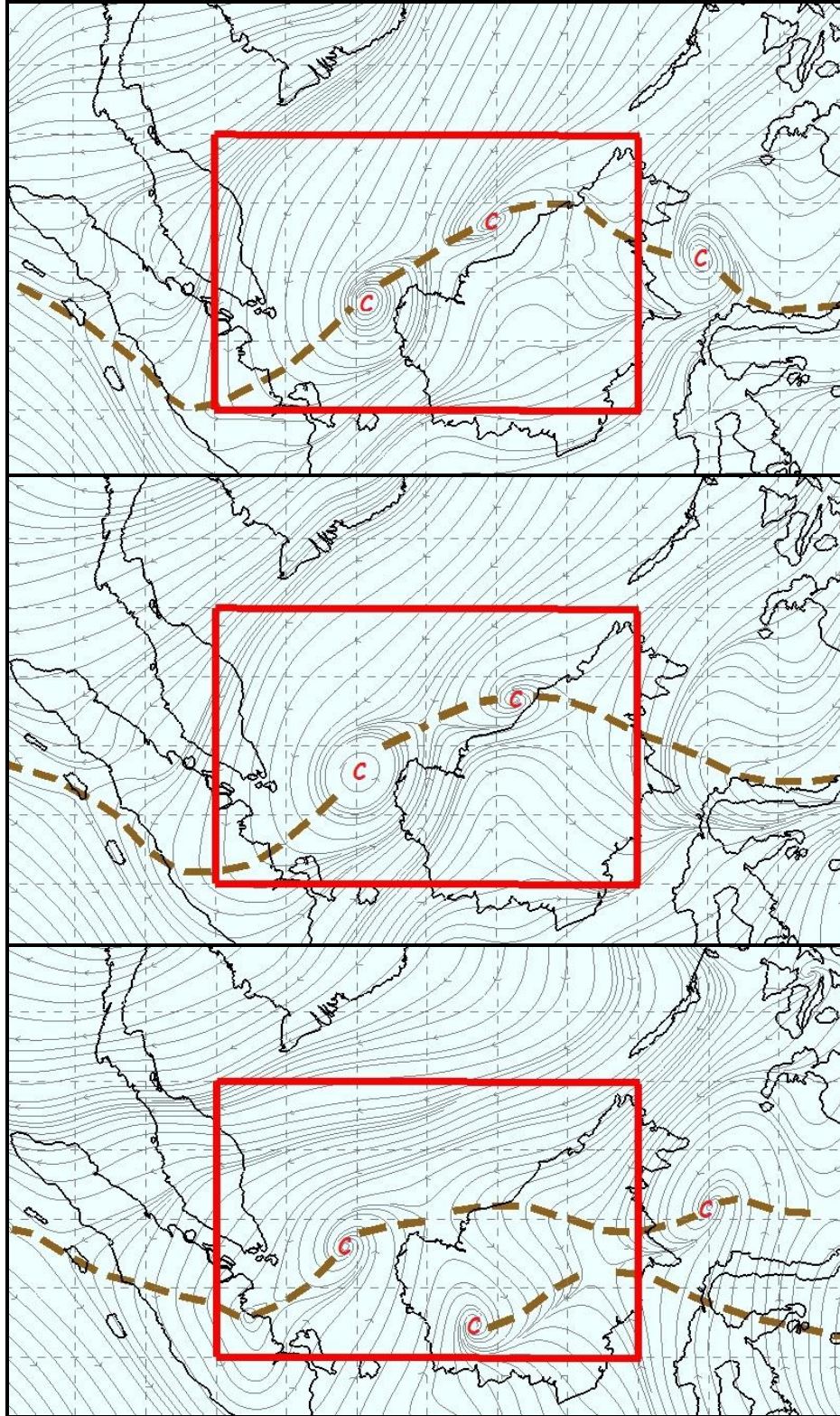


Fig 4.2.2: The analysis charts of 0000 UTC wind at 925 (top), 850 (middle) and 700 (bottom) hPa pressure levels on 3 December 1991. Brown-dashed line is the trough and "C" is the center of cyclonic circulation.

The existence of both vortices is principally possible with the support of favorable convective fields. The 925 hPa divergence map in Fig. 4.2.3 shows that both vortices are located not within but at the edge of strong convergence zone. Averaging the pre-calculated gridded value of 0000 UTC divergence at 925 hPa level from ERA-Interim reanalysis data, the mean divergence of the domain has been estimated to be $-4.62 \times 10^{-6} \text{ s}^{-1}$, which is in the same order of magnitude as the long-term seasonal mean determined in previous section. The center of moderate vortex has divergence value of $-1.10 \times 10^{-5} \text{ s}^{-1}$, one order of magnitude higher than the study area mean, while it is $-4.93 \times 10^{-6} \text{ s}^{-1}$ for the weak vortex, which is comparable with the domain average value. Both intensities are within a typical value of any large-scale convective weather system.

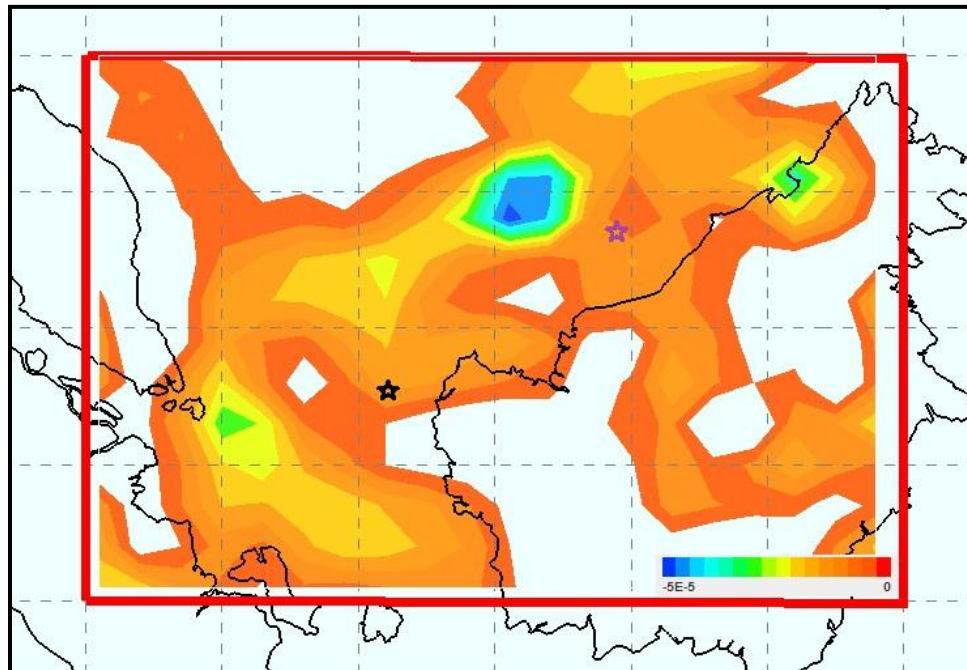


Fig. 4.2.3: The analysis of 0000 UTC horizontal divergence (s^{-1}) at 925 hPa chart on 3 December 1991. The black and purple stars are the center of moderate and weak vortices, respectively.

As for 925 hPa relative vorticity parameter analyzed in Fig. 4.2.4, the estimated mean value for the whole study domain is $1.33 \times 10^{-5} \text{ s}^{-1}$, which is 30% stronger than the long-term seasonal mean determined before, thus making it conducive for cyclonic activity to develop. The center of moderate vortex is located almost at the core of the strongest cyclonic zone with interpolated vorticity magnitude of $1.41 \times 10^{-4} \text{ s}^{-1}$, which is within a typical value for large-scale convective storm system and about 10 times stronger than the domain average. As for the case of weak vortex, its center is situated over the next strongest vorticity region with vorticity strength of $5.46 \times 10^{-5} \text{ s}^{-1}$, slightly less than half of the moderate vortex intensity.

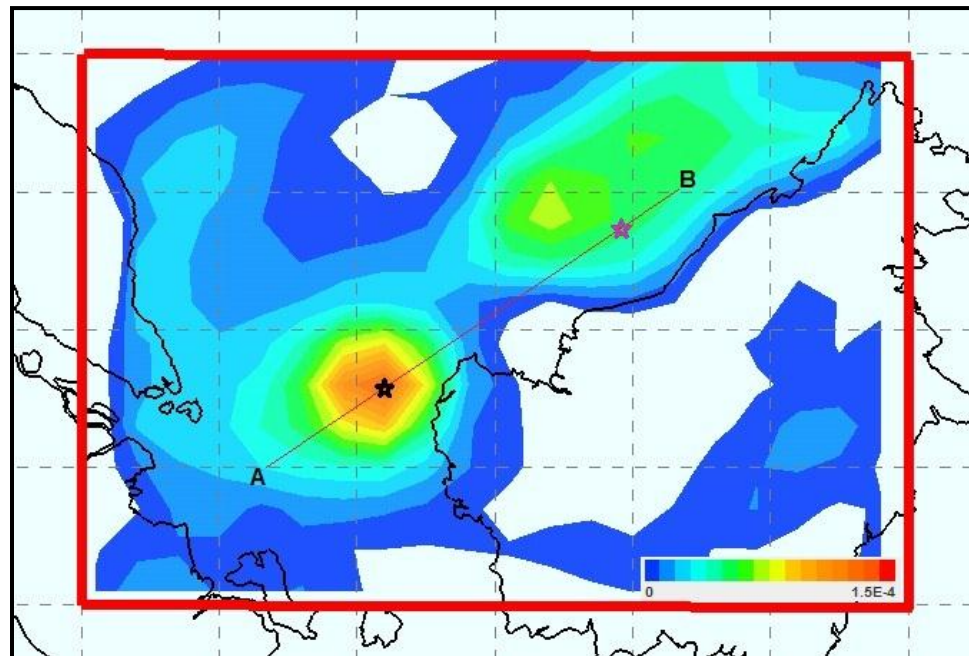


Fig. 4.2.4: The analysis of 0000 UTC horizontal relative vorticity (s^{-1}) at 925 hPa chart on 3 December 1991. The black and purple stars are the center of moderate and weak vortices, respectively.

The cross section of relative vorticity between 1000 and 100 hPa levels that cut through the center of both vortices displayed in Fig. 4.2.5 clearly shows that the vertical extent of the weak vortex sustained by intense vorticity is only limited within the lower tropospheric level. By considering the vorticity value of $5 \times 10^{-5} \text{ s}^{-1}$ as strong enough to support the development of the Borneo vortex, it is found that such a value for this vortex only exist within the altitude of less than 2,000 meters or roughly at about 800 hPa pressure level.

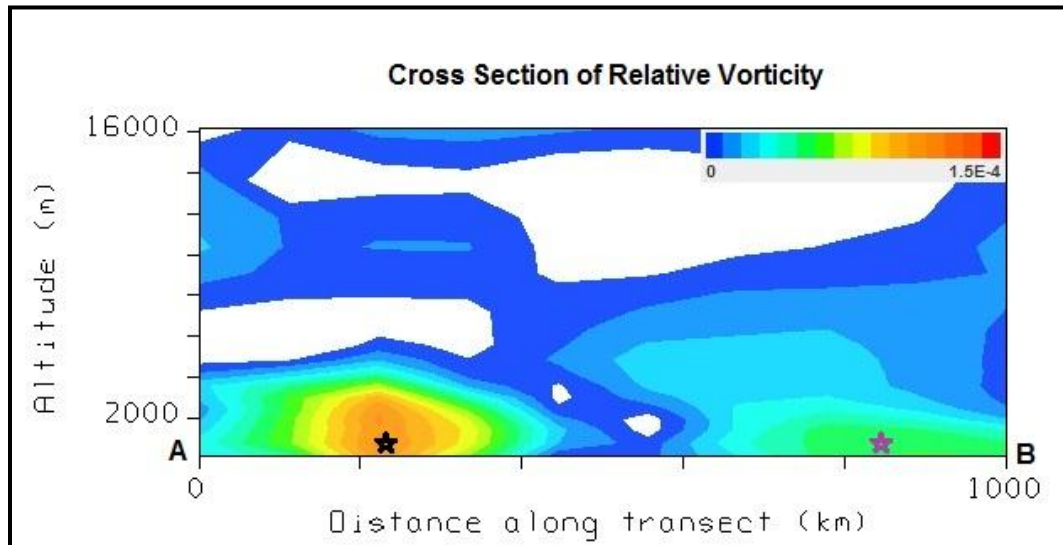


Fig. 4.2.5: The vertical cross section between A and B in Fig. 4.2.4 of 0000 UTC horizontal relative vorticity (s^{-1}) at 1000 to 100 hPa pressure levels on 3 December 1991. The black and purple stars are the center of moderate and weak vortices, respectively.

As for the moderate vortex, the vorticity with such strength is noticed within 4,000 meters altitude or slightly below the 600 hPa pressure level. Fig. 4.2.5 also reveals that this strong vorticity force has spread horizontally to over more than 200 km in diameter for both cases. Taking this to be the size of the

vortices, hence both of them can be categorized as a synoptic-scale weather system, as claimed by many scholars.

In the case of vertical velocity parameter depicted in Fig. 4.2.6, the location of its greatest strength coincides with the region of strongest convergence and cyclonic circulation zones displayed in Fig. 4.2.3 and Fig. 4.2.4. The mean value found within the domain is -0.025 Pa s^{-1} , which indicates that majority of air in this region is rising possibly due to unstable atmospheric condition. This value is almost the same as the long-term mean of December determined in previous section.

Both moderate and weak vortices were embedded in the region of upward motion but not placed in the strongest sector. The center of moderate vortex has omega amount of -0.15 Pa s^{-1} , which is within the typical value of large-scale convective weather system. On the contrary, the force of vertical motion of weak vortex is relatively weak with the value of only -0.032 Pa s^{-1} , which suggests that this type of vortex is unlikely to turn into severe convective weather system.

Regarding the potential vorticity field, its 925 hPa analysis chart in Fig. 4.2.7 portrays almost the same pattern as the vorticity field shown in Fig. 4.2.4. The center of moderate Borneo vortex is located close to the core of maximum potential vorticity quantity while the weak one is placed just over the edge of another maximum zone. The approximated mean value of potential vorticity within the domain is 0.094 PVU , which is in the same order of magnitude as December long-term quantity determined in section 4.1. However, the strength is

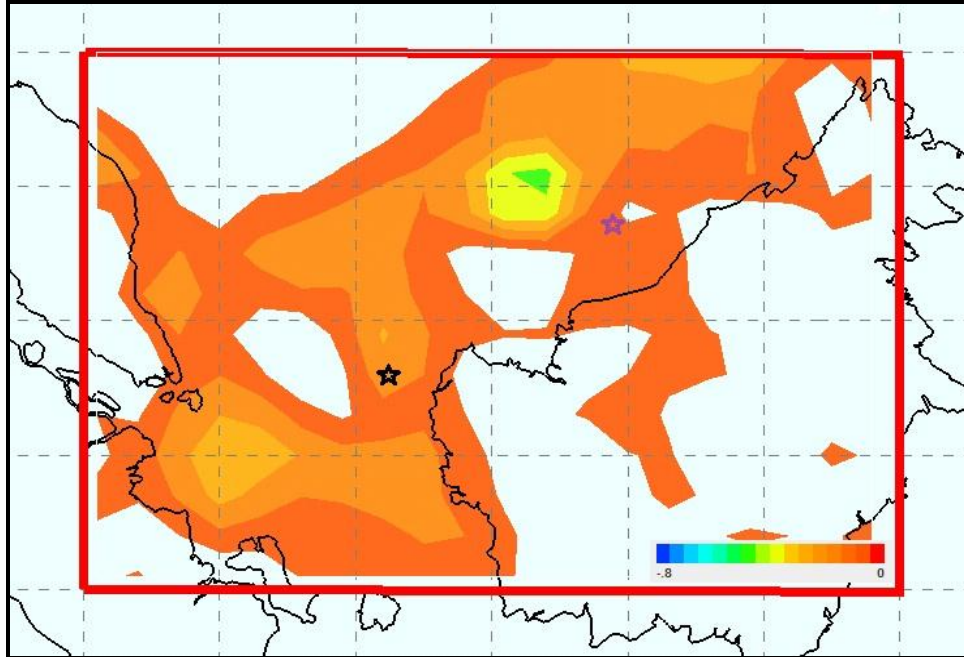


Fig. 4.2.6: The analysis of 0000 UTC vertical velocity/omega (Pa s^{-1}) at 925 hPa chart on 3 December 1991. The black and purple stars are the center of moderate and weak vortices, respectively.

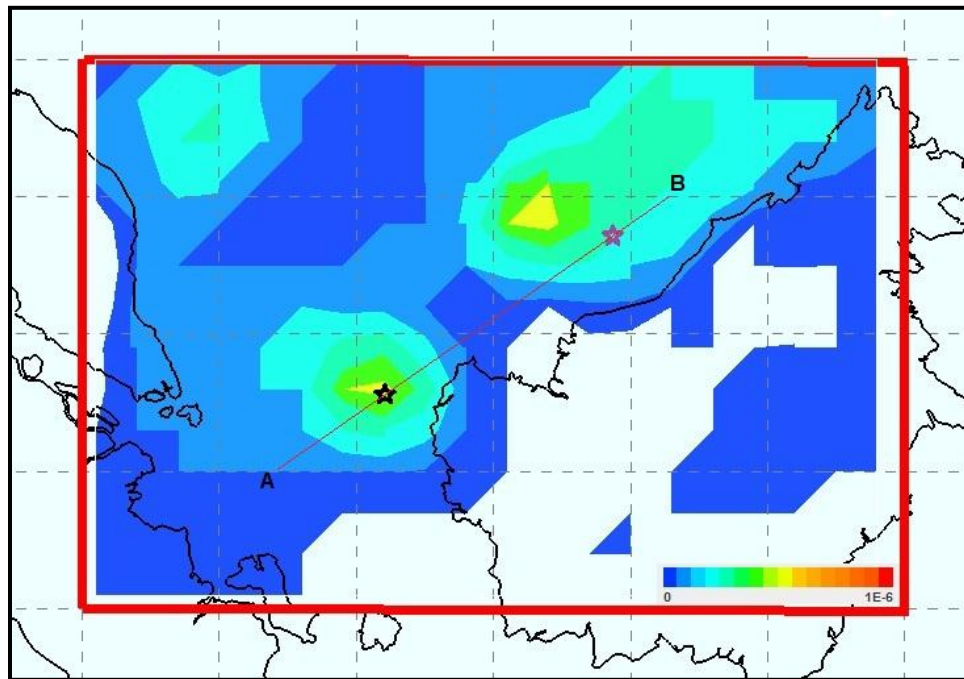


Fig. 4.2.7: The analysis of 0000 UTC potential vorticity ($\text{K m}^2 \text{Kg}^{-1} \text{s}^{-1}$) at 925 hPa chart on 3 December 1991. The black and purple stars are the center of moderate and weak vortices, respectively.

far greater at the center of moderate vortex with the value of 0.504 PVU, while it is not as high at the weak center, having value of only 0.332 PVU.

The cross section along the center of both vortices between 1000 and 100 hPa pressure levels presented in Fig. 4.2.8 shows that the vertical extent and the strength of the potential vorticity for the moderate vortex is much superior than the weak one. The depth of potential vorticity within the moderate vortex with the intensity of 0.25 PVU or greater stays within 4,000 meters in altitude but not surpassed 2,000 meters for the case of weak vortex. Since the quantity of potential vorticity within the troposphere region is associated with the amount of latent heat released, therefore one can imply that moderate vortex is a weather system that could generate large volume of rainfall compared to weak vortex.

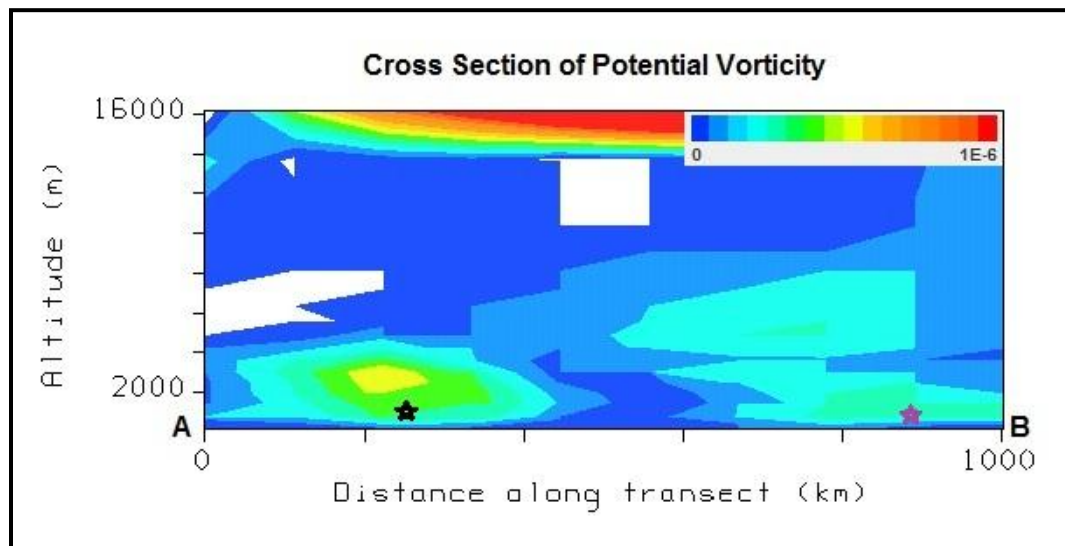


Fig. 4.2.8: The vertical cross section between A and B in Fig. 4.2.6 of 0000 UTC potential vorticity ($K m^2 Kg^{-1} s^{-1}$) at 1000 to 100 pressure levels on 3 December 1991. The black and purple stars are the center of moderate and weak vortices, respectively.

Through the analyses of this specific event, it can be deduced that the occurrence of weak Borneo vortex only requires very minimal amount of convective forces, but most of their magnitudes are greater than the domain averages. Its existence on the upper level synoptic charts is only limited within the lower tropospheric level and comes with small amount of rainfall. All these imply that this kind of vortex is a weak disturbance and not capable of inducing any large-scale severe convective weather system to strengthen the winter monsoon season over the study area. However, it could intensify and turn itself into stronger type of vortex system with the enhancement of its background conditions.

As for Borneo vortex with moderate intensity, all its convective parameters are within typical values of large-scale weather systems, which suggests that this kind of vortex might have a capability to support the formation of any stormy weather phenomenon. Since the vortex comes with large amount of rainfall, its occurrences could possibly intensify the winter monsoon season in the area. In spite of the availability of all these active ingredients, the presence of this particular moderate vortex on the upper level weather charts is only limited between the lower and middle tropospheric levels. This indicates that the vertical growth of such vortex throughout the atmosphere is not deep enough to enable it to become a large-scale severe weather system with great strength like mid-latitude and tropical cyclones.

4.3 Strong Borneo Vortex (9 January 2009)

The vortex is categorized of having strong intensity based on the requirements set in section 2.3 where the wind speed over its northwest segment was found to be greater than 10 ms^{-1} . Its center was placed at 2.3°N latitude and 112.1°E longitude, which is situated on the land mass of Borneo Island, as depicted in Fig. 4.3.1. This vortex is part of long-lived vortex system that was first seen on the 925 hPa wind chart of 23 December 2008 and withstood for 21 day until 12 January 2009.

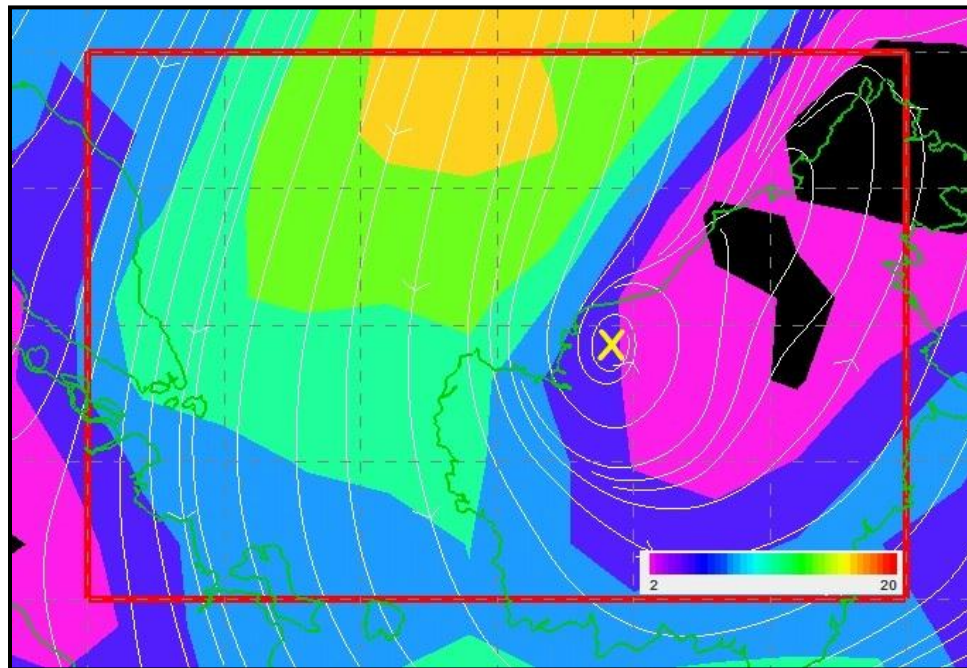


Fig. 4.3.1: The analysis chart of 925 hPa wind direction (white lines) and speed (color-shaded area in ms^{-1}) at 0000 UTC on 9 January 2009. The yellow 'X' is the center of Borneo vortex.

Through its lifespan, the system bore 9 vortices with weak intensity, 9 moderate and 3 strong. On 9 January 2009, the intense northeasterly wind in

association with the cold surge coming from central Asia entered the study domain and elevated the vortex intensity from moderate to strong. This kind of interaction enhances the Borneo vortex as well as winter monsoon intensity over the region, and has been observed and studied by many researchers, such as Ramage (1968), Cheang (1977 and 1987), Johnson and Houze (1987), Zhang et al. (1997b) and Chang et al. (2005b).

During 2008/09 winter monsoon, the climate was influenced by neutral ENSO condition together with PDO2, while the TBO was in strong mode. According to the climatological analyses done earlier, the number of Borneo vortices tends to be larger than the long-term mean during PDO2 and strong TBO phases. However, in the event of NEU years, the vortex quantity is likely to remain the same as the long-term value. Anyhow, 73 Borneo vortices were documented during this monsoon season, which were about 30% more than the long-term mean, while the number of strong vortices were doubled.

The 925 hPa synoptic chart at 0000 UTC of 9 January 2009 in Fig. 4.3.2 clearly exhibits that the vortex is located at the center of the monsoon trough line that lies diagonally along the Borneo coast and crosses the southern tips of the South China Sea. The orientation of this trough seems to be comparable to the mean position of January long-term vortex center plotted in Fig. 3.2.6. Unlike in previous cases, the presence of this vortex can be detected at much higher levels over the upper air chart.

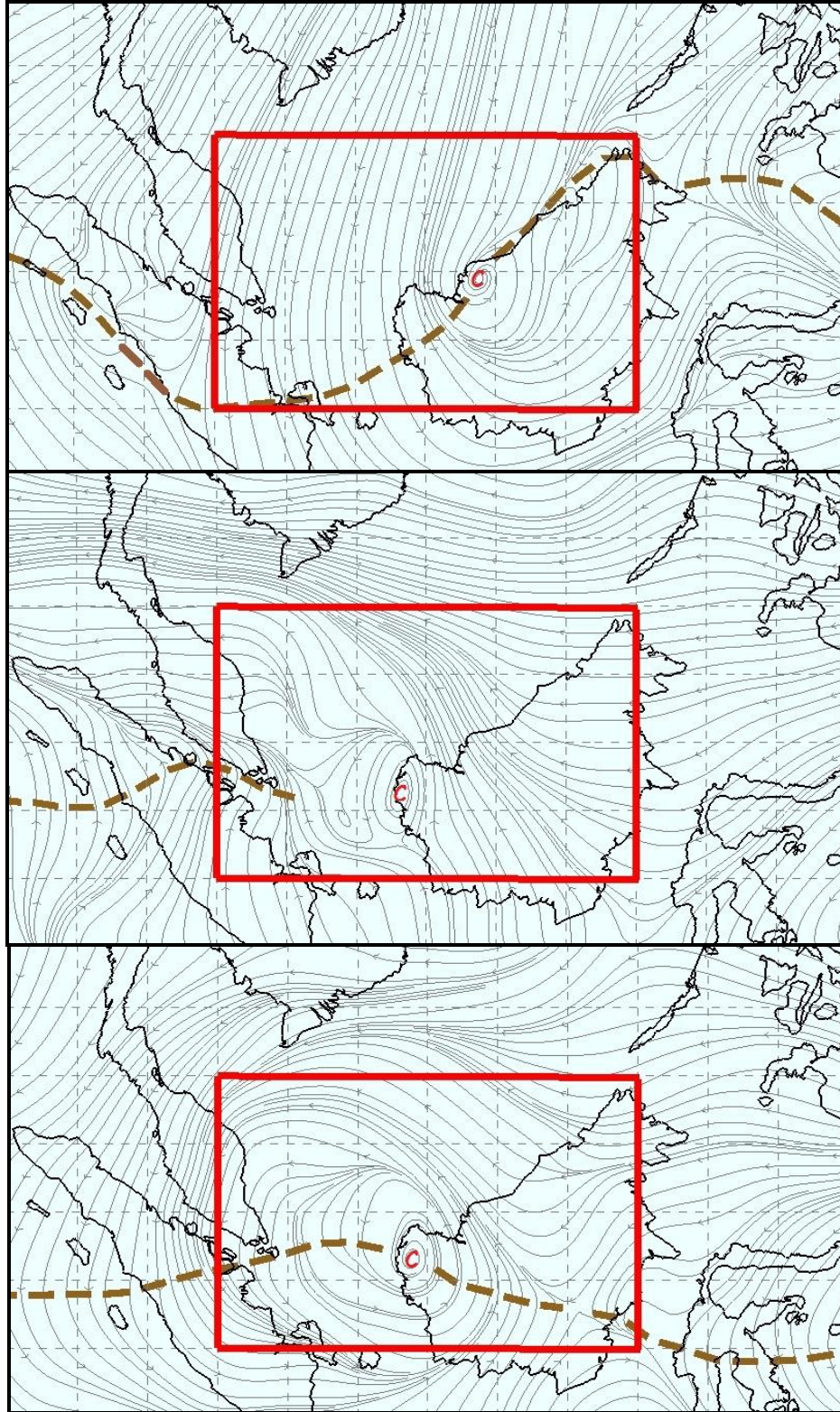


Fig 4.3.2: The analysis charts of 0000 UTC wind at 925 (top), 500 (center) and 400 (bottom) hPa pressure levels on 9 January 2009. Brown-dashed line is the trough and “C” is the cyclonic circulation center.

At 500 hPa level, the position of the vortex center has shifted southwestward from its original location found in lower altitude. This indicates that the vortex has tilted toward the southwest direction, possibly due to strong shear associated with robust upper level wind. The vortex was observed to dissipate from the charts as the analyses went beyond 400 hPa level, which suggests that the vortex only manages to penetrate into middle troposphere and possibly able to reach the bottom part of upper atmospheric level.

The existence of strong vortex should come with strong convective fields. In term of its divergence magnitude, the mean value has been calculated as $-2.33 \times 10^{-6} \text{ s}^{-1}$, which is in the same order of magnitude as the long-term seasonal mean estimated earlier. Fig. 4.3.4 shows that the vortex center is located not exactly inside the strongest divergence zone but rather only at the edge of it. The estimated divergence value at the center is $-2.66 \times 10^{-5} \text{ s}^{-1}$, one order of magnitude higher than the region mean. This is considered within a typical value of large-scale convective system for a development of any stormy weather.

As for relative vorticity field depicted in Fig. 4.3.4, the average cyclonic force for the whole study area was calculated as $1.66 \times 10^{-5} \text{ s}^{-1}$, which is 25% stronger than the background state of former case study. However, the center of strong vortex for this event is not located exactly at the core of the greatest vorticity like in the earlier case of moderate vortex. This is probably owing to the impact of strong northeastly cold surge that penetrated into the domain and

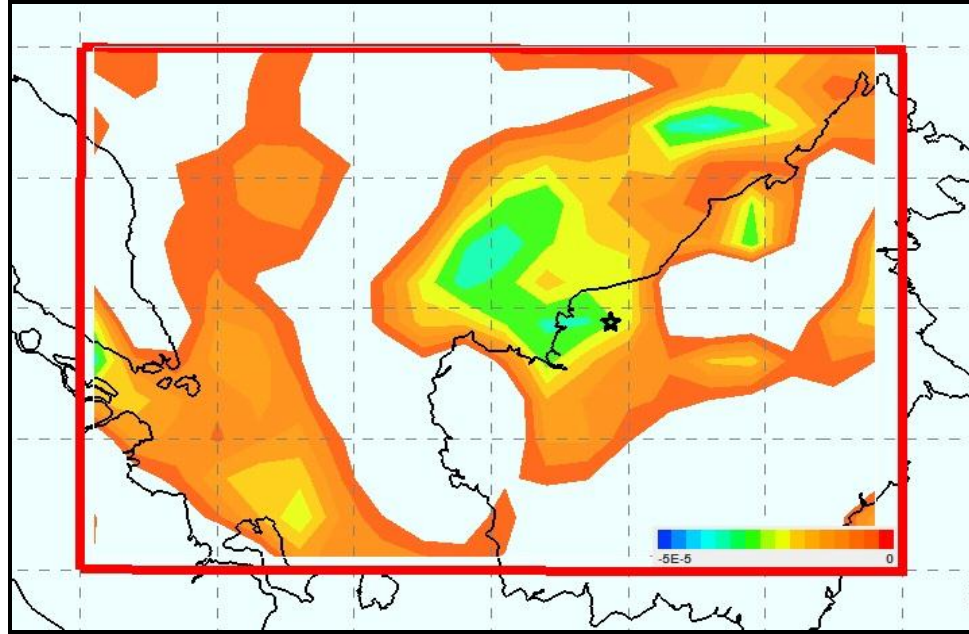


Fig. 4.3.3: The analysis of 0000 UTC horizontal divergence (s^{-1}) at 925 hPa chart on 9 January 2009. The black star is the center of strong vortex.

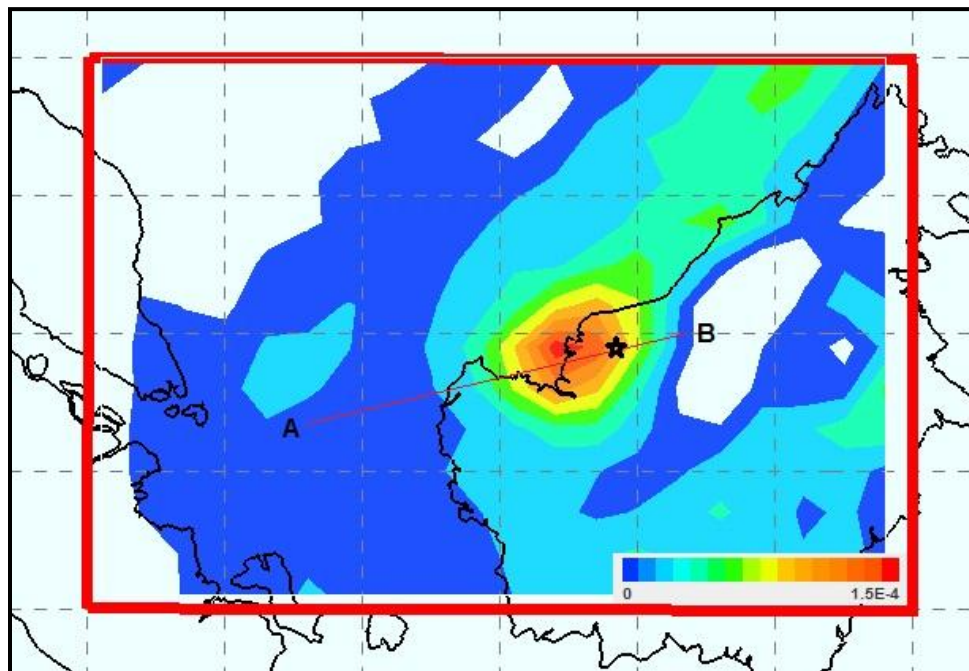


Fig. 4.3.4: The analysis of 0000 UTC horizontal relative vorticity (s^{-1}) at 925 hPa chart on 9 January 2009. The black star is the center of strong vortex.

pushed the center away to the edge of maximum vorticity region. As a result, the vorticity determined at this center was slightly weaker than the moderate event with a value of $1.21 \times 10^{-4} \text{ s}^{-1}$ compared to $1.41 \times 10^{-4} \text{ s}^{-1}$. Yet, it is still within a typical value of large-scale convective weather system, which could support the development of disastrous weather event.

The cross section of relative vorticity that cut through the center of this vortex between 1000 and 50 hPa levels displayed in Fig. 4.3.5 reveals that the vortex is significantly tilted westward, possibly as a result of strong vertical wind shear in association with the cold surge. The vertical extent of strong vorticity of at least $5 \times 10^{-5} \text{ s}^{-1}$ in strength is available within the altitude of slightly below 10,000 meters or equivalent to about 350 hPa pressure level. The presence of such amount of vorticity up to this elevation, which is between the middle and upper atmospheric levels, is considered deep enough to support the development of any large-scale severe convective weather system. Its horizontal span seems to exceed 200 km, which suggests that it is a synoptic-scale weather system, as cited in many works.

Meanwhile, the vertical velocity field depicted in Fig. 4.3.6 shows that the location of its maximum quantity matches well with the region of greatest convergence and cyclonic circulation zones presented in Fig. 4.3.3 and Fig. 4.3.4. The estimated mean value within the domain is -0.009 Pa s^{-1} , which is considered as very weak rising force since more than half of the atmospheric state in the study domain is either in a stagnant or sinking (non-shaded area)

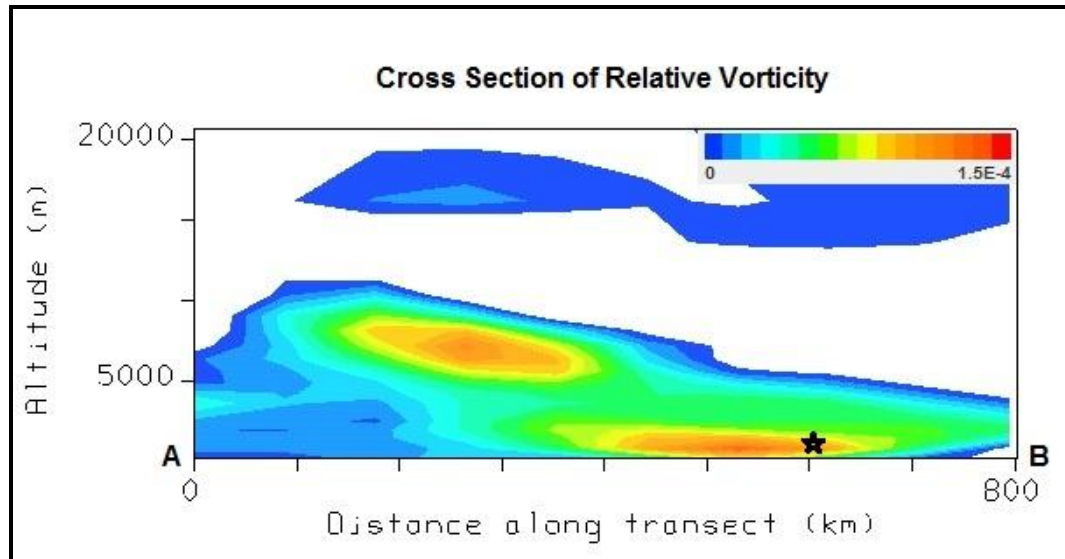


Fig. 4.3.5: The cross section between A and B in Fig. 4.3.4 of 0000 UTC relative vorticity (s^{-1}) at 1,000 to 50 hPa pressure levels on 9 January 2009. The black star is the center of strong vortex.

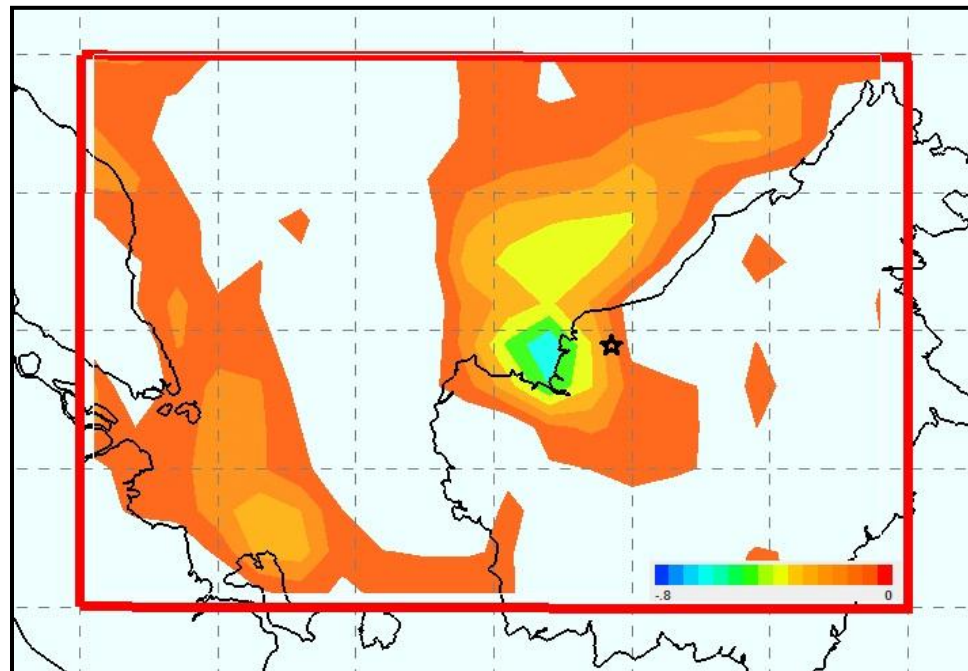


Fig. 4.3.6: The analysis of 0000 UTC vertical velocity/omega (Pa s^{-1}) at 925 hPa chart on 9 January 2009. The black star is the center of strong vortex.

condition. Even though the vertical extent of the vortex was able to penetrate into the upper layer of the troposphere, its omega value of -0.143 Pa s^{-1} was actually slightly weaker than the case of moderate vortex. This is possibly due to the extreme tilt of the vortex as a result of strong vertical wind shear under the influence of cold surge.

Since relative vorticity is a part of the compositions that is required in quantifying potential vorticity, it is not surprising to see that its 925 hPa field analysis in Fig. 4.3.7 depicts almost the same pattern as the relative vorticity chart in Fig. 4.3.4. The center of strong Borneo vortex is found to be located at the periphery of the maximum value zone, just similar to the analyses of other convective parameters. Its domain mean field comprises nearly as the same amount of potential vorticity as in previous event, which is approximated to be 0.094 PVU. Meanwhile, at the vortex center, the value is about the same as in the case of moderate vortex with 0.498 PVU compared to 0.504 PVU, which implies the presence of large quantity of latent heat in association with abundant amount of rainfall availability within the strong vortex system.

The cross section of potential vorticity that cut through the center of strong vortex between 1000 and 50 hPa pressure levels presented in Fig. 4.3.8 reveals that the vertical and horizontal extents and its intensity are much more significant than the previous event. The depth of potential vorticity within the strong vortex with intensity of 0.25 PVU or greater is about to reach the 10,000 meters altitude. Since the quantity of potential vorticity within the troposphere region is

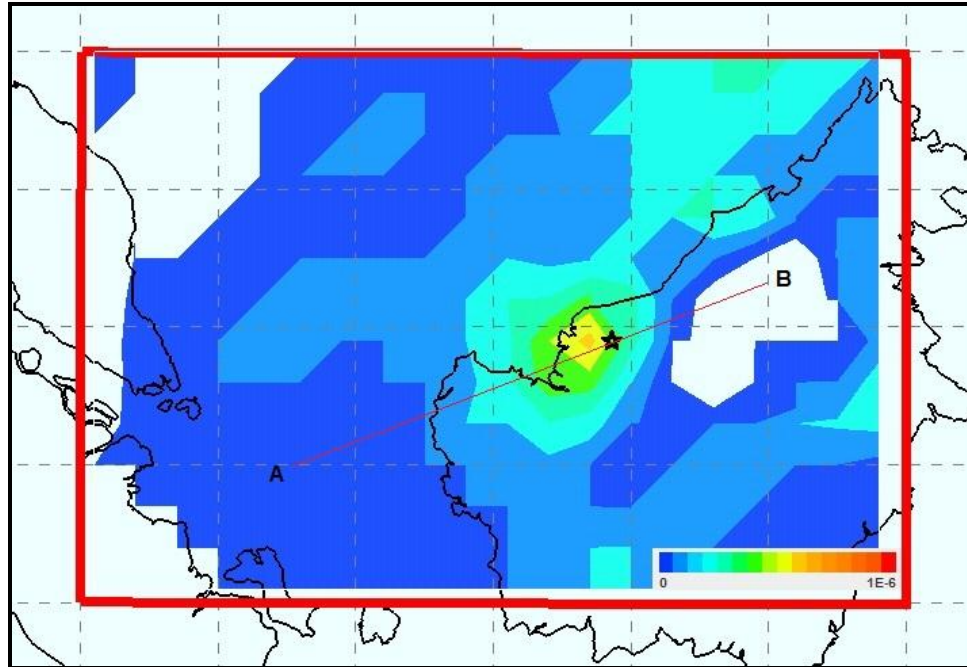


Fig. 4.3.7: The analysis of 0000 UTC potential vorticity ($\text{K m}^2 \text{ Kg}^{-1} \text{ s}^{-1}$) at 925 hPa chart on 9 January 2009. The black star is the center of strong vortex.

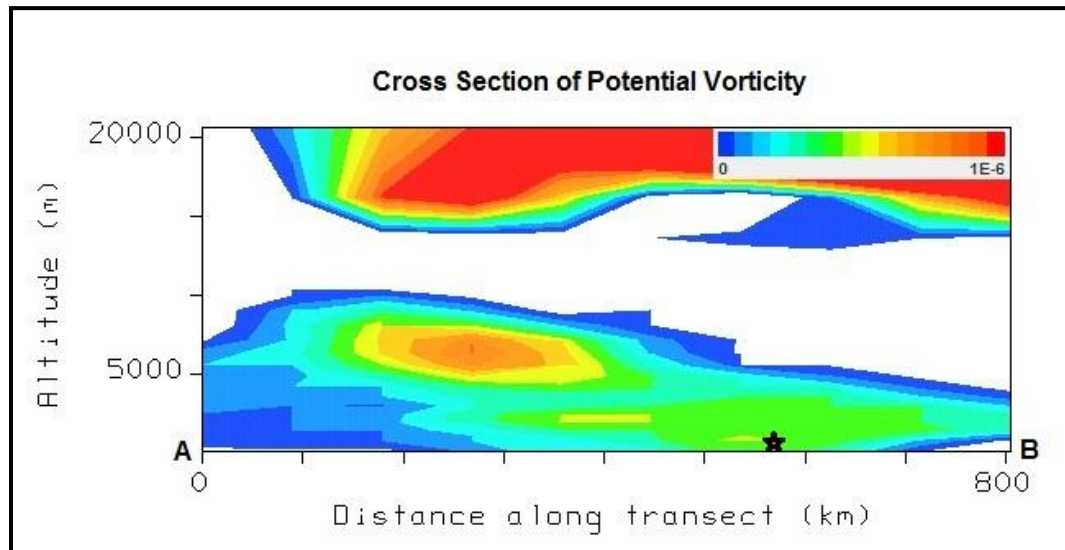


Fig. 4.3.8: The cross section between A and B in Fig. 4.3.7 of 0000 UTC potential vorticity ($\text{K m}^2 \text{ Kg}^{-1} \text{ s}^{-1}$) at 1,000 to 50 hPa pressure levels on 9 January 2009. The black star is the center of strong vortex.

corresponded to the amount of latent heat released, therefore it could be implied that strong vortex is a weather system that comes with large volume of rainfall, and hence could probably boost the winter monsoon intensity.

Another interesting feature that was discovered in Fig. 4.3.8 is the fold of potential vorticity field at the upper part of the cross section, normally known as tropopause undulation, which could lead to the emergence of upper atmospheric trough. Over the mid-latitude region, this setup generally follows by the onset of surface cyclogenesis of baroclinic weather systems as observed and discussed by many researchers, namely Hirschberg and Fristch (1991).

However, in the tropics, this kind of phenomenon is called tropical upper-tropospheric trough (TUTT), which is believed to form on account of the extrusions of mid-latitude stratospheric air (Nieto and Schubert, 1999). In this event, the culprit that leads to such action could probably due to the effect of cold surge that came all the way from mid-latitude of Asian continent and channeled the cold air into the domain.

Lots of studies have shown that the presence of TUTTs have been related to the wake of tropical cyclones. Therefore, what was identified here indicates that the existence of strong vortices and tropical cyclones is probably a product of the same process. That is why in some occasions the Borneo vortex of this strength managed to evolve into tropical depressions and tropical storms like in the case of Tropical Storm Greg (Lander et al., 1999) and Typhoon Vamei (Chang et al., 2003).

In summary, based on the above analyses, one can generalize that the presence of strong Borneo vortex within the study domain needs to be supported by relatively strong convective fields compared to previous event of weak and moderate vortex intensities. Even though some of the field magnitudes were slightly weaker than the moderate vortex, they were all within typical values of any large-scale convective weather system.

In term of its vertical extent, this kind of vortex able to grow much taller than the weak and moderate cases, which make it possible for large-scale deep convection to take place. Besides, the vortex is capable of holding large amount of rainfall, and hence releases more latent heat, which could permit the intensification of winter monsoon activity over this region under the support of CISK mechanism. In addition to that, the vortex is also comparable to tropical cyclones since both of them share certain behaviors and structure, probably owing to the strong contribution of not only the barotropic but also baroclinic instability as assumed by Cheang (1977).

CHAPTER 5

Summary and conclusions

All this while, the majority of the earlier studies of the Borneo vortices were focused on their synoptic and dynamics behaviors. It is aware that these vortices are a semi-permanent feature of the Malaysian winter monsoon since they frequently appear here owing to the region orientation. The presence or absence of these vortices in the monsoon trough is believed to be one of the key ingredients in modulating the monsoon activities, which are mainly associated with rainfall intensity. However, very limited attempts have been made to examine the vortices climatological characteristics in order to understand their variability so that the output can be used by operational meteorologists as an additional tool in improving the seasonal weather forecasts for this region.

Therefore, extensive efforts were carried out here so as to establish the comprehensive analyses of the Borneo vortices climatology with respect to its interannual and interdecadal variability. The study domain was set within 15° X 10° of longitude and latitude dimensions, which covered an area of intense vortex occurrences. The identification of the vortices was done through the method

suggested by Chang et al. (2003 and 2005a) using the ECMWF reanalysis data for 41 winter monsoon between November and February that ran from 1970/71 until 2010/11 seasons. The vortices were divided into different seasonal aspects, which include the frequency, center position, intensity, lifespan, onset and retreat dates.

2,278 Borneo vortices were identified throughout 4,810 days of 41 winter monsoon seasons, which indicate that the vortices could be found at almost 50% of the study period. Out of these numbers, about 77% were considered as weak type of vortices, 17% moderate and 5% strong. The mean position of the vortex center was located at 2.4°N and 110.6°E, which is just off coast of the Borneo. This is taking place mainly because more than 60% of the vortices were formed on a water body. On average, the vortex systems have a lifespan of 3.6 days, which suggest that they are a synoptic type of weather event.

The first Borneo vortex of the season tends to form in the early of November while the last one left the region by end of February. If both of these events are taken as the onset and retreat dates of the winter monsoon, the mean duration of the monsoon period over this region was turned out to be about 112 days. On monthly basis, December is considered as the peak period of the winter monsoon season based on the number of vortices and its vortex system lifespan. The monthly position of the vortex center shifted southeastward as the winter monsoon progresses, which coincides with the transition of the monsoon trough

and winter monsoon seasons studied by Sandler and Harris (1970), Lau and Chan (1983) and Tanaka (1994).

Throughout the study period, the majority of the seasonal Borneo vortex aspects show that their polynomial regressions tend to follow the interdecadal variability of the PDO. More number of Borneo vortices was spotted during cold PDO and less in warm PDO. In addition, the monsoon period tends to be long in PDO2 and short during PDO1. However, most of these mean values are statistically insignificant except in the case of strong vortices. In term of the vortex seasonal mean center, the influence of the PDO is found to be statistically significant on the vortex latitudinal position but not to its longitudinal variation. These demonstrate that the PDO2 has a tendency to force more vortices to get formed northward of its long-term mean position while more are developed in the south during the PDO1.

By transforming the time-series data into a function of cycle through the Fourier power spectral methods, it was revealed that most of the Borneo vortex aspects emulate the interannual periodicities similar to ENSO, QBO and TBO oscillations. Among them, ENSO is found to be the major climate factor in influencing most of the seasonal aspects of the Borneo vortices throughout this study. In LN years, more Borneo vortices were formed mainly of weak and strong intensities; the vortex lifespan was long, the last vortex of the season left the domain very late and the monsoon period turned lengthy, which are all considered statistically significant with at least 90% confidence level or close.

Meanwhile, the outcomes are the opposite during the EN events, even though some of them are statistically insignificant. In addition, the occurrence of first vortex of the season is likely to be early under the influence of EN years, but not for LN case.

Some of these effects become more apparent when the ENSO is stratified by the PDO period. The influence of EN is found to be relatively stronger in PDO1 period in most of the vortex aspects, similar to what have been demonstrated in Zhang et al (1997a), Gershunov and Barnett (1998), and Birk et al. (2010). However, only the cases of vortex quantity with strong intensity and the onset date of first vortex are found to be statistically significant at 90% confidence level. On the other hand, the signal of LN is relatively stronger in the PDO2 period, but very limited number of vortex aspects is considered to be statistically significant at 90% confidence level, which includes the number of weak vortices that have the tendency to occur more in this climate condition and the seasonal vortex mean center position that tends to stay further northeastward from its mean position.

Besides the ENSO, the signal of interannual variability that is similar to the TBO oscillation has also been found to influence the variation of some of the Borneo vortex seasonal aspects. Although the TBO is believed to have a strong connection with the ENSO events, yet its impact is not as significant as the ENSO. Most of the influence of strong TBO tends to be similar to LN, while the weak TBO tend to follow the EN. However, through statistical tests, only the

limited numbers of vortex aspects are found to be statistically significant with at least 90% confidence level, which includes the decrease in strong vortex quantity during weak TBO phase, an early onset of the first vortex and the extension of the monsoon duration in strong TBO event.

When considering the TBO events in ENSO phases, the effects turn more prominent. The TBO signal becomes strong in LN years and weak in EN events, which are clearly demonstrated the role of ENSO in modulating the TBO events as stressed by earlier works. However, not all impacts are found to be statistically significant. In the analyses on the influence of the QBO oscillation toward the variability of the Borneo vortex seasonal aspects, the majority of the results show that none of them is statistically significant even at 50% confidence level. These outcomes strongly suggest that the effect of QBO oscillation on the climate variability over the tropics has been very nominal, similar to what have been emphasized by many scholars, such as Baldwin et al. (2001).

The case studies performed in chapter 4 revealed that the presence of weak vortices was insignificant in enhancing the monsoon activity due to their weak convective forcings. However, the moderate and strong vortices demonstrated much stronger convection, which probably allowed the winter monsoon to get intensified. Therefore, with regard to their impacts, it is suggested that, in the near future, any study of these events should be limited to Borneo vortices of moderate and greater intensities, where the wind speed should be greater than 5 ms^{-1} in any segment of $2.5^\circ \times 2.5^\circ$ grid square within

which the vortex center is located. By doing so, only Borneo vortices that are considered significant would be taken into consideration for further analyses.

In these case studies, it is also surprised to discover that the Borneo vortices structure and behaviors of strong intensity are comparable with the tropical cyclones. Owing to this, some of the vortices were able to transform into tropical cyclones with the support of right atmospheric ingredients. The additional analyses done on strong vortices through the test of Zuki and Lupo (2008) findings show that the presence of this type of vortices is strongly significant during the active tropical cyclone periods. This suggests that the atmospheric background during strong vortex events is as favorable as the one that support the formation and maintenance of the tropical cyclones.

One possible contributor for such condition to appear is from the penetration of strong cold surge that come all the way from the middle latitude of central Asia into the study domain, which provides strong baroclinic instability for the Borneo vortices to enhance. The presence of this strong cold surge could also be sensed through the formation of TUTT on the potential vorticity field. However, thorough studies need to be done before further assumptions are made with regard to the Borneo vortices of strong intensity.

APPENDIX A

Tests of statistical significance using two-tailed p-value from t-test. The shaded columns are the cases that reach at least 90% confidence level.

A) Section 3.1 (Borneo vortex frequency)

PARAMETER	PDO1	PDO2	EN	LN	NEU	PDO1/EN	PDO1/LN	PDO1/NEU
Population mean	55.6	55.6	55.6	55.6	55.6	53.1	53.1	53.1
Sample mean	53.1	58.4	50.8	61.9	54.8	45.6	53.0	55.6
Sample size	22	19	10	10	21	5	2	15
Standard deviation	11.414	11.573	12.550	9.769	11.223	11.371	0.000	11.475
t-score	-1.004	1.026	-1.147	1.935	-0.319	-1.319	XXX	0.815
p-value (%)	67	68	72	92	25	74	-	57

PARAMETER	PDO2/EN	PDO2/LN	PDO2/NEU	West QBO	East QBO	Str TBO	Weak TBO
Population mean	58.4	58.4	58.4	55.6	55.6	55.6	55.6
Sample mean	56	64.1	52.8	57.1	54.1	58.5	52.5
Sample size	5	8	6	20	21	21	20
Standard deviation	12.500	9.717	11.339	11.698	11.697	11.936	10.782
t-score	-0.384	1.552	-1.104	0.559	-0.573	1.087	-1.253
p-value (%)	28	84	68	42	43	71	77

PARAMETER	Str TBO/EN	Str TBO/LN	Str TBO/NEU	Weak TBO/EN	Weak TBO/LN	Weak TBO/NEU
Population mean	58.5	58.5	58.5	52.5	52.5	52.5
Sample mean	56.2	60.7	58.1	45.4	64.7	52.3
Sample size	5	7	9	5	3	12
Standard deviation	15.691	9.144	13.287	5.941	14.468	9.306
t-score	-0.293	0.589	-0.085	-2.390	1.192	-0.071
p-value (%)	22	42	7	92	64	6

B) Section 3.2 (Borneo vortex center)

i) Latitudinal position

PARAMETER	PDO1	PDO2	EN	LN	NEU	PDO1/EN	PDO1/LN	PDO1/NEU
Population mean	2.4	2.4	2.4	2.4	2.4	2.2	2.2	2.2
Sample mean	2.2	2.7	2.0	3.1	2.3	1.8	2.9	2.3
Sample size	22	19	10	10	21	5	2	15
Standard deviation	0.782	0.678	0.770	0.423	0.716	0.895	0.424	0.691
t-score	-1.172	1.877	-1.558	4.965	-0.625	-0.894	1.651	0.541
p-value (%)	75	92	85	100	46	68	65	40

PARAMETER	PDO2/EN	PDO2/LN	PDO2/NEU	West QBO	East QBO	Str TBO	Weak TBO
Population mean	2.7	2.7	2.7	2.4	2.4	2.4	2.4
Sample mean	2.3	3.2	2.4	2.5	2.4	2.5	2.4
Sample size	5	8	6	20	21	21	20
Standard deviation	0.460	0.423	0.820	0.894	0.658	0.839	0.708
t-score	-1.739	3.127	-0.818	0.488	0.000	0.533	0.000
p-value (%)	84	98	55	37	0	40	0

PARAMETER	Str TBO/EN	Str TBO/LN	Str TBO/NEU	Weak TBO/EN	Weak TBO/LN	Weak TBO/NEU
Population mean	2.5	2.5	2.5	2.2	2.2	2.2
Sample mean	2.2	3.1	2.3	1.9	2.4	2.3
Sample size	5	7	9	5	3	12
Standard deviation	0.976	0.384	0.873	0.573	0.603	0.620
t-score	-0.615	3.828	-0.648	-1.047	0.469	0.535
p-value (%)	42	99	46	65	31	40

ii) Longitudinal position

PARAMETER	PDO1	PDO2	EN	LN	NEU	PDO1/EN	PDO1/LN	PDO1/NEU
Population mean	110.6	110.6	110.6	110.6	110.6	110.5	110.5	110.5
Sample mean	110.5	110.7	110.4	111.0	110.5	110.3	110.6	110.5
Sample size	22	19	10	10	21	5	2	15
Standard deviation	0.589	0.623	0.589	0.734	0.618	0.524	0.972	0.594
t-score	-0.778	0.681	-1.019	1.635	-0.724	-0.763	0.103	0.000
p-value (%)	31	50	77	86	52	51	7	0

PARAMETER	PDO2/EN	PDO2/LN	PDO2/NEU	West QBO	East QBO	Str TBO	Weak TBO
Population mean	110.7	110.7	110.7	110.6	110.6	110.6	110.6
Sample mean	110.6	111.1	110.3	110.5	110.6	110.7	110.4
Sample size	5	8	6	20	21	21	20
Standard deviation	0.719	0.553	0.452	0.693	0.593	0.662	0.590
t-score	-0.278	1.914	-1.979	-0.629	0.000	0.676	-1.478
p-value (%)	21	90	89	46	0	49	84

PARAMETER	Str TBO/EN	Str TBO/LN	Str TBO/NEU	Weak TBO/EN	Weak TBO/LN	Weak TBO/NEU
Population mean	110.7	110.7	110.7	110.4	110.4	110.4
Sample mean	110.5	111.1	110.6	110.3	110.8	110.4
Sample size	5	7	9	5	3	12
Standard deviation	0.622	0.724	0.593	0.588	0.050	0.651
t-score	-0.643	1.352	-0.477	-0.340	11.314	0.000
p-value (%)	44	77	36	25	99	0

C) Section 3.3 (Borneo vortex system and lifespan)

PARAMETER	EN	LN	NEU	West QBO	East QBO	Str TBO	Weak TBO
Population mean	3.6	3.6	3.6	3.6	3.6	3.6	3.6
Sample mean	3.2	4.1	3.5	3.6	3.6	3.7	3.5
Sample size	10	10	21	20	21	21	20
Standard deviation	0.888	0.883	0.776	0.785	0.964	0.915	0.832
t-score	-1.351	1.699	-0.576	0.000	0.000	0.489	-0.524
p-value (%)	79	88	43	0	0	37	40

PARAMETER	Str TBO/EN	Str TBO/LN	Str TBO/NEU	Weak TBO/EN	Weak TBO/LN	Weak TBO/NEU
Population mean	3.7	3.7	3.7	3.5	3.5	3.5
Sample mean	3.1	4.1	3.6	3.0	4.1	3.5
Sample size	5	7	9	5	3	12
Standard deviation	1.183	0.910	0.819	0.564	1.260	0.779
t-score	-1.015	1.076	-0.346	-1.774	0.674	0.000
p-value (%)	63	68	22	85	45	0

PARAMETER	Active	Non-active (warmest SSTs)	Non-active (coldest SSTs)
Population mean	3.6	3.6	3.6
Sample mean	4.8	3.2	3.7
Sample size	4	3	5
Standard deviation	0.238	0.306	0.610
t-score	8.733	-1.849	0.328
p-value (%)	100	79	24

D) Section 3.4 (Borneo vortex intensity)

i) Weak

PARAMETER	PDO1	PDO2	EN	LN	NEU	PDO1/EN	PDO1/LN	PDO1/NEU
Population mean	42.9	42.9	42.9	42.9	42.9	42.4	42.4	42.4
Sample mean	42.4	43.4	39.7	46.9	42.4	38.8	42.0	43.5
Sample size	22	19	10	10	21	5	2	15
Standard deviation	8.753	7.904	8.324	5.301	8.681	9.094	2.828	9.211
t-score	-0.262	0.268	-1.153	2.264	-0.258	-0.792	-0.141	0.447
p-value (%)	20	21	72	95	20	53	9	34

PARAMETER	PDO2/EN	PDO2/LN	PDO2/NEU	West QBO	East QBO	Str TBO	Weak TBO
Population mean	43.4	43.4	43.4	42.9	42.9	42.9	42.9
Sample mean	40.6	47.9	39.8	43.8	42.0	44.5	41.1
Sample size	5	8	6	20	21	21	20
Standard deviation	9.737	5.436	7.250	7.326	9.203	8.548	7.849
t-score	-0.575	2.190	-1.110	0.535	-0.437	0.837	-1.000
p-value (%)	40	94	68	40	33	59	67

PARAMETER	Str TBO/EN	Str TBO/LN	Str TBO/NEU	Weak TBO/EN	Weak TBO/LN	Weak TBO/NEU
Population mean	44.5	44.5	44.5	41.1	41.1	41.1
Sample mean	43.2	45.7	44.2	36.2	49.7	41.1
Sample size	5	7	9	5	3	12
Standard deviation	9.731	5.559	11.196	7.362	4.163	7.255
t-score	-0.267	0.529	-0.076	-1.331	2.921	0.000
p-value (%)	20	38	6	75	90	0

ii) Moderate

PARAMETER	PDO1	PDO2	EN	LN	NEU	PDO1/EN	PDO1/LN	PDO1/NEU
Population mean	9.7	9.7	9.7	9.7	9.7	8.8	8.8	8.8
Sample mean	8.8	10.7	8.4	10.0	10.1	6.2	6.5	9.9
Sample size	22	19	10	10	21	5	2	15
Standard deviation	3.951	4.631	6.147	4.714	4.158	4.438	3.536	3.515
t-score	-1.044	0.916	-0.634	0.191	0.430	-1.172	-0.651	1.171
p-value (%)	69	63	46	15	33	69	37	74

PARAMETER	PDO2/EN	PDO2/LN	PDO2/NEU	West QBO	East QBO	Str TBO	Weak TBO
Population mean	10.7	10.7	10.7	9.7	9.7	9.7	9.7
Sample mean	10.6	10.9	10.5	10.3	9.0	9.9	9.4
Sample size	5	8	6	20	21	21	20
Standard deviation	3.782	4.734	5.857	5.100	3.471	4.277	4.489
t-score	-0.053	0.112	-0.076	0.513	-0.902	0.296	-0.405
p-value (%)	4	7	6	49	62	23	31

PARAMETER	Str TBO/EN	Str TBO/LN	Str TBO/NEU	Weak TBO/EN	Weak TBO/LN	Weak TBO/NEU
Population mean	9.9	9.9	9.9	9.4	9.4	9.4
Sample mean	9.8	10.3	9.9	7.0	11.7	9.8
Sample size	5	7	9	5	3	12
Standard deviation	4.868	3.546	2.390	4.183	7.506	3.738
t-score	-0.041	0.276	0.000	-1.147	0.433	0.355
p-value (%)	3	21	0	68	30	27

iii) Strong

PARAMETER	PDO1	PDO2	EN	LN	NEU	PDO1/EN	PDO1/LN	PDO1/NEU
Population mean	3.0	3.0	3.0	3.0	3.0	2.0	2.0	2.0
Sample mean	2.0	4.3	2.7	5.0	2.3	0.6	3.5	2.2
Sample size	22	19	10	10	21	5	2	15
Standard deviation	2.214	3.367	3.529	2.828	2.533	0.548	0.707	2.484
t-score	-2.070	1.638	-0.255	2.122	-1.236	-5.112	2.121	0.301
p-value (%)	95	88	20	94	77	99	72	23

PARAMETER	PDO2/EN	PDO2/LN	PDO2/NEU	West QBO	East QBO	Str TBO	Weak TBO
Population mean	4.3	4.3	4.3	3.0	3.0	3.0	3.0
Sample mean	4.8	5.3	2.5	3.2	2.9	4.1	1.9
Sample size	5	8	6	20	21	21	20
Standard deviation	4.087	3.068	2.881	3.086	3.025	3.229	2.337
t-score	0.245	0.862	-1.397	0.282	-0.148	1.523	-2.051
p-value (%)	18	58	78	22	12	86	95

PARAMETER	Str TBO/EN	Str TBO/LN	Str TBO/NEU	Weak TBO/EN	Weak TBO/LN	Weak TBO/NEU
Population mean	4.1	4.1	4.1	1.9	1.9	1.9
Sample mean	3.2	5.5	3.4	2.2	3.3	1.4
Sample size	5	7	9	5	3	12
Standard deviation	4.494	2.690	2.507	2.683	2.887	2.109
t-score	-0.400	1.275	-0.790	0.224	0.686	-0.786
p-value (%)	29	75	55	17	44	65

E) Section 3.5 (The onset and retreat dates of the Borneo vortex)

i) Commencement date

PARAMETER	PDO1	PDO2	EN	LN	NEU	PDO1/EN	PDO1/LN	PDO1/NEU
Population mean	5.2	5.2	5.2	5.2	5.2	5.7	5.7	5.7
Sample mean	5.7	4.7	3.0	4.0	6.9	3	1	7.2
Sample size	22	19	10	10	21	5	2	15
Standard deviation	6.160	4.370	1.886	5.011	6.196	1.581	0.000	6.930
t-score	0.372	-0.485	-3.499	-0.718	1.227	-3.415	XXX	0.810
p-value (%)	29	37	99	51	77	92	-	57

PARAMETER	PDO2/EN	PDO2/LN	PDO2/NEU	West QBO	East QBO	Str TBO	Weak TBO
Population mean	4.7	4.7	4.7	5.2	5.2	5.2	5.2
Sample mean	3.0	4.8	6.2	5.5	5.0	3.8	6.8
Sample size	5	8	6	20	21	21	20
Standard deviation	2.345	5.392	4.262	6.100	4.680	3.430	6.592
t-score	-1.450	0.049	0.787	0.214	-0.191	-1.825	1.058
p-value (%)	78	4	53	17	15	92	70

PARAMETER	Str TBO/EN	Str TBO/LN	Str TBO/NEU	Weak TBO/EN	Weak TBO/LN	Weak TBO/NEU
Population mean	3.8	3.8	3.8	6.8	6.8	6.8
Sample mean	3.4	3.9	4.0	2.4	4.3	9.2
Sample size	5	7	9	5	3	12
Standard deviation	1.817	5.146	2.804	1.949	5.774	7.146
t-score	-0.440	0.048	0.202	-4.514	-0.612	1.114
p-value (%)	32	4	16	99	40	71

ii) Departure date

PARAMETER	PDO1	PDO2	EN	LN	NEU	PDO1/EN	PDO1/LN	PDO1/NEU
Population mean	24.0	24.0	24.0	24.0	24.0	23.0	23.0	23.0
Sample mean	23.0	25.1	20.9	26.7	24.1	20.0	27.5	25.1
Sample size	22	19	10	10	21	5	2	15
Standard deviation	6.200	3.519	5.301	1.829	5.567	5.831	0.707	6.445
t-score	-0.739	1.326	-1.754	4.429	0.080	-1.029	6.364	1.219
p-value (%)	53	80	89	100	6	64	90	76

PARAMETER	PDO2/EN	PDO2/LN	PDO2/NEU	West QBO	East QBO	Str TBO	Weak TBO
Population mean	25.1	25.1	25.1	24.0	24.0	24.0	24.0
Sample mean	21.8	26.5	25.8	24.8	23.2	25.0	22.8
Sample size	5	8	6	20	21	21	20
Standard deviation	5.215	2.000	1.602	3.000	6.600	4.364	5.800
t-score	-1.265	1.852	0.977	1.162	-0.542	1.025	-0.902
p-value (%)	73	75	63	74	40	68	62

PARAMETER	Str TBO/EN	Str TBO/LN	Str TBO/NEU	Weak TBO/EN	Weak TBO/LN	Weak TBO/NEU
Population mean	25.0	25.0	25.0	22.8	22.8	22.8
Sample mean	21.0	27.3	25.6	20.8	25.3	23.0
Sample size	5	7	9	5	3	12
Standard deviation	6.671	1.380	3.005	4.324	2.309	6.836
t-score	-1.199	4.082	0.565	-0.925	1.531	0.097
p-value (%)	70	99	41	60	73	8

iii) Monsoon Duration

PARAMETER	PDO1	PDO2	EN	LN	NEU	PDO1/EN	PDO1/LN	PDO1/NEU
Population mean	111.8	111.8	111.8	111.8	111.8	110.3	110.3	110.3
Sample mean	110.3	113.4	110.9	115.7	110.2	110.0	119.5	110.9
Sample size	22	19	10	10	21	5	2	15
Standard deviation	8.521	5.110	6.000	4.692	8.280	6.403	0.707	9.151
t-score	-0.807	1.328	-0.450	2.494	-0.864	-0.094	13.013	0.245
p-value (%)	57	80	44	97	60	7	95	19

PARAMETER	PDO2/EN	PDO2/LN	PDO2/NEU	West QBO	East QBO	Str TBO	Weak TBO
Population mean	113.4	113.4	113.4	111.8	111.8	111.8	111.8
Sample mean	111.8	114.7	112.6	112.3	111.2	114.2	109.0
Sample size	5	8	6	20	21	21	20
Standard deviation	5.718	4.803	5.428	6.189	8.207	5.522	7.950
t-score	-0.560	0.716	-0.330	0.352	-0.327	1.944	-1.535
p-value (%)	39	50	25	27	25	93	86

PARAMETER	Str TBO/EN	Str TBO/LN	Str TBO/NEU	Weak TBO/EN	Weak TBO/LN	Weak TBO/NEU
Population mean	114.2	114.2	114.2	109.0	109.0	109.0
Sample mean	110.6	116.4	114.6	111.4	114.0	106.8
Sample size	5	7	9	5	3	12
Standard deviation	6.542	5.192	2.440	5.683	3.464	9.418
t-score	-1.101	1.038	0.464	0.845	2.041	-0.775
p-value (%)	67	66	34	55	82	55

REFERENCES

- Ahrens, C. Donalds, 2009: *Meteorology Today: An introduction to weather, climate and the environment*. Ninth Edition, Brooks Cole, 624pp.
- Baldwin, M. P., L. J. Gray, T. J. Dunkerton, K. Hamilton, P. H. Haynes, W. J. Randel, J. R. Holton, M. J. Alexander, I. Hirota, T. Horinouchi, D. B. A. Jones, J. S. Kinnersley, C. Marquardt, K. Sato, and M. Takahashi, 2001: The Quasi-Biennial Oscillation, *Rev. Geophys.*, 39, 179-229.
- Bate, P. W., G. S. Garden, G. E. Jackson, B. K. Cheang and P. Sankaran, 1989: The tropical circulation in the Australian/Asian region – November 1987 to April 1988. *Aust. Met. Mag.*, 37, 201-216.
- Birk, K., A. R. Lupo, P. Guinan, and C. E. Barbieri, 2010: The interannual variability of midwestern temperatures and precipitation as related to the ENSO and PDO. *Atmosfera*, 23, 95–128.
- Bjerknes, J., 1969: Atmospheric teleconnections from the equatorial Pacific. *Mon. Wea. Rev.*, 97, 163 – 172.
- Bloomfield, Peter, 2000: *Fourier Analysis of Time Series: An Introduction*. Second Edition, John Wiley & Sons, New York, 261pp.
- Brooks, Bjorn-Gustaf J., 2011: Fourier Transforms – New Analytical Approaches and FTIR Strategies. Goran Nikolic, InTech Pub., 481 – 492.
- Chang, C. P., C. H. Liu and H. C. Kuo, 2003: Typhoon Vamei: An equatorial tropical cyclone formation. *Geophys. Res. Lett.*, 30(3), 1150.
- Chang, C. P and E. Maas Jr., 1976: A case of cross-equatorial displacement of a vortex. *Mon. Wea. Rev.*, 104, 653-655.
- Chang, C. P, J. E. Erickson and K. M. Lau, 1979: Northerly cold surges and near-equatorial disturbances over the winter MONEX area during December 1974, Part I: Synoptic aspects. *Mon. Wea. Rev.*, 107, 812-829.
- Chang, C. P., J. McBride, and C. H. Liu, 2005a: Annual cycle of Southeast Asia—Maritime Continent rainfall and the asymmetric monsoon transition. *J. Climate*, 18, 287-301.

- Chang, C. P. and K. M. Lau, 1980: Northerly cold surges and near-equatorial disturbances over the winter MONEX area during December 1974, Part II: Planetary-scale aspects. *Mon. Wea. Rev.*, 108, 298-312.
- Chang, C. P., P. A. Harr, and H. J. Chen, 2005b: Synoptic disturbances over the equatorial South China Sea and western Maritime Continent during boreal winter. *Mon. Wea. Rev.*, 133, 489-503.
- Chang, C. P., P. A. Harr, and J. McBride and H. H. Hsu, 2004b: Maritime Continent monsoon: Annular cycle and boreal winter variability, *East Asian Monsoon*, Vol. 2, C. P. Chang (Ed.), World Scientific, 107-150.
- Chang, C. P. and T. Li, 2000: A theory for tropical tropospheric biennial oscillation. *J. Atmos. Sci.* 57, 2209-2224.
- Chang, C. P., Z. Wang, J. Ju, and T. Li, 2004a: On the relationship between western Maritime Continent monsoon rainfall and ENSO during northern winter. *J. Climate*, 17, 665-672.
- Cheang, B. K., 1977: Synoptic features and structures of some equatorial vortices over the South China Sea in the Malaysian region during the winter monsoon of December 1973. *Pure Appl. Geophys.*, 115, 1303–1333.
- Cheang, B. K., 1978: Structure of a cyclonic disturbance over the South China Sea and the Malaysian region during the winter monsoon. *Indian J. Met. Hydro. and Geophys.*, 29, 16-25.
- Cheang, B. K., 1987: Short and long-range monsoon prediction in Southeast Asia. *Monsoons*, Jay S. Fein and Pamela L. Stephens (Eds.), John Wiley & Sons, New York, 579-606.
- Chen, G. and H. Lin, 2005: Impact of El-Nino/La-Nina on the seasonality of oceanic water vapor: A proposed scheme for determining the ITCZ. *Mon. Weather Rev.*, 133, 2940–2946.
- Chen, G. T. J., T. E. Gerish, and C. P. Chang, 1986: Structure variations of the synoptic-scale cyclonic disturbances near Borneo during the WMONEX period. *Pap. Meteor. Res.*, 9, 117-135.
- Enfield, D. B., and A. M. Mestas-Nuñez, 1999: Multiscale variabilities in global sea surface temperatures and their relationships with tropospheric climate patterns. *J. Climate*, 12, 2719–2733.
- Fasullo, J., 2004: Biennial characteristics of All India rainfall. *J. Climate*, 17, 2972-2982.

- Fett, R. W., 1966: Upper-level structure of the formation tropical cyclone. *Mon. Wea. Rev.*, 94, 9-18
- Gershunov, A. and T. P. Barnett, 1998: Interdecadal modulation of ENSO teleconnections. *Bull. Am. Meteor. Soc.*, 79, 2715–2725.
- Gray, W. M., 1968: Global view of the origin of tropical disturbances and storms. *Mon. Wea. Rev.*, 96, 669-700.
- Gray, W. M., 1975: Tropical cyclone genesis. Dept. of Atmos. Sci. Paper No 323, Colorado State University, 121pp.
- Gray, W. M., 1984: Atlantic seasonal hurricane frequency, Part I: El Nino and 30 mb quasi-biennial oscillation influences. *Mon. Wea. Rev.*, 112, 1649–1668.
- Gray, W. M., J. D. Sheaffer, and J. A. Knaff, 1992: Influence of the stratospheric QBO on ENSO variability. *J. Meteor. Soc. Japan*, 70, 975-995.
- Greenfield, R. S. and T. N. Krishnamurti, 1979: The winter monsoon experiment - report of December 1978 field phase. *Bull. Amer. Meteor. Soc.*, 60, 439-445.
- Hare, S. R., 1996: Low frequency climate variability and salmon production. Ph.D. dissertation, School of Fisheries, University of Washington, Seattle.
- Hendon, H. H., 2003: Indonesia rainfall variability: Impacts of ENSO and local air-sea interaction. *J. Climate*, 16, 1775–1790.
- Hirschberg, P. A. and J. M. Fritsch, 1991: Tropopause undulations and the development of extratropical cyclones, Part I: Overview and observations from a cyclone event. *Mon. Wea. Rev.*, 119, 496-517.
- Holton, J. R., 1979: *An Introduction to Dynamic Meteorology*. Academic Press, New York, 391pp.
- Houghton, J. T., 2001. *Climate change 2001: The scientific basis*. Cambridge University Press, Cambridge, UK, 857pp.
- Houze, R. A. Jr., S. G. Geotis, F. D. Marks and A. K. West, 1981: Winter monsoon convection in the vicinity of North Borneo, Part I: Structure and time variation of the clouds and precipitation. *Mon. Wea. Rev.*, 109, 1595-1614.
- Johnson, R. H. and C. P. Chang, 2007: Winter MONEX: A quarter-century and beyond. *Bull. Am. Met. Soc.*, 88, 385-388.

- Johnson, R. H., and D. L. Priegnitz, 1981: Winter monsoon convection in the vicinity of north Borneo, Part II: Effects on large-scale fields. *Mon. Wea. Rev.*, 109, 1615-1628.
- Johnson, R. H. and J. R. Zimmerman, 1986: Modification of the boundary layer over the South China Sea during a Winter MONEX cold surge event. *Mon. Wea. Rev.*, 114, 2004–2015.
- Johnson, R. H. and R. A. Houze Jr., 1987: Precipitating cloud systems of the Asian monsoon. *Monsoon Meteorology*. Vol. X, C. P. Chang and T. N. Krishnamurti (Eds.), Oxford University Press, 298–353.
- Juneng, L. and F. T. Tangang, 2005: Evolution of ENSO-related rainfall anomalies in Southeast Asia region and its relationship with atmosphere-ocean variations in Indo-Pacific sector. *Climate Dynamics*, 25:337-350.
- Juneng, L. and F. T. Tangang, 2010: Long-term trends of winter monsoon synoptic circulations over Maritime Continent: 1962-2007. *Atmos. Sci. Lett.*, 11, 199-203.
- Kerr, R. A., 1999: Big El Ninos ride the back of slower climate change. *Science*, 283, 1108-1109.
- Krishnamurti, T. N., M. Kanamitsu, W. J. Ross and J. D. Lee, 1973: Tropical east-west circulations during the northern winter. *J. Atmos. Sci.*, 30, 780-787.
- Krishnamurti, T. N., N. Surgi and J. Manobianco, 1985: Recent results on divergent circulations over the global tropics. *Pap. Meteor. Res.*, 6(1), 41-62.
- Lander, M. A., E. J. Trehubenko and C. P. Guard, 1999: Eastern Hemisphere tropical cyclones of 1996. *Mon. Wea. Rev.*, 127, 1274-1300.
- Lau, K. M. and P. H. Chan, 1983: Short-term climate variability and atmospheric teleconnection from satellite-observed outgoing longwave radiation, Part II: Lagged correlations. *J. Atmos. Sci.*, 40, 2751-2767.
- Lin, H. J., Z. Y. Guan, D. L. Qian, Q. L. Wan and L. J. Wang, 2009: Occurrences of wintertime tropical cyclones in the Western North Pacific under the background of global warming. *Atmos. Oceanic Sci. Lett.*, 2, 6, 333–338.
- Lin, C. Y., C. R. Ho, Q. Zheng, S. J. Huang and N. J. Kuo, 2011: Variability of sea surface temperature and warm pool area in the South China Sea and its relationship to the western Pacific warm pool. *J Oceanogr.*, 67, 719–724.

- Lin, Y. L. and C. S. Lee, 2011: An analysis of tropical cyclone formations in the South China Sea during the late season. *Mon. Wea. Rev.*, 139, 2748-2760.
- Lupo A. R., 2011: Interannual and Interdecadal variability in hurricane activity. *Recent Hurricane Research - Climate, Dynamics, and Societal Impacts*. A. R. Lupo (Ed.), Intech Publishers, Vienna, 3-40pp
- Lupo, A.R., E. P. Kelsey, D. K. Weitlich, I. I. Mokhov, F. A. Akyuz, P. E. Guinan, J. E. Woolard, 2007: Interannual and interdecadal variability in the predominant Pacific Region SST anomaly patterns and their impact on a local climate. *Atmosfera*, 20, 171-196.
- Lupo, A. R., and G. Johnston, 2000: The variability in Atlantic Ocean Basin hurricane occurrence and intensity as related to ENSO and the North Pacific Oscillation. *Nat. Wea. Dig.*, 24:1, 2, 3 – 13.
- Lupo, A. R., Latham, T. K., Magill, T., Clark, J. V., Melick, C. J., and Market, P. S., 2008. The Interannual Variability of Hurricane Activity in the Atlantic and East Pacific Regions. *Nat. Wea. Digest*, 32(2),119–135
- Malaysian Meteorological Department (MMD), 2012: Agro-climatic analysis and outlook. MMD Publication, Volume 9, No.01.
- Mantua, N. J., S. R. Hare, Y. Zhang, J. M. Wallace and R. C. Francis, 1997: A Pacific decadal climate oscillation with impacts on salmon. *Bull. Am. Meteor. Soc.*, 78, 1069-1079.
- Meehl, G. A., 1987: The annual cycle and interannual variability in the tropical Indian and Pacific Ocean regions. *Mon. Wea. Rev.*, 115, 27–50.
- Meehl, G. A., 1997: The South Asian monsoon and the tropospheric biennial oscillation (TBO). *J. Climate*, 10, 1921-1943.
- Meehl, G. A., and J. M. Arblaster, 2002: The tropospheric biennial oscillation and Asian-Australian monsoon rainfall. *J. Climate*, 15, 722–744.
- Meehl, G. A., and J. M. Arblaster, 2011: Decadal Variability of Asian–Australian Monsoon–ENSO–TBO Relationships. *J. Climate*, 24, 4925-4949.
- Minobe, S., 1997: A 50-70 year climatic oscillation over the North Pacific and North America. *Geophys. Res. Lett.*, 24, 683-686.
- Mower, R. N., J. H. Chu, D. W. Martin and B. Auvine, 1984: Mean state of the troposphere over south-east Asia and the East Indies, December 1978. *Quart. J. Roy. Meteor. Soc.*, 110, 1023–1033.

- Murakami, T., 1977: Changes in regional energetics over the North Pacific, South China Sea and the Indonesia Seas during winter. *Mon. Wea. Rev.*, 105, 1508 - 1520.
- Murakami, T., 1979: Winter Monsoon surges over East and Southeast Asia, *J. Meteor. Soc. Japan*, 57, 133-158.
- Neter, J., W. Wasserman, and G. A. Whitmore, 1993: *Applied Statistics*. 4th ed. Prentice Hall, 989 pp.
- Nieto Ferreira, R. and W. H. Schubert, 1999: On the role of tropical cyclones in the formation of tropical upper tropospheric troughs. *J. Atmos. Sci.*, 56, 2891-2907.
- Ooi, S. H. and L. K. Ling, 1996: Observational and Analytical Studies on Tropical Greg (9627) Affecting Sabah and its Vicinity in Late December 1996. ESCAP/WMO Typhoon Committee Annual Review 1996
- Oort, A. H., and J. J. Yienger, 1996: Observed interannual variability in the Hadley circulation and its connection to ENSO. *J. Climate*, 9, 2751–2767.
- Palmer, C. E., 1952: Tropical meteorology. *Quart. J. Roy. Meteor. Soc.*, 78, 126-163.
- Ramage, C. S., 1955: The cold-season tropical disturbances of Southeast Asia. *J. Meteor.*, 12, 252-262.
- Ramage, C. S., 1968: Role of a tropical “Maritime Continent” in the atmospheric circulation. *Mon. Wea. Rev.*, 96, 365–37.
- Ramage, C.S., 1971: *Monsoon Meteorology*. Academic Press, New York, 344pp.
- Reed, R. J., W. J. Campbell, L. A. Rasmussen, and D. G. Rogers, 1961: Evidence of a downward propagating annual wind reversal in the equatorial stratosphere. *J. Geophys. Res.*, 66, 813-818.
- Riehl, H., 1948: On the formation of typhoons. *J. Meteor.*, 5, 247-264.
- Riehl, H., 1969: Some aspects of cumulonimbus convection in relation to tropical weather disturbances. *Bull. Am. Meteor. Soc.*, 50, 587-595.
- Sadler, J. C., 1967: On the origin of tropical vortices. Working Panel on Trop. Dyn. Meteor. Naval Post Graduate School, Monterey, CA, 39-75

- Sadler, J. C. and B. E. Harris, 1970: The mean tropospheric circulation and cloudiness over Southeast Asia and neighboring areas. Hawaii Inst. Geophys. Sci. Report No. 1.
- Saji, N. H., Goswami B. N., Vinayachandran P. N., and Yamagata T., 1999: A dipole mode in the tropical Indian Ocean. *Nature*, 401, 360-363.
- Simmons, A, S. Uppala, D. Dee, and S. Kobayashi, 2007: ERA-Interim: New ECMWF reanalysis products from 1989 onwards. Newsletter 110 - Winter 2006/07, ECMWF, 11 pp.
- Tanaka, M., 1994: The onset and retreat dates of the Austral summer monsoon over Indonesia, Australia and New Guinea, *J. Meteor. Soc. Japan*, 72, 255-267.
- Tangang, F. T., E. Salimun, L. Juneng, P. N. Vinayachandran, K. S. Yap, C. J. C. Reason, S. K. Behera and T. Yasunari, 2008: On the roles of northeast cold surge, the Borneo vortex, the Madden-Julian Oscillation and the Indian Ocean Dipole during the worst 2006/2007 flood in Peninsular Malaysia. *Geophys. Res. Lett.*, 35: L14S07. DOI:10.1029/2008GL033429.
- Tangang, F. T. and L. Juneng, 2004: Mechanisms of Malaysia rainfall anomalies. *J. Climate*, 17, 3616–3622.
- Tangang F. T, L. Juneng, C. J. C Reason, S. Moten and W. A. W. Hassan, 2007: Simulation of tropical cyclone Vamei (2001) using the PSU/NCAR MM5 model. *Meteor. Atmos. Phys.*, 97, 273–290
- Trenberth, K. E., 1976: Spatial and temporal variations of the Southern Oscillation. *Quart. J. Roy. Meteor. Soc.*, 102, 639-653.
- Trenberth, K. E., 1997: The definition of El Nino. *Bull. Am. Meteor. Soc.*, 78, 2771-2777.
- Vinayachandran, P. N., J. Kurian, and C. P. Neema, 2007: Indian Ocean response to anomalous conditions in 2006, *Geophys. Res. Lett.*, 34, L15602, doi:10.1029/2007GL030194.
- Wang, B., 2006: *The Asian Monsoon*. Published by Springer and Praxis Publishing, 787pp.
- Wang, B., F. Huang, Z. Wu, J. Yang, X. Fu, and K. Kikuchi, 2009: Multi-Scale Climate Variability of the South China Sea Monsoon: A Review. *Dyn. Atmos. Ocean*, 47, 15-37.

- Wang, C., 2002: Atmospheric circulation cells associated with the El Niño-Southern Oscillation. *J. Climate*, 15, 399-419.
- Wexler, H., 1951: Anticyclones. *Compendium of Meteorology*, Amer. Meteor. Soc., 621-629.
- Wu, R. G. and B. P. Kirtman, 2004: The tropospheric biennial oscillation of the monsoon-ENSO system in an interactive ensemble coupled GCM. *J. Climate*, 17, 1623-1640.
- Yanai, M., T. Maruyama, Tsuyoshi Nitta and Y. Hayashi, 1968: Power Spectra of Large-Scale Disturbances over the Tropical Pacific. *J. Meteor. Soc. Japan*, 46, 4, 308-323.
- Yang, S., K. M. Lau, and K. M. Kim, 2002: Variations of the East Asian jet stream and Asian–Pacific–American winter climate anomalies. *J. Climate*, 15, 306-325
- Yasunari, T., 1990: Impact of Indian monsoon on the coupled atmosphere-ocean system in the tropical Pacific. *Meteor. Atmos. Phys.*, 44, 29–41.
- Yasunari, T. and R. Suppiah, 1988: Some problems on the interannual variability of Indonesian monsoon rainfall. *Tropical rainfall measurements*. J. S. Theon and N. Fugono (Eds.), Deepak, 113–122.
- Zhang, Y., J. M. Wallace and D. S. Battisti, 1997a: ENSO-like interdecadal variability: 1900-93. *J. Climate*, 10, 1004-1020.
- Zhang, Y., K. R. Sperber, and J. S. Boyle, 1997b: Climatology and interannual variation of the East Asian winter monsoon: Results from the 1979–95 NCEP/NCAR Reanalysis. *Mon. Wea. Rev.*, 125, 2605–2619.
- Zuki, Md. Z., and A. R. Lupo, 2008: The interannual variability of tropical cyclone activity in the southern South China Sea. *J. Geophys. Res.*, 113, D06106, doi:10.1029/2007JD009218.

VITA AUCTORIS

Mohd Hisham Mohd Anip was born on 2nd March 1969 in Kuala Lumpur, Malaysia. After completing his elementary education at Sultan Sulaiman Primary School, Terengganu in 1981, he was accepted into a boarding school, Science Dungun Secondary School, which is also in Terengganu, to pursue his secondary study before enrolling into University of Malaya in 1987.

After graduating in 1993 with a bachelor's degree in Science Mathematics, he temporarily worked as a tutor with the university before being offered to join the Malaysian Meteorological Department (MMD) in 1994 working as a meteorologist. The career has landed him with lots of opportunity to learn and explore various meteorological stuffs from different meteorological agencies, such as WMO (Geneva), KMA (Korea), IMD (India) and MSS (Singapore).

In 2005, he earned his master's degree in Atmospheric Science from University of Missouri-Columbia (MIZZOU). Three years later, he came back to MIZZOU to join the PhD. program after being granted a 4-year study leave that comes with full sponsorship from the Malaysian Government. Once completed, he needs to go back to serve his country as a meteorologist.

He got married in 1995 to a beautiful teacher, Zuana Tahir, one year after joining the MMD, and they now are blessed with three wonderful children, Hazman (15), Hanah (12) and Hilman(8).